Lehigh University
Lehigh Preserve

Theses and Dissertations

2011

Using Kriging Methods to Estimate Damage Distribution

Bing Wang
Lehigh University

Follow this and additional works at: http://preserve.lehigh.edu/etd

Recommended Citation
Wang, Bing, "Using Kriging Methods to Estimate Damage Distribution" (2011). *Theses and Dissertations.* Paper 1383.

This Thesis is brought to you for free and open access by Lehigh Preserve. It has been accepted for inclusion in Theses and Dissertations by an authorized administrator of Lehigh Preserve. For more information, please contact preserve@lehigh.edu.

Using Kriging Methods to Estimate Damage Distribution

by

Bing Wang

A Thesis
Presented to the Graduate and Research Committee
of Lehigh University
in Candidacy for the Degree of
Master of Science
in
Mechanical Engineering and Mechanics

Lehigh University

April 2011

This thesis is accepted and approved in partial fulfillment of the requirements for the Master of Science.

April 22, 2011

Date

D G Harlow

Thesis Advisor

D G Harlow

Chairperson of Department

ACKNOWLEDGEMENT

Primarily, I would like to express my sincere gratitude to my advisor Professor D. Gary Harlow. Without his inspiration, enthusiasm, patient, motivation and his great efforts to guide me during writing this thesis, this thesis could not be completed.

Lastly, and most importantly, I wish to indicate the great appreciation to my family: my parents, Lezhi Wang and Lanying Zhang, for giving me a life, supporting me and loving me and my wife, Yuanyuan Wang, for her patience and sacrifice during my studying in U.S.

TABLE OF CONTENTS

ACKNOWLEDGEMENT……...III

TABLE OF CONTENTS……IV

LIST OF FIGURES……...…VII

LIST OF TABLES……X

ABSTRACT……...1

Chapter 1 Introduction 2

1.1 The Statement of Problem 2

1.2 Purpose of the Study 2

1.3 Outline of Thesis 3

Chapter 2 Kriging and Related Software Programs 5

2.1 Introduction to Kriging 5

2.1.1 Simple Kriging 7
2.1.2 Ordinary Kriging 9
2.1.3 Universal Kriging 10
2.1.4 Other Kriging Methods 11

2.2 Reason of Choosing Kriging 11

2.3 Software Be Applied 13

2.3.1 ArcGIS 13
2.3.2 Golden Surfer 14
2.3.3 SGeMS 14
2.3.4 Image Pro-Plus 15

Chapter 3 Kriging Estimation 16

3.1 Introduction to Kriging Estimation 16

3.1.1 Creating a Simulation Grid 16
3.1.2 Loading the Data Set 17
3.1.3 Operation the Kriging Algorithm 17
3.1.4 Displaying and Analyzing Results 19

3.2 Pre Kriging Data Processing 19
3.3 Effect of Radius 25
3.3.1 Creating Data Set 25
3.3.2 Simulation of All Four Holes with 1/16ft Radius 25
3.3.3 Simulation of All Four Holes with 1/8ft Radius 29
3.3.4 Simulation of All Four Holes with 1/2ft Radius 31
3.3.5 Simulation of All Four Holes with 1ft Radius 34
3.3.5 Conclusion of Radius Effect 37
3.4 Effect of Different Radii Holes Arrangement 39
3.4.1 Creating Data Set 39
3.4.2 Simulation of the First Holes Arrangement 39
3.4.3 Simulation of the Second Holes Arrangement 42
3.4.4 Simulation of the Third Holes Arrangement 45
3.4.5 Conclusion of Different Holes Arrangement Effect 48
3.5 Effect of Different Distance between Holes 49
3.5.1 Creating Data Set 49
3.5.2 Simulation of Separation is 3 ft 50
3.5.3 Simulation of Separation is 5 ft 53
3.5.4 Conclusion of Different Distance between Holes 56
3.6 Effect of Different Patterns of Holes 56
3.6.1 Creating Data Set 56
3.6.2 Simulation of 1 Hole 58
3.6.3 Simulation of 2 Holes 61
3.6.4 Simulation of 3 Holes 64
3.6.5 Simulation of 5 Holes 67
3.6.6 Simulation of 6 Holes 70
3.6.4 Conclusion of Different Patterns of Holes 73
3.7 Relationship between Radius and Distance 73
3.7.1 Creating Data Set 74
3.7.2 Relationship of Radius and Distance for 1/16ft radius 74
3.7.3 Relationship of Radius and Distance for 1/8ft radius 77
3.7.4 Relationship of Radius and Distance for 1/2ft radius 79
Chapter 4 Conclusion and Future Work 83
4.1 Conclusion 83
4.2 Suggestions for Future Work 84
REFERENCE 86

APPENDIX…… 88

LIST OF FIRURES

Figure 1 Curve of variogram function about spherical model, exponential model and Gaussian model 18
Figure 2 Two Patterns Used to Express Circles 20
Figure 3 9 Points Used to Represent a Circle of Radius 0.25in 21
Figure 4 17 Points Used to Represent a Circle of Radius 0.25in 21
Figure 5 9 Points Used to Represent a Circle of Radius 0.5in 22
Figure 6 17 Points Used to Represent a Circle of Radius 0.5in 22
Figure 7 9 Points Used to Represent a Circle of Radius 1 in 23
Figure 8 17 Points Used to Represent a Circle of Radius 1 in 23
Figure 9 Curve of Variogram Function for 1/16ft Radius 26
Figure 10 Contour of Thickness Distribution from ArcGIS for 1/16ft Radius 27
Figure 11 Contour of Thickness Distribution from Surfer for 1/16ft Radius 27
Figure 12 Contour of Thickness Distribution from SGeMS for 1/16ft Radius 28
Figure 13 3-D Model of Thickness Distribution from SGeMS for 1/16ft Radius 28
Figure 14 Curve of Variogram Function for 1/16ft Radius 29
Figure 15 Contour of Thickness Distribution from ArcGIS for 1/16ft Radius 30
Figure 16 Contour of Thickness Distribution from Surfer for 1/16ft Radius 30
Figure 17 Contour of Thickness Distribution from SGeMS for 1/8ft Radius 31
Figure 18 3-D Model of Thickness Distribution from SGeMS for 1/8ft Radius 31
Figure 19 Curve of Variogram Function for 1/2ft Radius 32
Figure 20 Contour of Thickness Distribution from ArcGIS for 1/2ft Radius 33
Figure 21 Contour of Thickness Distribution from Surfer for 1/2ft Radius 33
Figure 22 Contour of Thickness Distribution from SGeMS for 1/2ft Radius 34
Figure 23 3-D Model of Thickness Distribution from SGeMS for 1/2ft Radius 34
Figure 24 Curve of Variogram Function for 1ft Radius 35
Figure 25 Contour of Thickness Distribution from ArcGIS for 1ft Radius 36
Figure 26 Contour of Thickness Distribution from Surfer for 1ft Radius 36
Figure 27 Contour of Thickness Distribution from SGeMS for 1ft Radius 37
Figure 28 3-D Model of Thickness Distribution from SGeMS for 1ft Radius 37
Figure 29 Curve of Variogram Function for the First Arrangement 39
Figure 30 Contour of Thickness Distribution from ArcGIS for the First Arrangement. 40
Figure 31 Contour of Thickness Distribution from Surfer for the First Arrangement ... 41
Figure 32 Contour of Thickness Distribution from SGeMS for the First Arrangement 41
Figure 33 3-D Model from SGeMS for the First Arrangement 42
Figure 34 Curve of Variogram Function for the Second Arrangement 42
Figure 35 Contour of Thickness Distribution from ArcGIS for the Second One 43
Figure 36 Contour of Thickness Distribution from Surfer for the Second One 44
Figure 37 Contour of Thickness Distribution from SGeMS for the Second One 44
Figure 38 3-D Model from SGeMS for the Second Arrangement 45
Figure 39 Curve of Variogram Function for the Third Arrangement 45
Figure 40 Contour of Thickness Distribution from ArcGIS for the Third One 46

Figure 41 Contour of Thickness Distribution from Surfer for the Third One……..….47
Figure 42 Contour of Thickness Distribution from SGeMS for the Third One…….47
Figure 43 3-D Model from SGeMS for the Third Arrangement 48
Figure 44 Curve of Variogram Function for Separation is 3ft 50
Figure 45 Contour of Thickness Distribution from ArcGIS for Separation is 3ft..... 51
Figure 46 Contour of Thickness Distribution from Surfer for Separation is 3ft..... 51
Figure 47 Contour of Thickness Distribution from SGeMS for Separation is 3ft 52
Figure 48 3-D Model of Thickness Distribution from SGeMS for Separation is 3ft..... 52
Figure 49 Curve of Variogram Function for Separation is 5ft 53
Figure 50 Contour of Thickness Distribution from ArcGIS for Separation is 5ft..... 54
Figure 51 Contour of Thickness Distribution from Surfer for Separation is 5ft..... 54
Figure 52 Contour of Thickness Distribution from SGeMS for Separation is 5ft 55
Figure 53 3-D Model of Thickness Distribution from SGeMS for Separation is 5ft..... 55
Figure 54 Different Patterns..... 57
Figure 55 Curve of Variogram Function for 1 Hole..... 58
Figure 56 Contour of Thickness Distribution from ArcGIS for 1 Hole 59
Figure 57 Contour of Thickness Distribution from Surfer for 1 Hole 59
Figure 58 Contour of Thickness Distribution from SGeMS for 1 Hole..... 60
Figure 59 3-D Model of Thickness Distribution from SGeMS for 1 Hole 60
Figure 60 Curve of Variogram Function for 2 Holes 61
Figure 61 Contour of Thickness Distribution from ArcGIS for 2 Holes 62
Figure 62 Contour of Thickness Distribution from Surfer for 2 Holes..... 62
Figure 63 Contour of Thickness Distribution from SGeMS for 2 Holes 63
Figure 64 3-D Model of Thickness Distribution from SGeMS for 2 Holes 63
Figure 65 Curve of Variogram Function for 3 Holes 64
Figure 66 Contour of Thickness Distribution from ArcGIS for 3 Holes 65
Figure 67 Contour of Thickness Distribution from Surfer for 3 Holes..... 65
Figure 68 Contour of Thickness Distribution from SGeMS for 3 Holes 66
Figure 69 3-D Model of Thickness Distribution from SGeMS for 3 Holes 66
Figure 70 Curve of Variogram Function for 5 Holes 67
Figure 71 Contour of Thickness Distribution from ArcGIS for 5 Holes 68
Figure 72 Contour of Thickness Distribution from Surfer for 5 Holes..... 68
Figure 73 Contour of Thickness Distribution from SGeMS for 5 Holes 69
Figure 74 3-D Model of Thickness Distribution from SGeMS for 5 Holes 69
Figure 75 Curve of Variogram Function for 6 Holes 70
Figure 76 Contour of Thickness Distribution from ArcGIS for 6 Holes 71
Figure 77 Contour of Thickness Distribution from Surfer for 6 Holes..... 71
Figure 78 Contour of Thickness Distribution from SGeMS for 6 Holes 72
Figure 79 3-D Model of Thickness Distribution from SGeMS for 6 Holes 72
Figure 80 Contour of Thickness Distribution from ArcGIS for 2ft Distance 75
Figure 81 Contour of Thickness Distribution from ArcGIS for 2.67ft Distance 76
Figure 82 Contour of Thickness Distribution from ArcGIS for 2.68ft Distance 76

Figure 83 Contour of Thickness Distribution from ArcGIS for 3ft Distance 77
Figure 84 Contour of Thickness Distribution from ArcGIS for 2.68ft Distance 78
Figure 85 Contour of Thickness Distribution from ArcGIS for 2.67ft Distance 78
Figure 86 Contour of Thickness Distribution from ArcGIS for 2.67ft Distance with No Additional Points..... 79
Figure 87 Contour of Thickness Distribution from ArcGIS for 2.67ft Distance with Additional Points..... 80
Figure 88 Contour of Thickness Distribution from ArcGIS for 3.2ft Distance 81
Figure 89 Contour of Thickness Distribution from ArcGIS for 3.3ft Distance 81
Figure 90 Contour of Thickness Distribution from ArcGIS for 3.35ft Distance 82

LIST OF TABLES

Table 1 Damage Effect Ratio with different radii 38
Table 2 Damage Effect Ratio with Different Radii Holes Arrangement.....48
Table 3 Damage Effect Ratio with Different Radii Holes Arrangement.....56
Table 4 Damage Effect Ratio with Different Patterns of Holes 73

ABSTRACT

The purpose of this thesis is to study the effect of the distribution damage holes in a plate by applying kriging methods. Considering the importance of uniform thickness in some industries, measuring the material thickness distribution is essential.

Assuming a thickness and location of damage, kriging methods could be used to estimate the thickness distribution to evaluate the effect of damage holes under several conditions. In this thesis, damage holes have been characterized with four conditions, which are different radii, different radii in hole arrangements, different distances between holes and different patterns of holes. A relationship between damage distance and size was developed.

The value of this thesis is to apply available programs using kriging methods to obtain the thickness distribution quickly and easily which could serve large scale industrialized applications.

Chapter 1

Introduction

Uniformity of plate thickness is one of the most significant factors in the processing and manufacturing of plates. This is related to the performance, safety and service life of plates used for structural components. Structural thickness is one of the most important concerns in the nuclear industry especially for components in containment vessels. A plate with sufficient thickness is an effective shield to prevent nuclear radiation leakage, so uniform thickness could guarantee that the plate prevents penetrability. In addition, areas subjected to stress, whose thickness is small, may grow into cracks that will affect the service life of plates. Above all, thickness is a crucial parameter for structural plates, and its estimation is warranted.

1.1 The Statement of Problem

Due to the importance of plate thickness, this article will consider a 20 ft × 20 ft plate which contains known damage. The goal of this thesis is to estimate the effect of the known damage on the thickness distribution. So that structural integrity assessments can be made.

1.2 Purpose of the Study

As a core factor, thickness is usually immeasurable for a whole plate, especially

large plates. For some applications even very small through – thickness holes can have severe consequences. Typical, measurement devices are not capable of scanning large structures in a timely fashion. The purpose of this research is to evaluate an estimation method for the thickness distribution and assess the rationality of this method. This method being considering is kriging, which was first used to weight average gold at the Witwatersrand reef complex in South Africa by Krige, D. G [1] for geostatistical analysis. The purpose of kriging is to forecast size at unobserved locations by spatial size which is partially observed. How kriging could be applied to calculate the thickness distribution is developed in this thesis.

1.3 Outline of Thesis

This thesis contains four other chapters:

Chapter 2 involves three parts. One is the introduction of kriging principles. The next part illustrates the reason why kriging methods are chosen for this research. The last part presents four softwares that are applied in this thesis. Three of them, ArcGIS, SGeMS and Surfer, are existing proven software programs for kriging methods. They are implemented to estimate the thickness distribution. Image-pro Plus is used for image measuring to compute the damage effect ratio.

Chapter 3, a key part of this thesis, describes the application of kriging methods to analyze and solve the problem stated above and gain images of the thickness distribution under five different conditions using the three Kriging related programs.

According to the results, some conclusions were inferred to show the effect of damage area relative to the whole plate.

Chapter 4 gives conclusions of this research and suggestions for future work.

Chapter 2

Kriging and Related Software Programs

As mentioned, measuring the thickness of every point on a plate is not practical, but the goal is for global estimation based on limited measurements. Using inferential statistics principles, patterns based on known thickness values from measured points can be developed to estimate the thickness distribution of the whole plate. The kriging method is one of the better choices to obtain such a distribution.

2.1 Introduction to Kriging

Kriging is one of the families of optimal interpolations used to estimate unknown values based on regression against observed values of surrounding data. Kriging is frequently used in geostatistics to interpolate the value of a random field. The coefficients of kriging methods and the associated error are weighted based upon observed patterns, which contain spatial data, the unobserved location relative to the data locations, and spatial correlation or the degree to which one location can be predicted from a second location as a function of spatial separation.

Goovaerts has an excellent presentation on kriging which is summarized as [2]: all kriging estimators are but variants of the basic linear regression estimator $Z^*(\mathbf{u})$ defined as [3]:

$$Z^*(\mathbf{u}) - m(\mathbf{u}) = \sum_{\alpha=1}^{n(u)} \lambda_\alpha [Z(\mathbf{u}_\alpha) - m(\mathbf{u}_\alpha)] \quad (1)$$

The meanings of the symbols are following as:

u, $\mathbf{u}_\alpha$: location vectors for a point to be estimated and one of the neighboring data points, indexed by α, respectively;

n(**u**) : number of data points in a local neighborhood of **u** used for the estimation of $Z^*(\mathbf{u})$;

m(**u**), m($\mathbf{u}_\alpha$) : expected values (means) of Z(**u**) and Z($\mathbf{u}_\alpha$), respectively;

$\lambda_\alpha(\mathbf{u})$: Kriging weight assigned to datum z($\mathbf{u}_\alpha$) for estimation at location **u**; same datum will receive different weight for different estimation location

Equation (1) is the basic form of the kriging estimator. The goal is to determine weights, λ_α , which minimize the variance of the estimator

$$\sigma_E^2(\mathbf{u}) = \mathrm{Var}\{Z^*(\mathbf{u}) - Z(\mathbf{u})\} \quad (2)$$

under the unbiasedness constraint $E\{Z^*(\mathbf{u}) - Z(\mathbf{u})\}=0$.

Z(**u**) is treated as a random field (RF) with a trend component, m(**u**), and a residual component, R(**u**) = Z(**u**) – m(**u**). The residual component treated as an RF with stationary with mean zero and a stationary covariance (a function of lag, **h**, but not of position, **u**):

$$E\{R(\mathbf{u})\} = 0 \quad (3)$$

$$\mathrm{Cov}\{R(\mathbf{u}), R(\mathbf{u}+\mathbf{h})\} = E\{R(\mathbf{u}) \cdot R(\mathbf{u}+\mathbf{h})\} = C_R(\mathbf{h}) \quad (4)$$

The residual covariance function is generally derived from the input semivariogram model,

$$C_R(\mathbf{h}) = C_R(\mathbf{0}) - \gamma(\mathbf{h}) = \text{Sill} - \gamma(\mathbf{h}) \quad (5)$$

Sill is the origin point of semivariogram curve, which is shown in Figure 1.

There are three main kriging variants, which are simple kriging, ordinary kriging and kriging with a trend. The differences among of them are their treatments of the trend of component, m(**u**).

2.1.1 Simple Kriging

For simple kriging, the trend component is assumed to be a constant and known, m(**u**) = m, which is assumed to be the case for the data in this project[4]. There,

$$Z^*_{SK}(u) = m + \sum_{\alpha=1}^{n(u)} \lambda_\alpha^{SK}(\mathbf{u})[Z(\mathbf{u}_\alpha) - m] \quad (6)$$

It is obvious that E[Z($\mathbf{u}_\alpha$)-m] = 0, so the estimation error $Z^*_{SK}(\mathbf{u}) - Z(\mathbf{u})$ is a linear combination of random variables representing residuals at the data points, $\mathbf{u}_\alpha$, and the estimation point, **u:**

$$Z^*_{SK}(\mathbf{u}) - Z(\mathbf{u}) = [Z^*_{SK}(\mathbf{u}) - m] - [Z(\mathbf{u}) - m]$$

$$= \sum_{\alpha=1}^{n(u)} \lambda_\alpha^{SK}(\mathbf{u})R(\mathbf{u}_\alpha) - R(\mathbf{u}) = R^*_{SK}(\mathbf{u}) - R(\mathbf{u}) \quad (7)$$

Using rules for the variance of a linear combination of random variables, the error variance is then given by

$$\sigma_E^2(\mathbf{u}) = \mathrm{Var}\{R_{SK}^*(\mathbf{u})\} + \mathrm{Var}\{R_{SK}(\mathbf{u})\} - 2\mathrm{Cov}\{R_{SK}^*(\mathbf{u}), R_{SK}(\mathbf{u})\}$$

$$= \sum_{\alpha=1}^{n(\mathbf{u})}\sum_{\beta=1}^{n(\mathbf{u})} \lambda_\alpha^{SK}(\mathbf{u})\lambda_\beta^{SK}(\mathbf{u})C_R(\mathbf{u}_\alpha - \mathbf{u}_\beta) + C_R(\mathbf{0})$$

$$- 2\sum_{\alpha=1}^{n(\mathbf{u})} \lambda_\alpha^{SK}(\mathbf{u})C_R(\mathbf{u}_\alpha - \mathbf{u}) \qquad (8)$$

To minimize the error variance, the derivative of the above expression with respect to each of the kriging weights is taken and set to zero. This leads to the following system of equations:

$$\sum_{\beta=1}^{n(\mathbf{u})} \lambda_\beta^{SK}(\mathbf{u})C_R(\mathbf{u}_\alpha - \mathbf{u}_\beta) = C_R(\mathbf{u}_\alpha - \mathbf{u}) \quad \alpha = 1, \dots, n(\mathbf{u}) \qquad (9)$$

From the assumption, the mean is constant, so the covariance function for $Z(\mathbf{u})$ is the same as that for the residual component, $C(\mathbf{h}) = C_R(\mathbf{h})$. The equation (9) can be written in terms of $C(\mathbf{h})$

$$\sum_{B=1}^{n(\mathbf{u})} \lambda_\beta^{SK}(\mathbf{u})C(\mathbf{u}_\alpha - \mathbf{u}_\beta) = C(\mathbf{u}_\alpha - \mathbf{u}) \quad \alpha = 1, \dots, n(\mathbf{u}) \qquad (10)$$

This can be written in matrix form as

$$\mathbf{K}\lambda_{SK}(\mathbf{u}) = \mathbf{k} \qquad (11)$$

Where **K** is the matrix of covariances between data points and **k** is the vector of covariances between the data points and the estimation points.

So the kriging weights can be solved by using

$$\lambda_{SK}(\mathbf{u}) = \mathbf{K}^{-1}\mathbf{k} \qquad (12)$$

Depend on the equation (6), the prediction can be obtained.

2.1.2 Ordinary Kriging

In ordinary kriging, the mean in the local neighborhood of each estimation point is assumed to be constant, rather than assuming that it is constant over the whole domain.[5] For each nearby data, the mean is that $m(\mathbf{u}_\alpha) = m(\mathbf{u})$ and $Z(\mathbf{u}_\alpha)$ is used to estimate $Z(\mathbf{u})$. Under such circumstances, the kriging estimator could be written as,

$$Z^*(\mathbf{u}) = m(\mathbf{u}) + \sum_{\alpha=1}^{n(\mathbf{u})} \lambda_\alpha(\mathbf{u})[Z(\mathbf{u}_\alpha) - m(\mathbf{u})]$$

$$= \sum_{\alpha=1}^{n(\mathbf{u})} \lambda_\alpha(\mathbf{u}) Z(\mathbf{u}_\alpha) + \left[1 - \sum_{\alpha=1}^{n(\mathbf{u})} \lambda_\alpha(\mathbf{u})\right] m(\mathbf{u}) \qquad (13)$$

under the condition that the kriging weights sum to 1, leading to an ordinary kriging estimator of

$$Z^*_{OK}(\mathbf{u}) = \sum_{\alpha=1}^{n(u)} \lambda_\alpha^{OK}(\mathbf{u}) Z(\mathbf{u}_\alpha) \quad \text{with} \quad \sum_{\alpha=1}^{n(u)} \lambda_\alpha^{OK}(\mathbf{u}) = 1 \qquad (14)$$

With the purpose of minimizing the error variance, a Lagrange parameter, $\mu_{OK}(\mathbf{u})$ is involved:

$$L = \sigma_E^2(\mathbf{u}) + 2\mu_{OK}(\mathbf{u}) \left[1 - \sum_{\alpha=1}^{n(\mathbf{u})} \lambda_\alpha(\mathbf{u})\right] \qquad (15)$$

There is a constraint that must be satisfied for the Lagrange parameters due to the minimization:

$$\frac{1}{2}\frac{\partial L}{\partial \mu} = 1 - \sum_{\alpha=1}^{n(\mathbf{u})} \lambda_\alpha(\mathbf{u}) = 0 \qquad (16)$$

From the above equations, the system of equations for the kriging weights turns out to be

$$\begin{cases} \sum_{\beta=1}^{n(\mathbf{u})} \lambda_{\beta}^{OK}(\mathbf{u}) C_R(\mathbf{u_\alpha} - \mathbf{u_\beta}) + \mu_{OK}(\mathbf{u}) = C_R(\mathbf{u_\alpha} - \mathbf{u}) & \alpha = 1, \dots, n(\mathbf{u}) \quad (17) \\ \sum_{\beta=1}^{n(\mathbf{u})} \lambda_{\beta}^{OK}(\mathbf{u}) = 1 & (18) \end{cases}$$

As for simple kriging, $C_R(\mathbf{h})$ and $C(\mathbf{h})$ could be calculated according to the assumption of a constant mean. In practice, the ordinary kriging system can be stated directly by a semivariogram instead of $C_R(\mathbf{h})$.

After obtaining the Lagrange parameters and kriging weights, the ordinary kriging error variance is solved by

$$\sigma_{OK}^2(\mathbf{u}) = C(0) - \sum_{\alpha=1}^{n(\mathbf{u})} \lambda_{\alpha}^{OK}(\mathbf{u}) C(\mathbf{u_\alpha} - \mathbf{u}) - \mu_{OK}(\mathbf{u}) \quad (19)$$

Depending on equations (11) and (12), the ordinary kriging weight $\lambda_{OK}(\mathbf{u})$ could be solved. Then the predicted value could be gained by using the equation (13).

2.1.3 Universal Kriging

The difference between universal kriging and ordinary kriging is that a linear or higher-order trend in the global coordinates is added in the ordinary kriging estimation. [3] In other words, ordinary kriging is universal kriging with zero-order trend. The assumed local mean in the neighborhood of the estimation point and added trend are two keys to estimate values of unobserved points for universal kriging. Considering the difficulty in obtaining the semivariogram after adding the trend, universal kriging is not applied widely in practice.

2.1.4 Other Kriging Methods

Some other kinds of kriging methods are illustrated as following [6][7][8][9]:

Indicator Kriging: This method is a nonlinear and nonparametric forecasting method which converts continuous variables to a range of binary string. Indicator kriging is useful to retain continuity of high and low permeability regions.

Disjunctive Kriging: This is a nonlinear kriging by transforming the observed data to a series of additive functions, like Hermite polynomials. Disjunctive kriging is very useful for decision but not predict.

Co-kriging: This method is expanding single variable to two or more correlated variables. It is useful for the condition that costly and rare samples are related with low-cost and large quantities' samples. Through applying co-kriging, forecast accuracy of rare samples could be raised by dense sampling.

Among these kriging methods, simple kriging which is employed in this thesis is the most steady and commonly applied method.

2.2 Reason of Choosing Kriging

In order to look for a method to measure the thickness distribution, interpolation, which is an estimation of a variable at an unobserved location from observed values at surrounding locations, is an effective and accuracy method relying on the strong computing capability.[9] Most interpolation (polynomial, splines, rational interpolation, etc.) algorithms use some functions to build models to estimate the unobserved values.

Their properties are stated below [10][11]:

Almost all interpolations would be reasonable estimations, if the data locations are distributed uniformly over the field.

Almost all interpolations will lose accurancy, if the data locations are distributed in clusters and the distance between clusters are large.

Due to the nature of averaging, interpolation algorithms underestimate high extremer and overestimate the low ones.

Kriging as an interpolation algorithm also has these properties, but it has these benefits [10][11][12]:

Kriging is based on by the best linear unbiased estimator. It reduces the effect of bias towards input sample values by kriging weights that are derived from a data-driven weighting function which requires that the sum of the weights is one.

The variogram of kriging does not rely on the actual value of samples, but their distribution. With construction of a perfect variogram model, prediction will represent a better value-distribution and error of estimation will be a minimum.

For the data locations that are distributed in a cluster, kriging assigns individual points within a cluster less weight than isolated data points.

Kriging provides estimation of errors that gives a basis for random simulation of possible realizations.

After the development of kriging, since its first use by Krige, D.G, kriging methods have become a large family including many branches. So kriging could be a

reasonable technique well suited for some particular interpolation problems.

2.3 Software Be Applied

Based on the advantages listed in part 2.2, a large number of programmers have focused on constructing softwares for kriging methods to solve related problems fast and efficiently. Many such software is commercial, but non-commercial software is employed widely in Geostatistics, Environmental Science, Mining, Remote Sensing, Hydrogeology, etc. Such large-scale applications indirectly prove the applicability kriging. From the now-commercial software, three were applied in this thesis; they are ArcGIS, Golden Surfer and SGeMS. The goal of using three programs is to compare the estimated thickness distribution from the different packages.

2.3.1 ArcGIS

ArcGIS includes a set of programs for geographic information system (GIS) programmed by Esri.[13] It is a complex and powerful commercial software which is a system for people who rely on accurate geographic information to make decisions. These packages contain ArcCatalog, ArcGlobe, ArcMap, and ArcScene. ArcMap whose functions are to view spatial data, create layered maps, and perform basic spatial analysis by some interpolation algorithms, one of which is kriging, was applied in this research to analyze samples to obtain the thickness distribution.

ArcMap is the central application in ArcGIS for all map-based tasks including map analysis and editing. It provides two ways to view map. One is a page layout

view which is to view geographic data as well as other map elements. The other is a geographic data view which transfers geographic layers to GIS datasets. The data view is a window for any GIS datasets for a given area. ArcMap is always applied to construct a virtual map on page for printing.

2.3.2 Golden Surfer

Golden Surfer is produced by Golden Software which has developed advanced mapping and graphing solutions since 1983. [14] Surfer is grid-based mapping software which transfers patchily spaced XYZ data into a regularly spaced grid. The best feature of Surfer is simulating a full-function three dimensions visualization contouring and surface model. Due to applying various available interpolation algorithms and controlling gridding parameters, Surfer is used for terrain modeling, landscape visualization, surface analysis, and other territories. It provides numerous excellent display methods like contour maps, 3D maps, 3D wireframe, vector and shaded relief that makes solutions represented and understood easily. Golden Surfer is not a huge and complex commercial software, but is easy to operate.

2.3.3 SGeMS

The Stanford Geostatistical Modeling Software (SGeMS) is a cross-platform (Windows, UNIX) and open-source software for solving problems involving spatially related variables by implementing most of the classical geostatistics algorithms (Kriging, Gaussian and indicator simulation, etc). [15]

SGeMS was designed with two objectives. One is to provide a user-friendly software that applies a large number of geostatistics tools. The user-friendliness means that is a non-obtrusive graphical user interface, it is easy to directly visualize data, and it gives results in a full three dimension interactive environment. Other functions of SGeMS could also conveniently be augmented. As an open-source software, SGeMS functions as a main software, and new tools could be added by other scientists.

2.3.4 Image Pro-Plus

Besides these three Geostatistical softwares, Image Pro-Plus was implemented to process the images. It can measure the area of color-coded colors, which shows the extent of damage areas. In this thesis, this software was used to measure the proportion of damage area, which is related by the damage effect ratio.

Chapter 3

Kriging Estimation

This chapter will clarify the overall process of implementing kriging method to estimate the thickness distribution in an assumed field. The entire processing contains creating a grid, loading data sets, setting up conditions and analyzing results. This chapter includes seven parts, which are required for pre kriging data processing and kriging estimation.

3.1 Introduction to Kriging Estimation

3.1.1 Creating a Simulation Grid

As stated in Part 1.1, the objectives are to consider a 20 ft × 20 ft plate to estimate the variability in thickness. Obtaining and analyzing the thickness distribution is the aim. Almost all simulations are started with creating an environment. The plate is divided into numerous cells in a three dimensional Cartesian grid. In kriging, units of all the location data are ignored, so the plate could be simplified to 20×20 without units. The environment contains the dimensions (20×20) of the grid, the coordinates of the origin of the grid which is from the lower left corner to the higher right corner and the dimensions of each grid cell. After setting this environment, all data in this simulation contain two properties: a point-set and a Cartesian grid.

3.1.2 Loading the Data Set

The basis for gaining an accurate solution is the input data set, so it is essential that correct and good data be loaded. Unfortunately, the three primary software packages require different file formats, but they can be transferred to be used for each. A Microsoft Excel file (.xls) is supported by Surfer and ArcGIS, but SGeMS requires using a GSLIB format.

3.1.3 Operation the Kriging Algorithm

After creating the grid and loading the data set, a kriging algorithm can be implemented. Before applying software, some parameters should be set to fit different input data. These parameters are solved by several algorithms called variogram models. [16][17][18][19] There are four basic linear models which are the core of the nugget effect model, the spherical model, the exponential model and the Gaussian model.

3.1.3.1 Nugget Effect Model

Nugget effect is only for h =0, which is for input data that are quite dissimilar and separated by small distances. If the value of variogram at the origin is not 0, it is called the Nugget Effect.[20][21]

$$\gamma(\mathbf{h}) = \begin{cases} 0 & \text{if } \left|\left|\mathbf{h}\right|\right| = \mathbf{0} \\ 1 & \text{Otherwise} \end{cases} \qquad (20)$$

3.1.3.2 Spherical Model

$$\gamma(\mathbf{h}) = c \cdot \mathrm{Sph}\left(\frac{\mathbf{h}}{a}\right) = \begin{cases} 0 & \mathbf{h} = 0 \\ c \cdot \left[\frac{3}{2}\frac{\mathbf{h}}{a} - \frac{1}{2}\left(\frac{\mathbf{h}}{a}\right)^3\right] & \mathbf{h} \le a \\ 0 & \mathbf{h} \ge a \end{cases} \quad (21)$$

3.1.3.3 Exponential Model

$$\gamma(\mathbf{h}) = c \cdot \mathrm{Exp}\left(\frac{\mathbf{h}}{a}\right) = c \cdot \left[1 - \exp\left(-\frac{3\mathbf{h}}{a}\right)\right] \quad (22)$$

3.1.3.4 Gaussian Model

$$\gamma(\mathbf{h}) = c \cdot \left[1 - \exp\left(-\frac{(3\mathbf{h})^2}{a^2}\right)\right] \quad (23)$$

For the spherical model, exponential model and Gaussian model, their values of the variogram at the origin are all zero and the values close to a constant along with the increasing values of the lag **h. Figure 1** shows the curve of variogram function about these effect models.

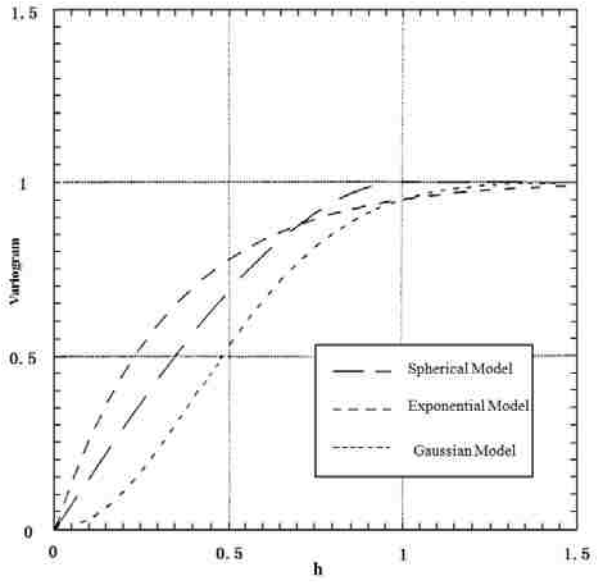

Figure 1 Curve of variogram function about spherical model, exponential model and Gaussian model

3.1.4 Displaying and Analyzing Results

After running these software programs, the thickness distribution was obatined as a data file. Based on these data, several types of images can be drawn, like contour maps, or 3D maps. These maps are colored with these different colors used to distinguish the different thickness.

The goal of this thesis is to measure the effect of observed damage against neighboring location by estimating the thickness distribution. Damage is considered as thickness that is decreased by 50%. The effect is indicated by the damage effect ratio (φ), which is defined by the follow formulation:

$$\varphi = \frac{\text{Total Damage Area}}{\text{Total Area of The Measured Pleat}} \times 100\% \qquad (24)$$

Depending on the color maps, Image Pro-Plus is employed to measure the total damage area, that is, areas whose color are represent thickness that is less than half the nominal thickness.

3.2 Pre Kriging Data Processing

The simulation environment and five conditions to be considered are described. All points are located in a 20ft × 20ft plate. The location and thickness of some points are assumed to be known. These are different and illustrated in every condition. The nominal thickness of the plate is 0.375 inch except for areas with damage.

It is assumed that holes whose radii are vary from 1/16 in, 1/8 in, 1/2 in and 1 in are representative of actual damage. Kriging method is based on numerous point

locations, so it is difficult to use circular damage. Considering that a plate is made up of infinitely many points, the holes are represented by several points. The next step is to test this assumption and determine the number of points needed to represent s the circle. **Figure 2** shows two patterns used to approximate circular damage. One has 9 points and the other was 17 points. For the one with 9 points, one point is on the centre of the circle, and the other 8 points are on the circumference. For the one with 17 points, 9 points locate in the same place as the other case and another 8 points are located on the midpoint of the radii between the center and the 8 points on the circumference.

Figure 2 Two Patterns Used to Represent Circles

In order to decide the number of points to be used, 3 simulations were done for radii of 0.25 inches, 0.5 inches, and 6 inches. The reason of choosing these three radii is assessing the applicability of this assumption and considering the effect of the distance between circle centers on the radius.

These simulations are performed in the following circumstance. The 20ft × 20ft plate is divided into 400 cells and 396 points are located in the center of these cells except for 4 cells in the center of the plate. The thicknesses of the 396 points are

0.375 inches. The other 4 cells are the locations of 4 holes which are of known damage. The following figures show the differences between holes represented by 9 points and 17 points for radii of 0.25 in, 0.5 in and 6 in.

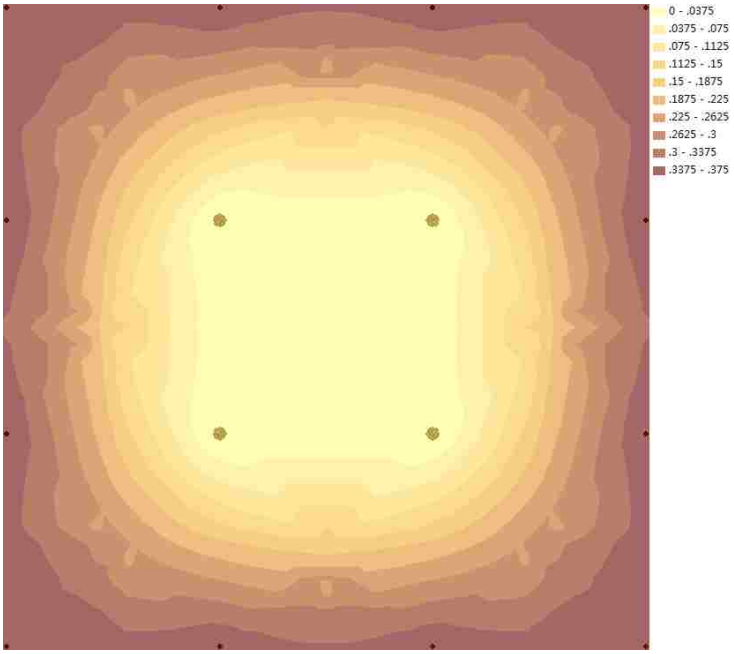

Figure 3 9 Points Used to Represent a Circle of Radius 0.25in

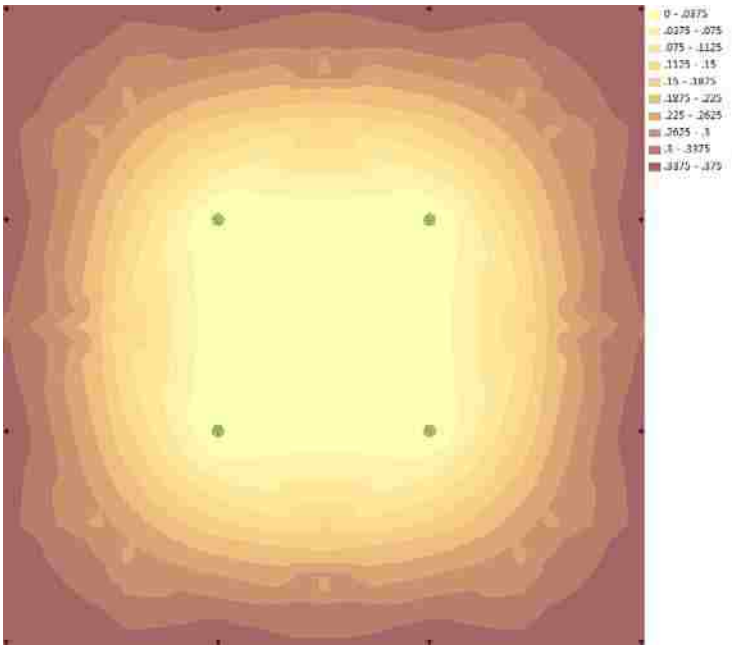

Figure 4 17 Points Used to Represent a Circle of Radius 0.25in

For Figures 3 and 4, the differences between them are slight.

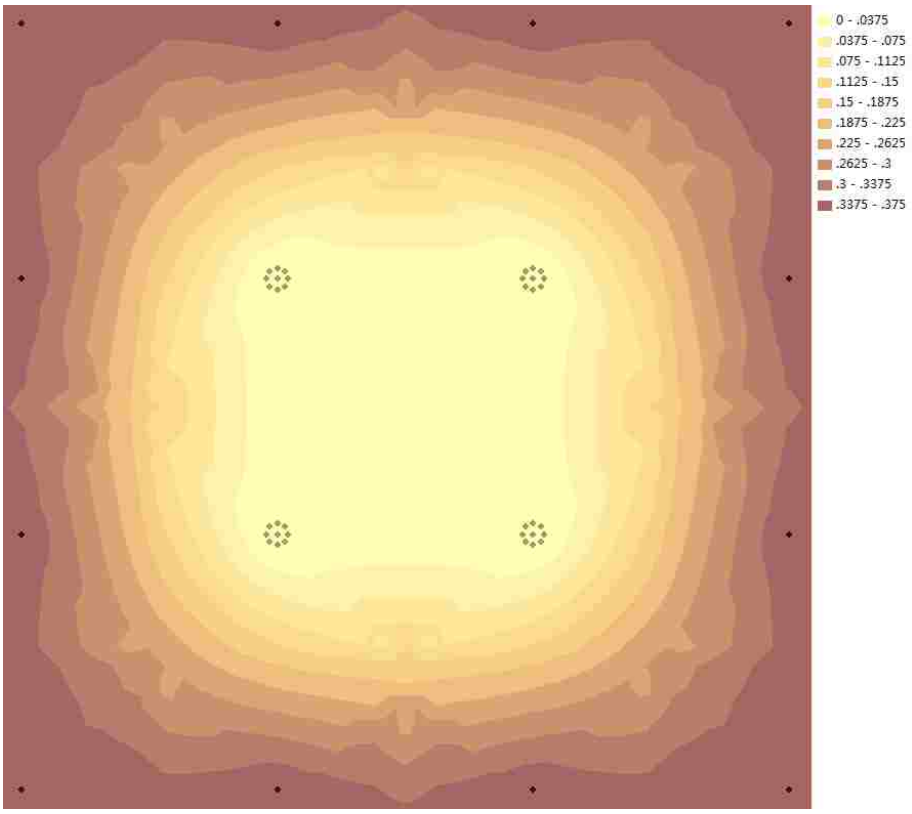

Figure 5 9 Points Used to Represent a Circle of Radius 0.5in

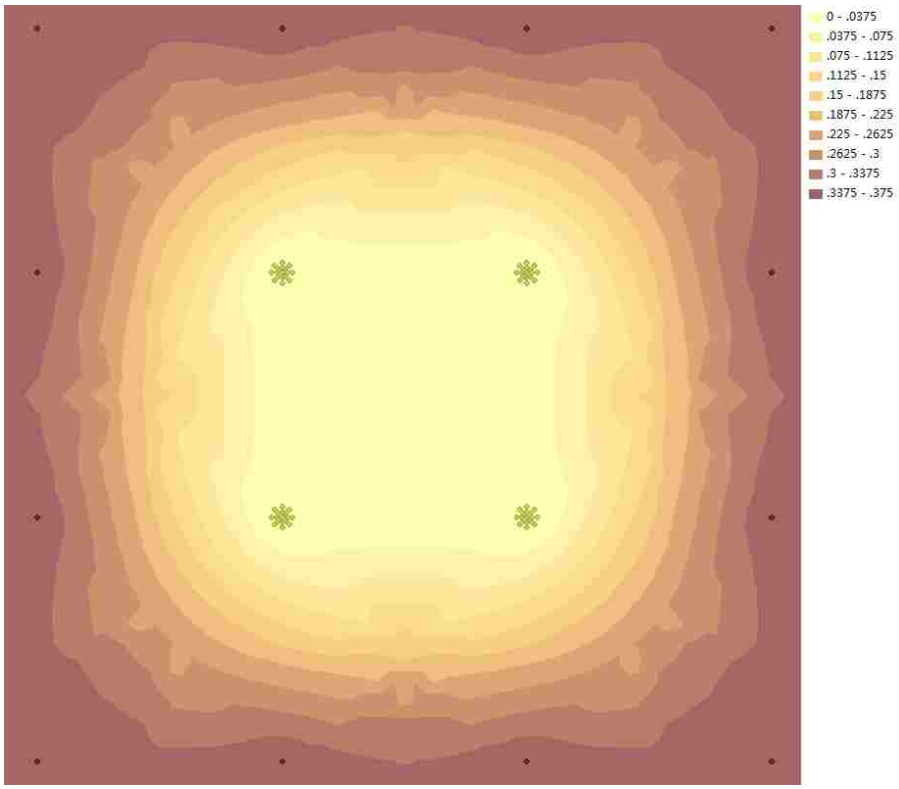

Figure 6 17 Points Used to Represent a Circle of Radius 0.5in

For Figure 5 and 6, the differences between them are minimal.

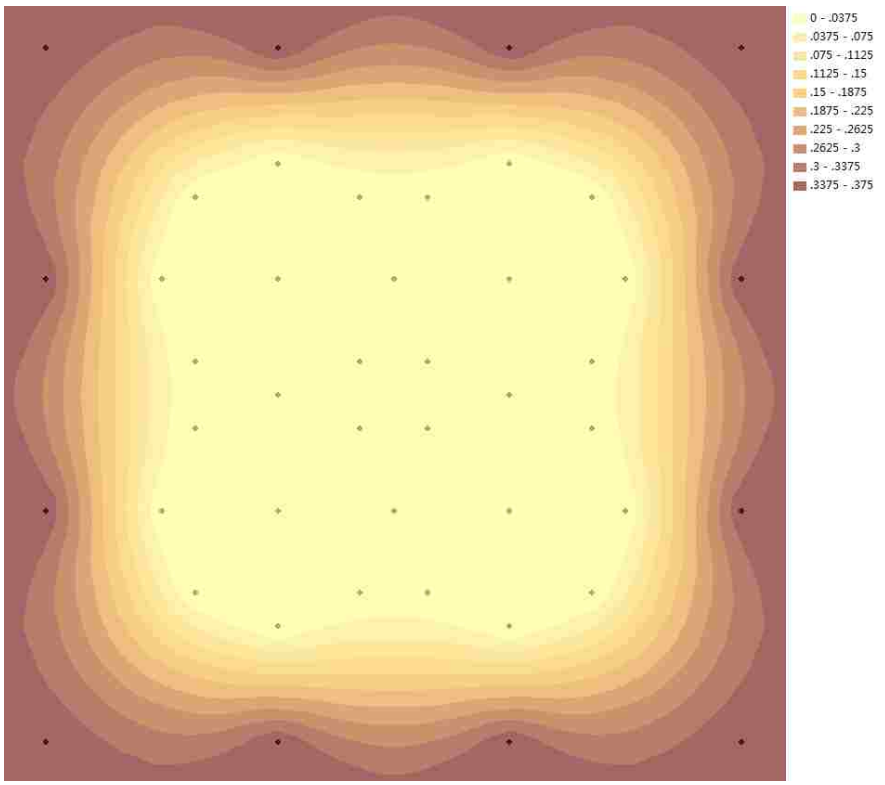

Figure 7 9 Points Used to Represent a Circle of Radius 1 in

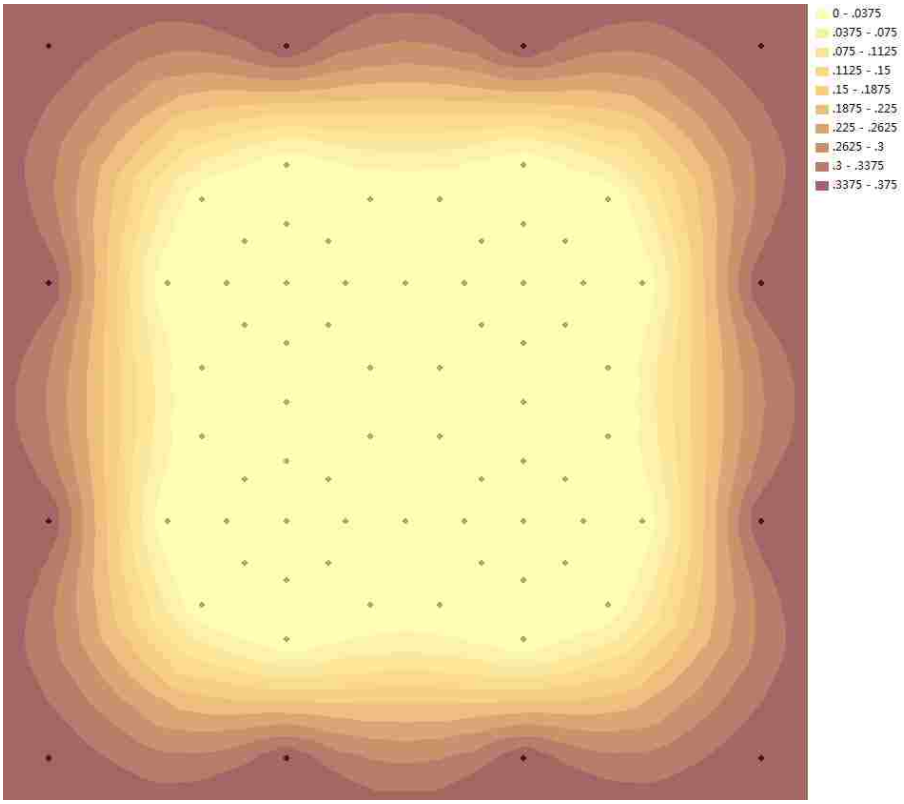

Figure 8 17 Points Used to Represent a Circle of Radius 1 in

For Figure 7 and 8, the differences between them are negligible.

From these six figures, it is concluded that both 9 points and17 points could represent a circle, even when the circles are positioned 0.25in, 0.5in and 1in from each other. In order to gain accuracy solution, 17 points was selected to represent circular damage.

Considering the difficulty of calculating the locations of the 17 points, a program was co structured with Matlab for the locations of the points which transferred them into an excel file as a data.

The program is presented in the appendix.

Completing the pre kriging data processing, the simulation of five conditions could be run. All five conditions are listed as following:

(1) All holes are located in the center of the plate and have the same radius, but the radii range over 1/16 ft, 1/8 ft, 1/2 ft and 1 ft. This is to evaluate the effect of relative hole location.

(2) The four holes are located in the center of the plate and each has a different radius for 1/16 ft, 1/8 ft, 1/2 ft and 1 ft. Considering the symmetry, there are three different arrangements. This is to evaluate the effect of different arrangements of hole size.

(3) All four holes have the same radius but different locations. They are located in the four corners of a square whose lengths of a side are assumed to be 1in, 3 in and 5 inch. This is to evaluate the effect of between holes distance.

(4) There are varying numbers of holes from 1 hole to 6 holes. These holes make

up different patterns which are located as a circle whose radius is 1 foot. This is to evaluate the effect of different patterns of holes.

(5) In this part, the location and radius of these holes are varied. This is to evaluate the relationship between the distance and radius to avoid the interaction.

3.3 Effect of Radius

3.3.1 Creating Data Set

The circumstance of this part is that the 20ft × 20ft plate is divided into 400 cells, and 396 are represented by a single point located in the center, and 4 cells near the center of the plate contain damage. The thicknesses of the 396 points are 0.375 in. The other 4 cells have known damage. These simulations will consider the effect of different radii of holes and different locations of holes.

3.3.2 Simulation of All Four Holes with 1/16ft Radius

3.3.2.1 Setting up Parameters

Figure 9 shows the curve of the variogram function for holes with a 1/16ft radius by using ArcGIS. The variogram was drawn based on the simple kriging methods which are gained by ArcGIS. The based principle is to use the points in clusters and neglect the signal point. So some following curves don’t look reasonable.

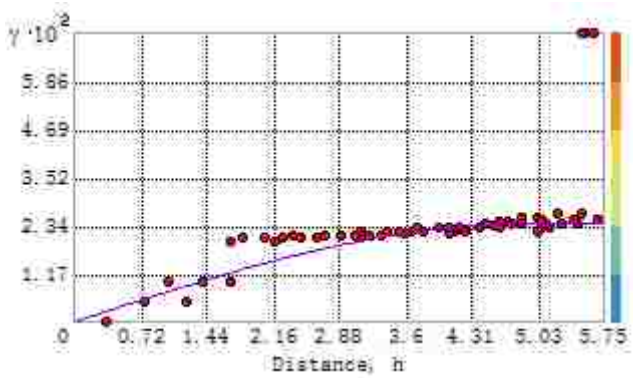

Figure 9 Curve of Variogram Function for 1/16ft Radius

Based on this curve, the spherical effect model was selected. The other parameters of the spherical model are as following:

Mean Value: 0.32004

Major range: 4.89919

3.3.2.2 Displaying the Images

Using the above parameters in the three softwares, the estimated thickness distribution was computed. Given on these files, the four figures are developed from the packages. Every software gives a contour map of the distribution and Surfer yields a 3-D distribution map.

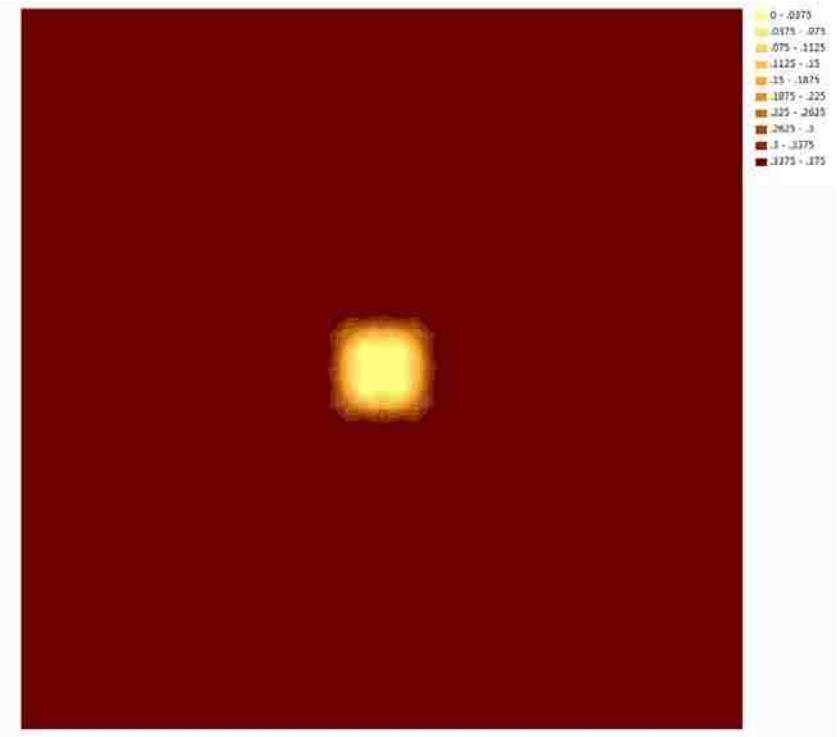

Figure 10 Contour of Thickness Distribution from ArcGIS for 1/16ft Radius

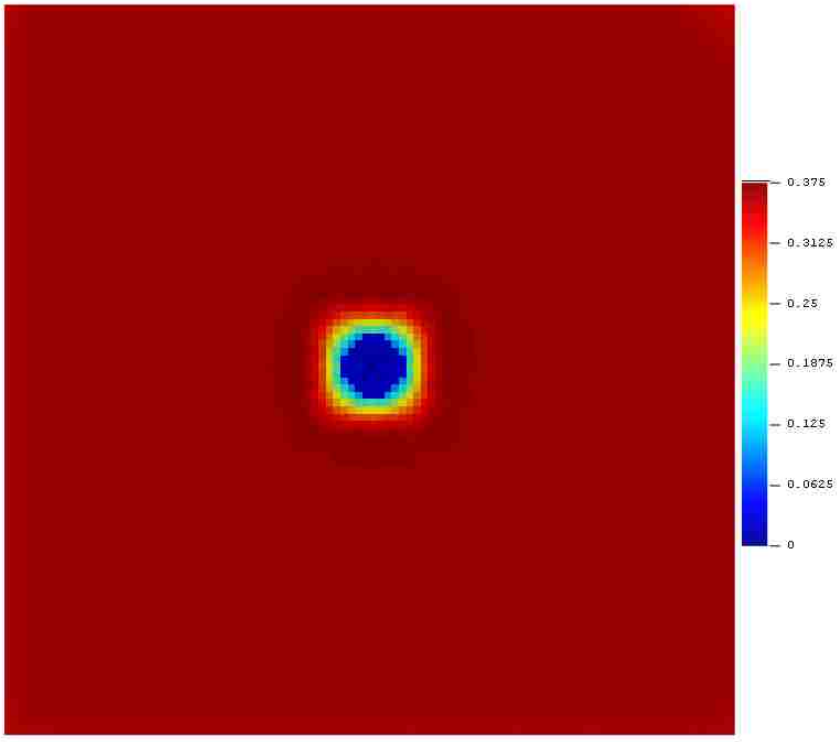

Figure 11 Contour of Thickness Distribution from Surfer for 1/16ft Radius

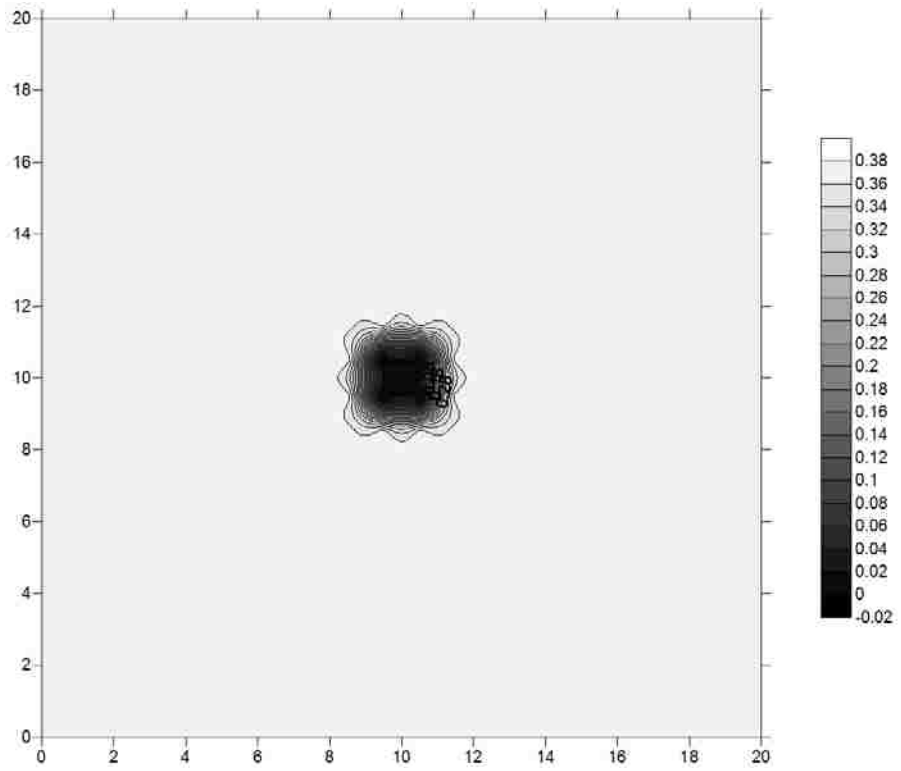

Figure 12 Contour of Thickness Distribution from SGeMS for 1/16ft Radius

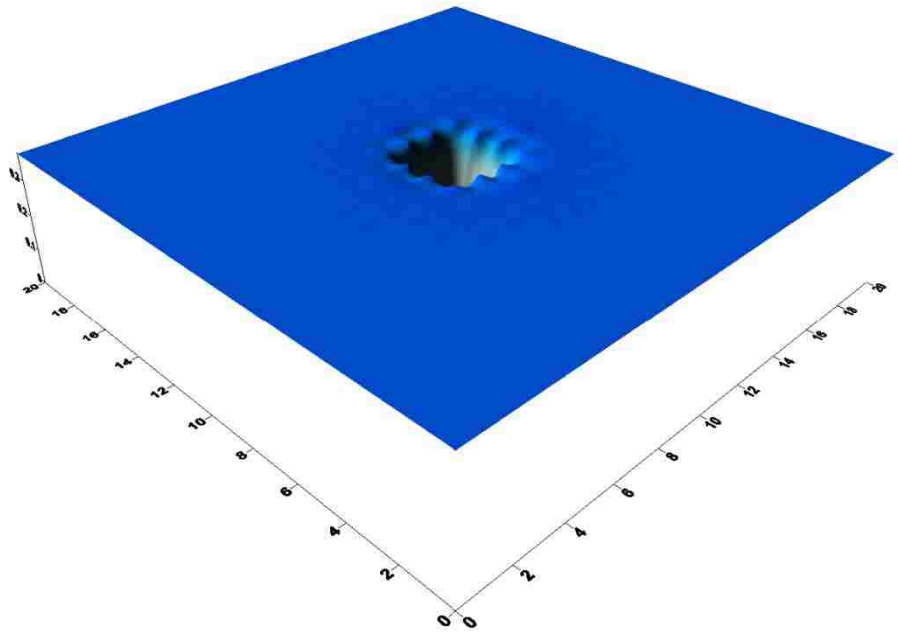

Figure 13 3-D Model of Thickness Distribution from SGeMS for 1/16ft Radius

The damage effect ration (φ) was measured from Figures 10, 11 and 12 by Image Pro-Plus, and Table 1 contains the results.

3.3.3 Simulation of All Four Holes with 1/8ft Radius

3.3.3.1 Setting up Parameters

Figure 14 shows the curve of variogram function for 1/8ft radius by ArcGIS.

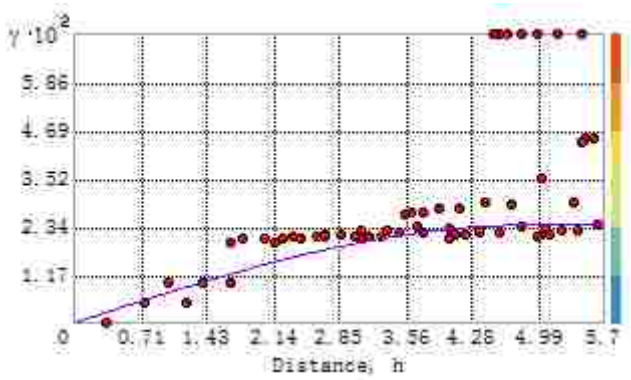

Figure 14 Curve of Variogram Function for 1/16ft Radius

Based on this curve, the spherical effect model was selected. The other parameters of the spherical model are as following:

Mean Value: 0.32004

Major range: 4.87849

3.3.3.2 Displaying the Images

Using the above parameters in the three softwares, the estimated thickness distribution was computed. Given on these files, the four figures are developed from the packages. Every software gives a contour map of the distribution and Surfer yields a 3-D distribution map.

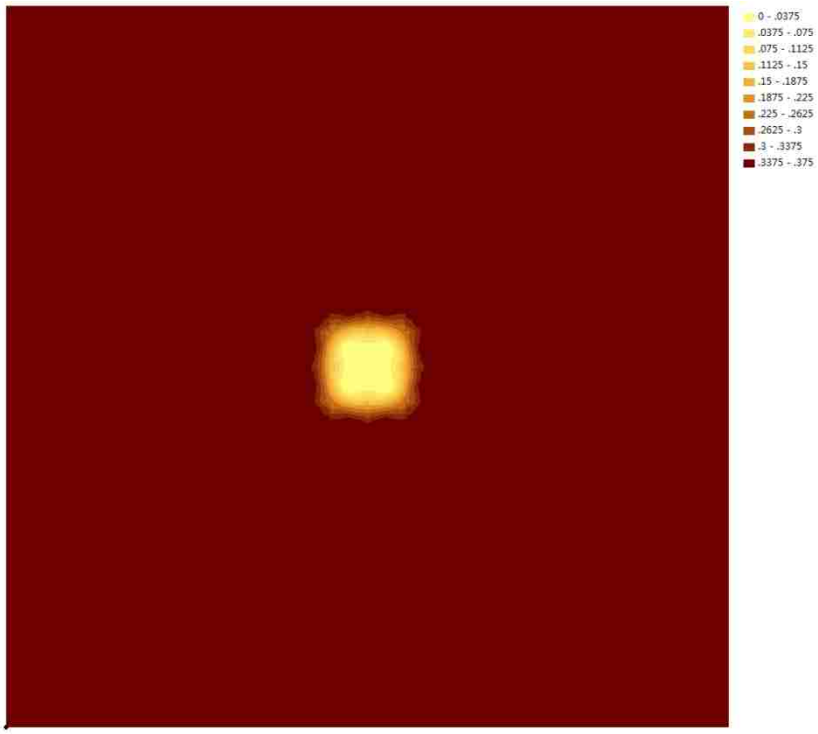

Figure 15 Contour of Thickness Distribution from ArcGIS for 1/16ft Radius

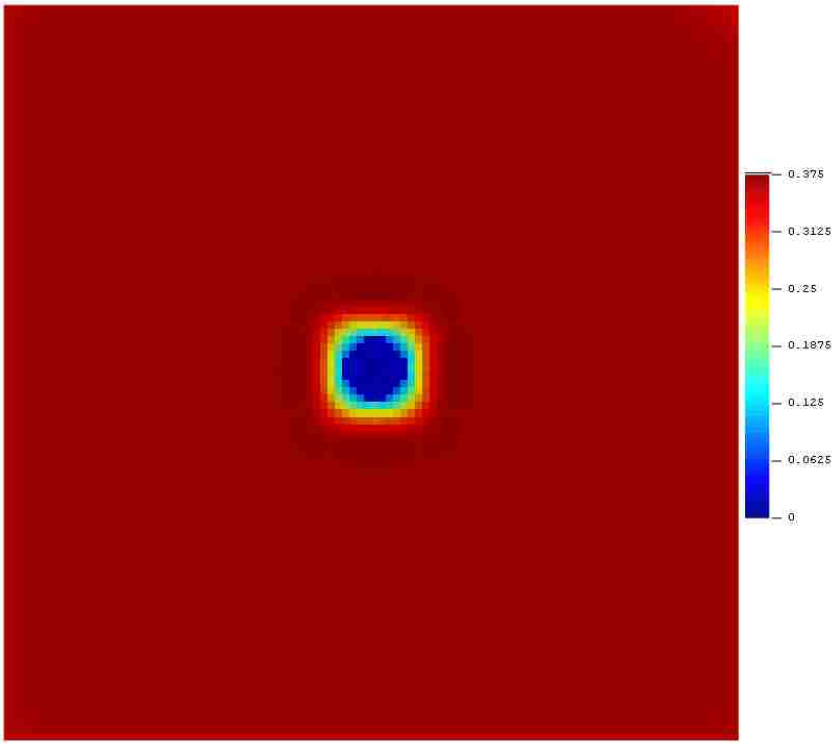

Figure 16 Contour of Thickness Distribution from Surfer for 1/16ft Radius

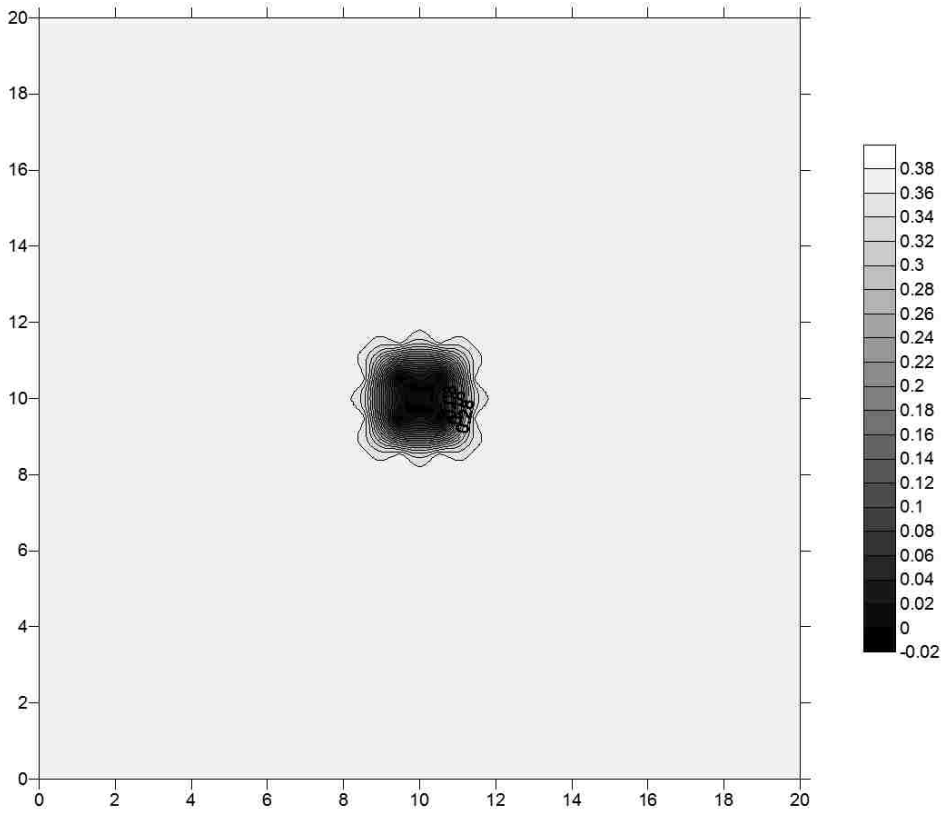

Figure 17 Contour of Thickness Distribution from SGeMS for 1/8ft Radius

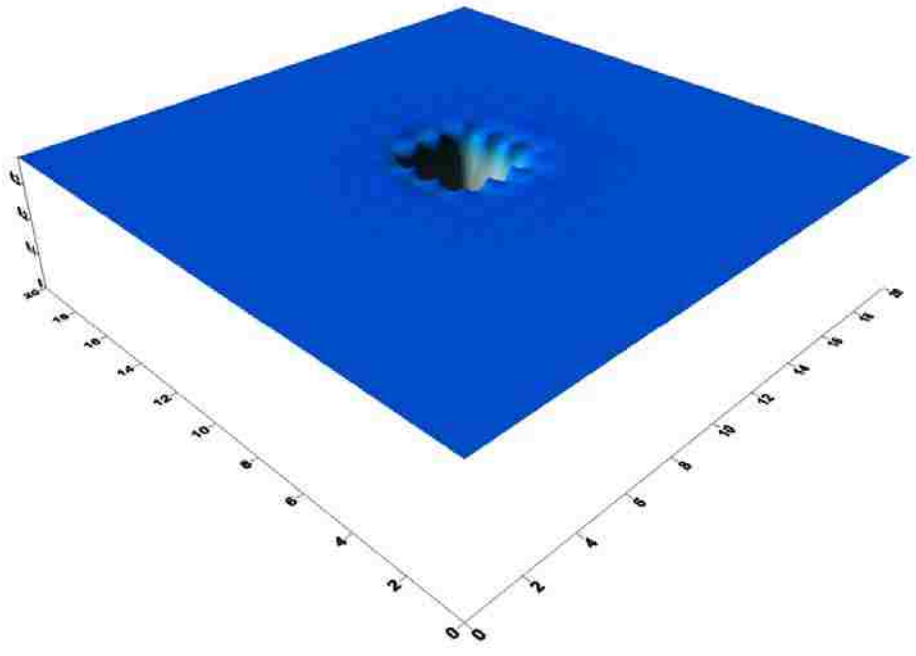

Figure 18 3-D Model of Thickness Distribution from SGeMS for 1/8ft Radius

The damage effect ration (φ) was measured from Figures 15, 16 and 17 by Image Pro-Plus, and Table 1 contains the results.

3.3.4 Simulation of All Four Holes with 1/2ft Radius

3.3.4.1 Setting up Parameters

Figure 19 shows the curve of variogram function for 1/2ft radius by ArcGIS.

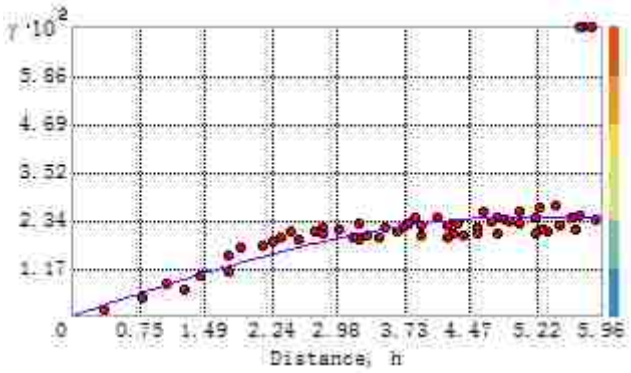

Figure 19 Curve of Variogram Function for 1/2ft Radius

Based on this curve, the spherical effect model was selected. The other parameters of the spherical model are as following:

Mean Value: 0.32283

Major range: 5.05648

3.3.4.2 Displaying the Images

Using the above parameters in the three softwares, the estimated thickness distribution was computed. Given on these files, the four figures are developed from the packages. Every software gives a contour map of the distribution and Surfer yields a 3-D distribution map.

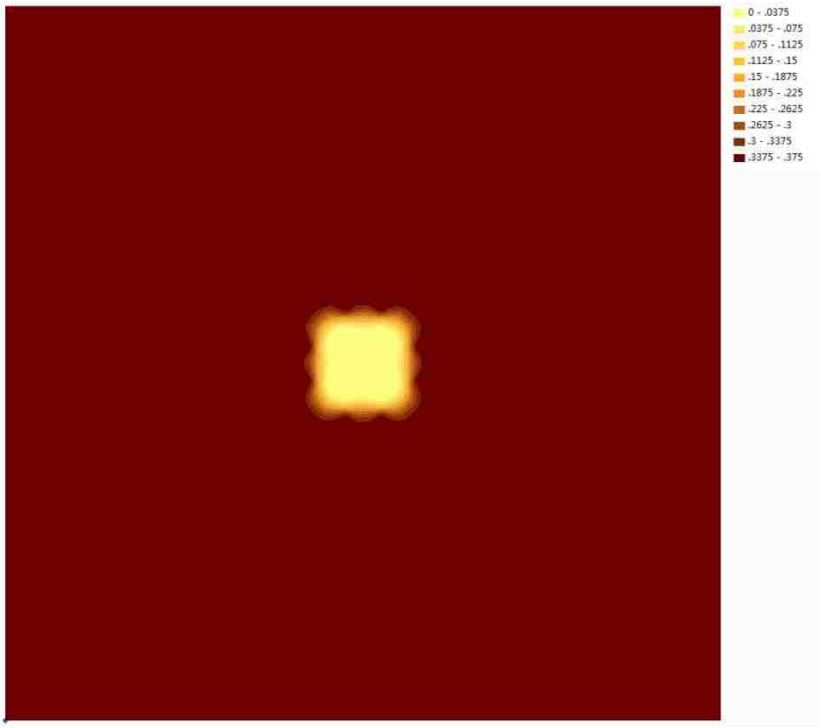

Figure 20 Contour of Thickness Distribution from ArcGIS for 1/2ft Radius

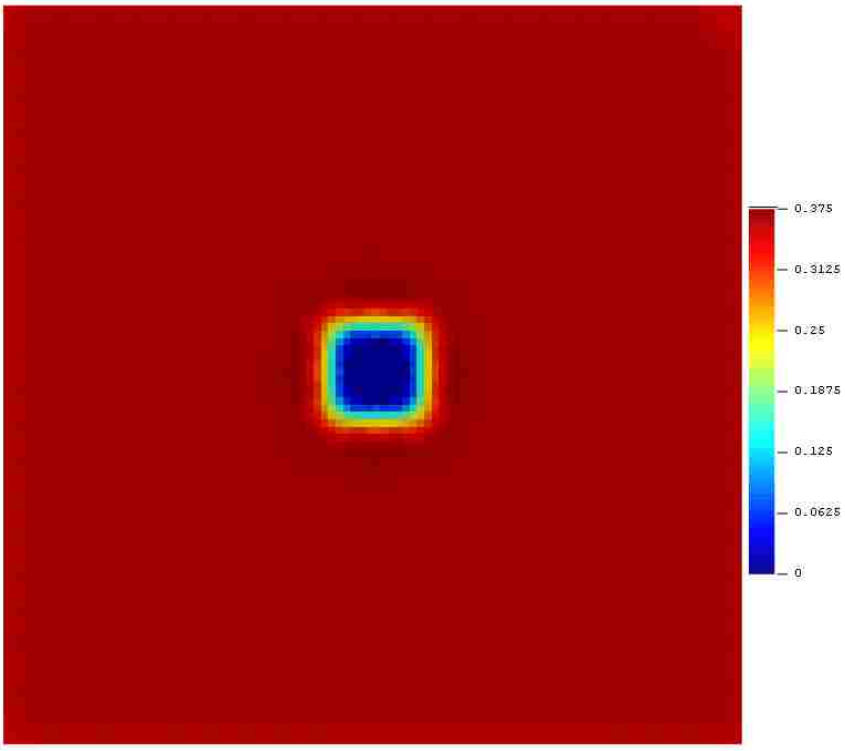

Figure 21 Contour of Thickness Distribution from Surfer for 1/2ft Radius

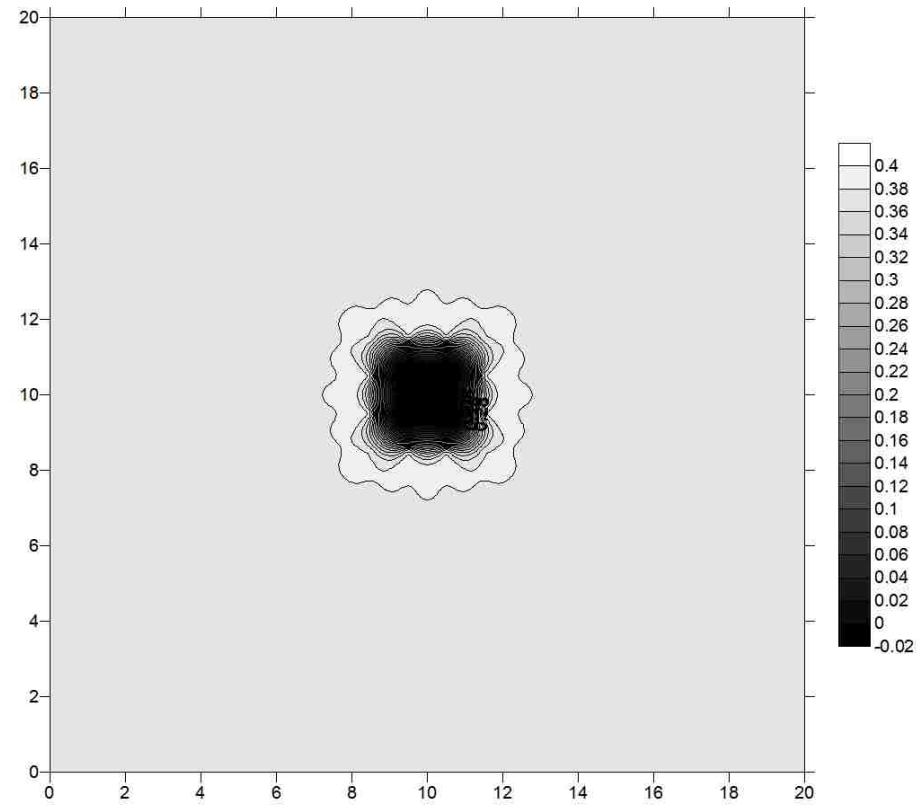

Figure 22 Contour of Thickness Distribution from SGeMS for 1/2ft Radius

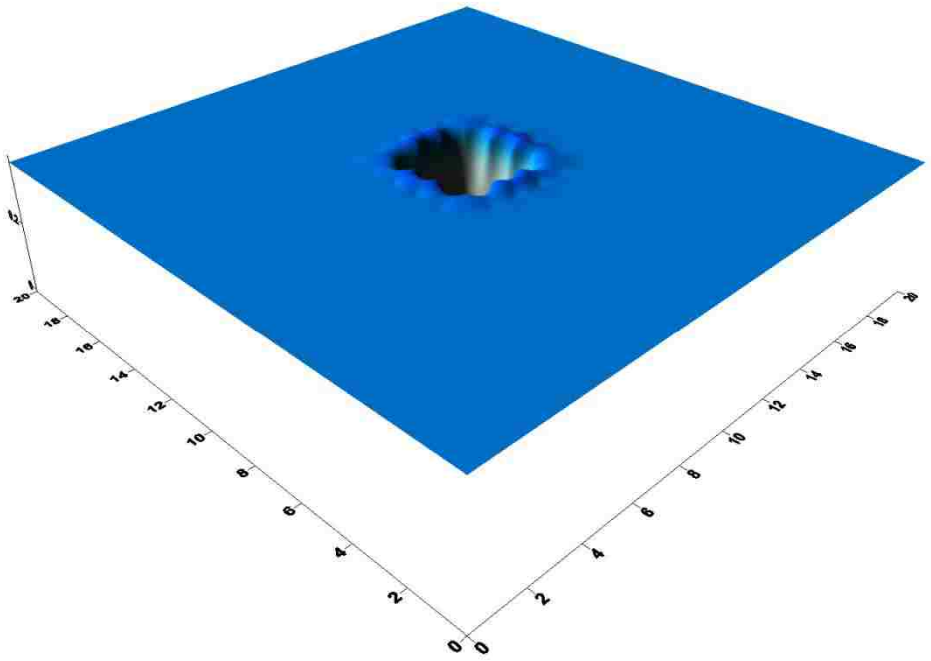

Figure 23 3-D Model of Thickness Distribution from SGeMS for 1/2ft Radius

The damage effect ration (φ) was measured from Figures 20, 21 and 22 by Image Pro-Plus, and Table 1 contains the results.

3.3.5 Simulation of All Four Holes with 1ft Radius

3.3.5.1 Setting up Parameters

Figure 24 shows the curve of variogram function for 1ft radius by ArcGIS.

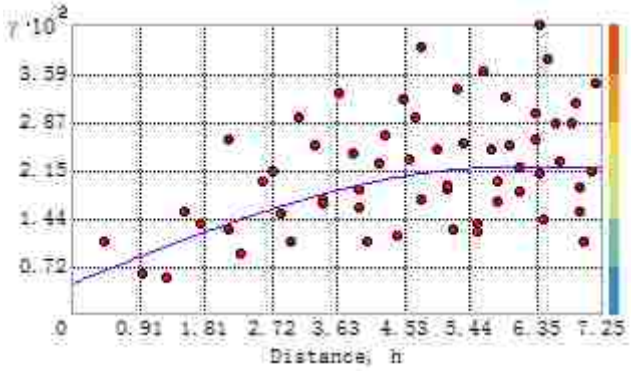

Figure 24 Curve of Variogram Function for 1ft Radius

Based on this curve, the spherical effect model was selected. The other parameters of the spherical model are as following:

Mean Value: 0.32854

Major range: 5.97872

3.3.4.2 Displaying the Images

Using the above parameters in the three softwares, the estimated thickness distribution was computed. Given on these files, the four figures are developed from the packages. Every software gives a contour map of the distribution and Surfer yields a 3-D distribution map.

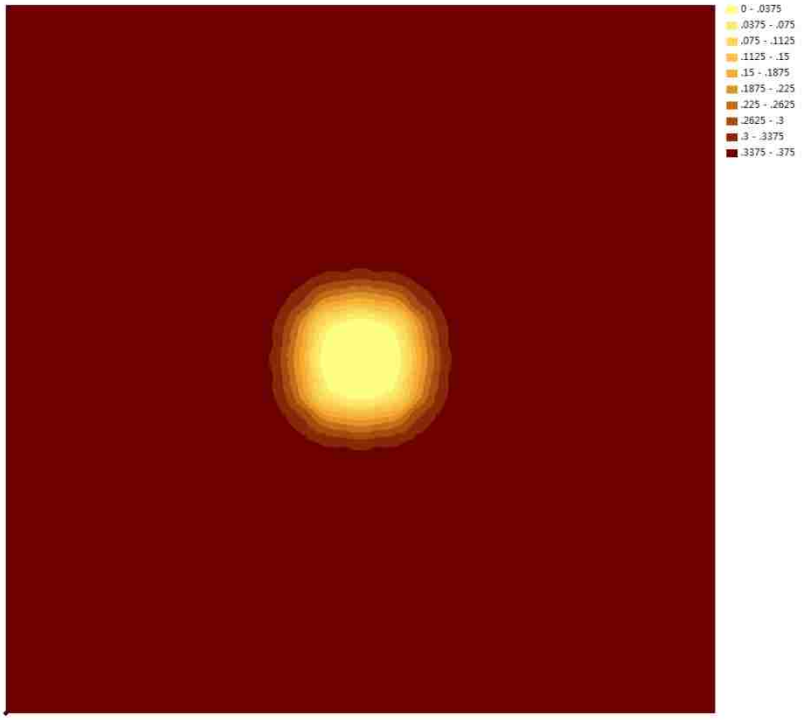

Figure 25 Contour of Thickness Distribution from ArcGIS for 1ft Radius

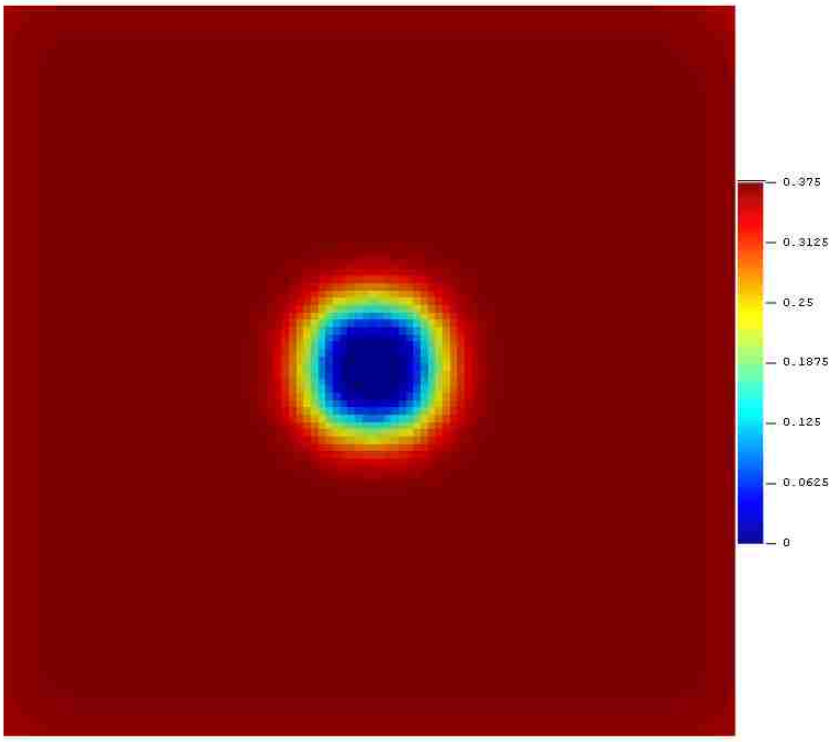

Figure 26 Contour of Thickness Distribution from Surfer for 1ft Radius

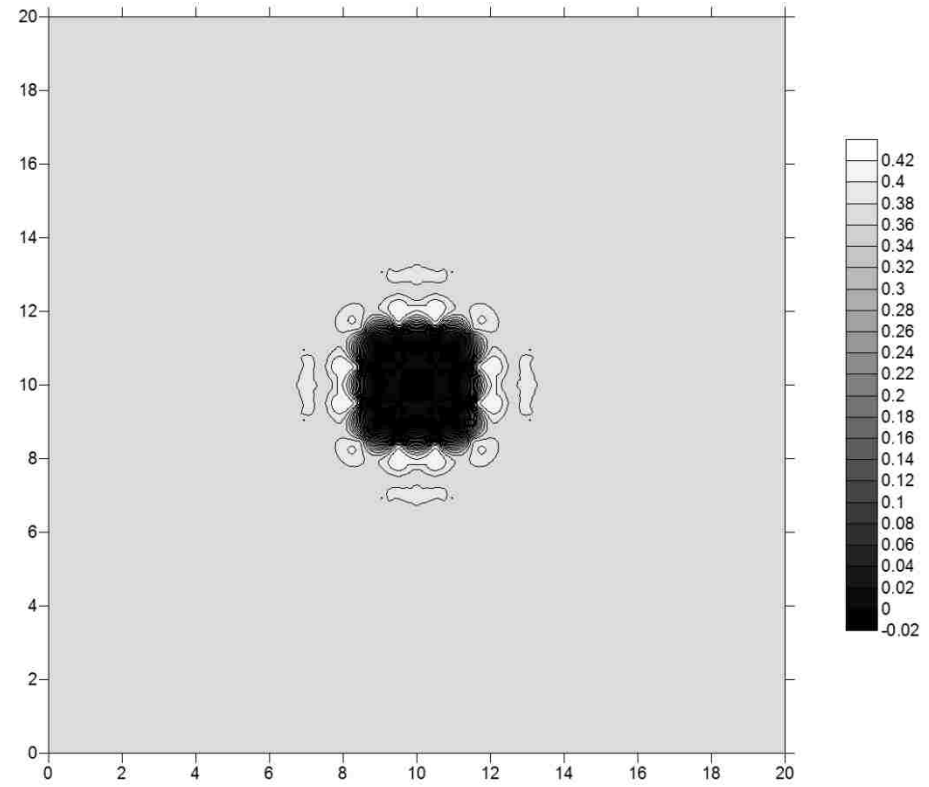

Figure 27 Contour of Thickness Distribution from SGeMS for 1ft Radius

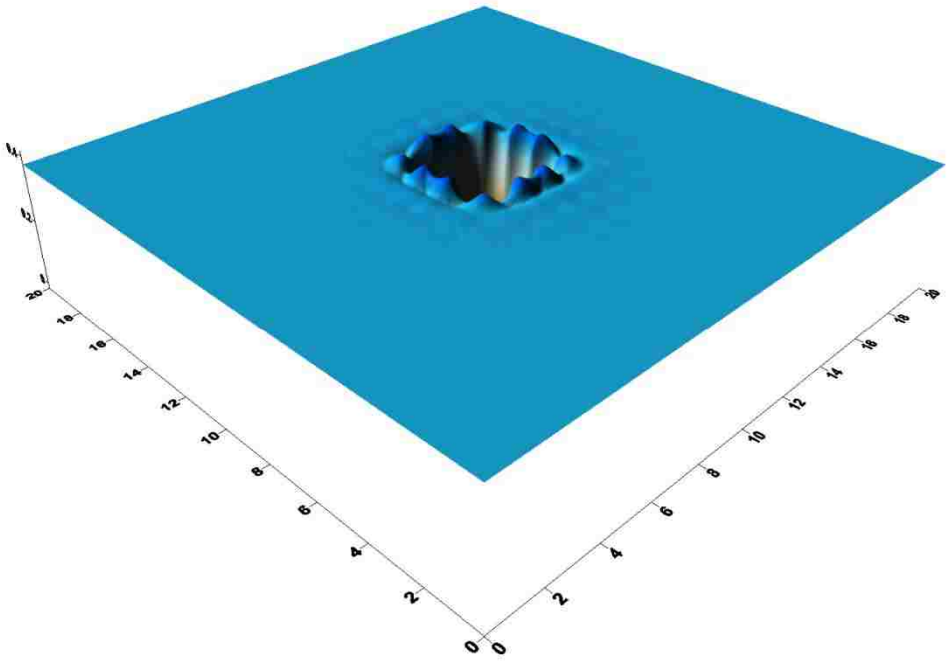

Figure 28 3-D Model of Thickness Distribution from SGeMS for 1ft Radius

The damage effect ration (φ) was measured from Figures 25, 26 and 27 by Image Pro-Plus, and Table 1 contains the results.

3.3.5 Conclusion of Radius Effect

By combined the above gained damage effect ratio, **Table 1,** it is easy to illustrate the damage effect ratio which is effect by changing radius.

Radius (feet)	**Damage Effect Ratio (φ): (%)**		
	ArcGIS	**Surfer**	**SGeMS**
1/16	0.99	0.97	1.41
1/8	1.06	1.07	1.67
1/2	1.52	1.56	2.22
1	2.50	2.27	3.06

Table 1 Damage Effect Ratio with different radii

Comparing the Table 1 and with the contour figures, the conclusions about the effect of the radius are stated as following:

(1) The damage effect ratio tends to increase with increasing radius, and the relationship between them is non-linear.

(2) The holes only affect their adjacent areas.

(3) The patterns of damage areas from the three softwares are similar. For the damage effect ratio, the difference between ArcGIS and Surfer is little, but the difference is significant for SGeMS, because the accuracy of SGeMS is lower than the other two softwares.

3.4 Effect of Different Radii Holes Arrangement

3.4.1 Creating Data Set

The condition for this section is that the 20ft × 20ft plate is divided into 400 cells with 396 cells represented by the nominal thickness of 0.375in which located in the center of these cells. The other 4 cells contain holes which have known damage. Each of the holes have a different radius, chosen from 1/16ft, 1/8ft, 1/2ft and 1ft. Considering symmetry, the four holes could have 3 different arrangements, which start from the left-low corner of a square as clockwise order:

(1) 1ft → 1/8ft → 1/16ft → 1/2ft;

(2) 1ft → 1/16ft → 1/2ft → 1/8ft;

(3) 1ft → 1/16ft → 1/8ft → 1/2ft;

3.4.2 Simulation of the First Holes Arrangement

3.4.2.1 Setting up Parameters

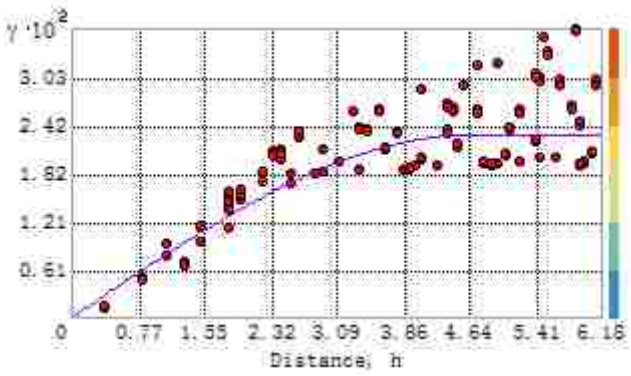

Figure 29 Curve of Variogram Function for the First Arrangement

Based on this curve, the spherical effect model was selected. The other

parameters of the spherical model are as following:

Mean Value: 0.32213

Major range: 4.68727

3.4.2.2 Displaying the Images

Using the above parameters in the three softwares, the estimated thickness distribution was computed. Given on these files, the four figures are developed from the packages. Every software gives a contour map of the distribution and Surfer yields a 3-D distribution map.

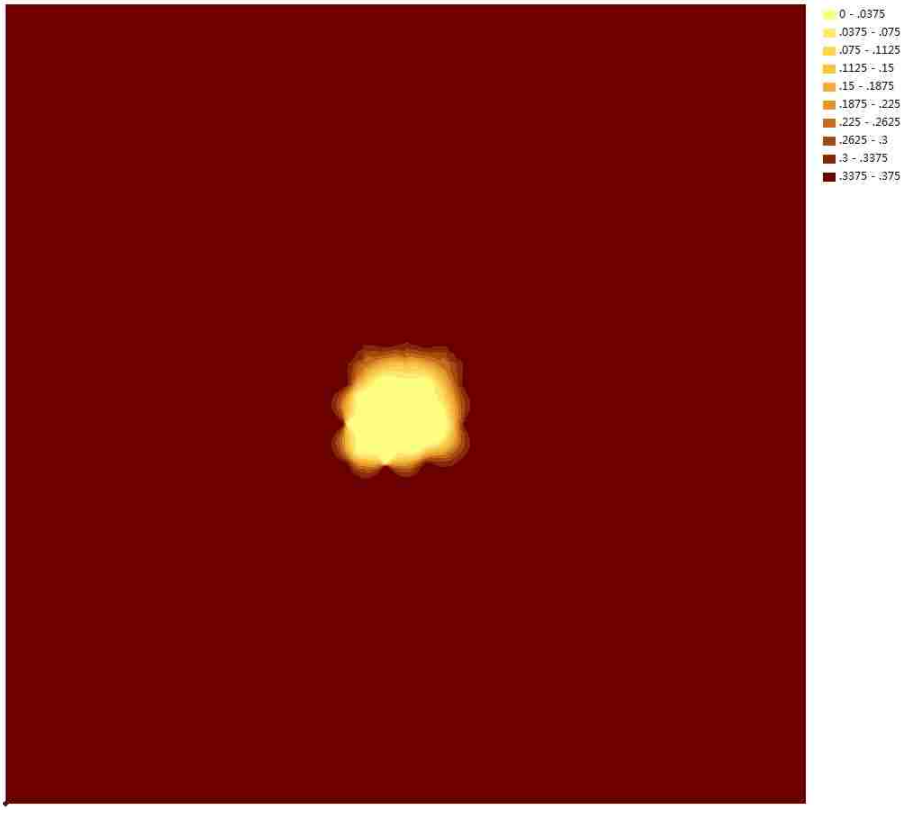

Figure 30 Contour of Thickness Distribution from ArcGIS for the First Arrangement

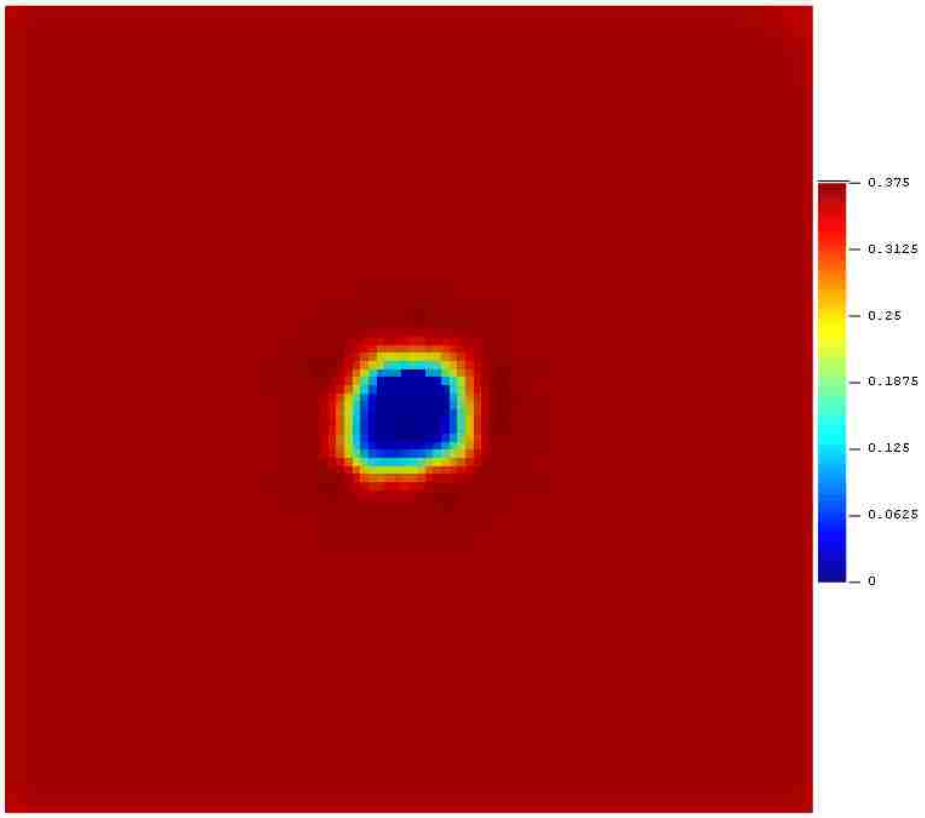

Figure 31 Contour of Thickness Distribution from Surfer for the First Arrangement

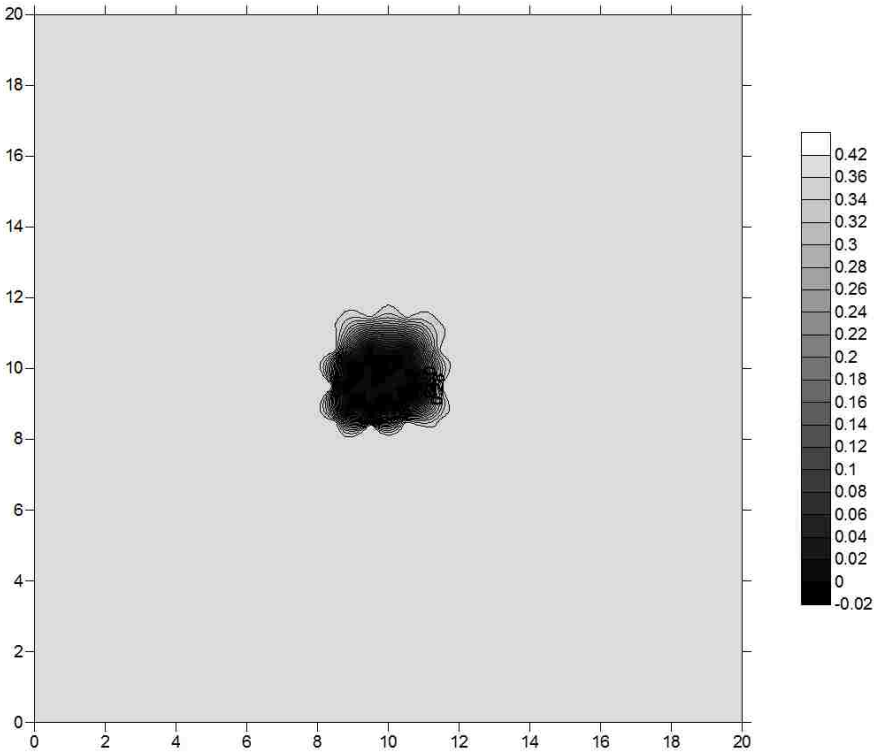

Figure 32 Contour of Thickness Distribution from SGeMS for the First Arrangement

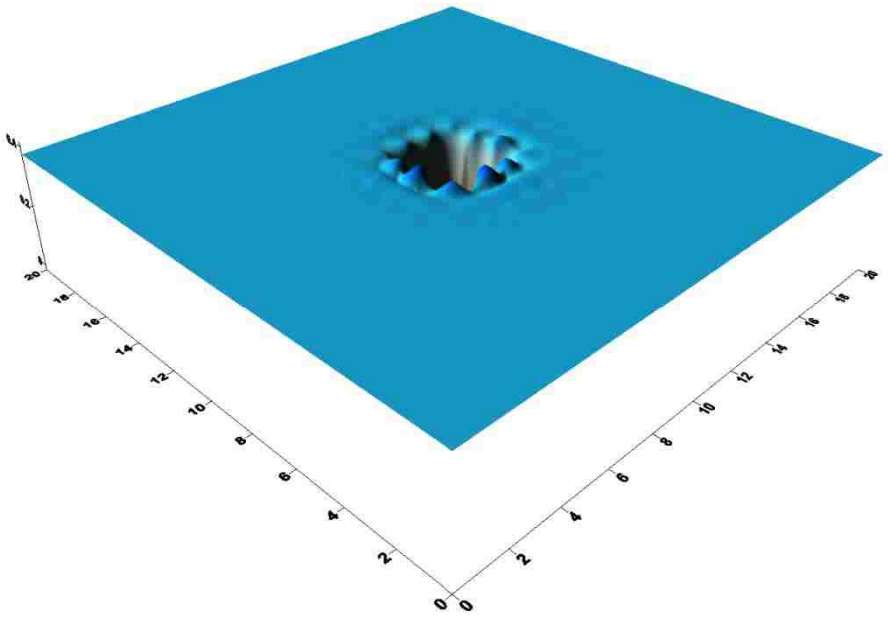

Figure 33 3-D Model of Thickness Distribution from SGeMS for the First Arrangement

The damage effect ration (φ) was measured from Figures 30, 31 and 32 by Image Pro-Plus, and Table 2 contains the results.

3.4.3 Simulation of the Second Holes Arrangement

3.4.3.1 Setting up Parameters

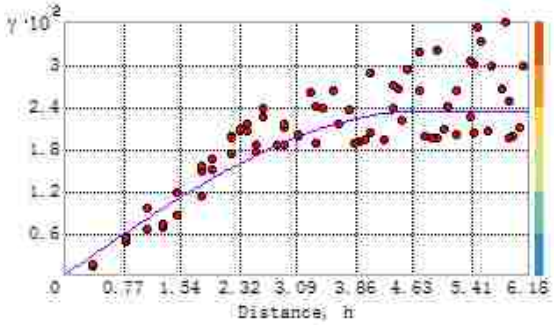

Figure 34 Curve of Variogram Function for the Second Arrangement

Based on this curve, the spherical effect model was selected. The other parameters of the spherical model are as following:

Mean Value: 0.32143 Major range: 4.72251

3.4.3.2 Displaying the Images

Using the above parameters in the three softwares, the estimated thickness distribution was computed. Given on these files, the four figures are developed from the packages. Every software gives a contour map of the distribution and Surfer yields a 3-D distribution map.

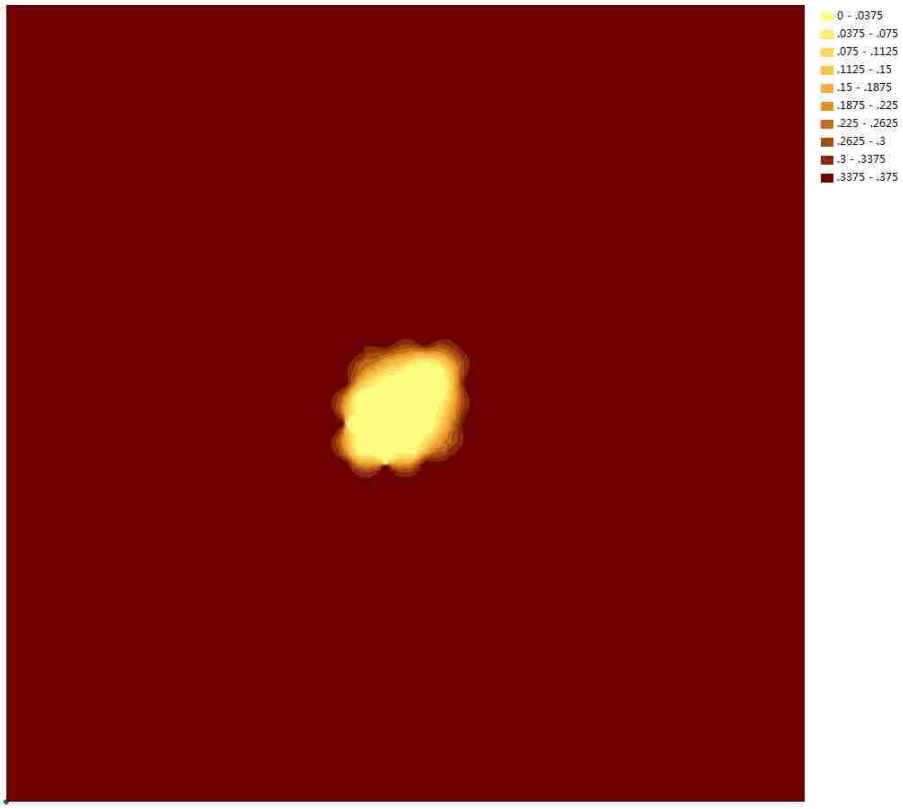

Figure 35 Contour of Thickness Distribution from ArcGIS for the Second Arrangement

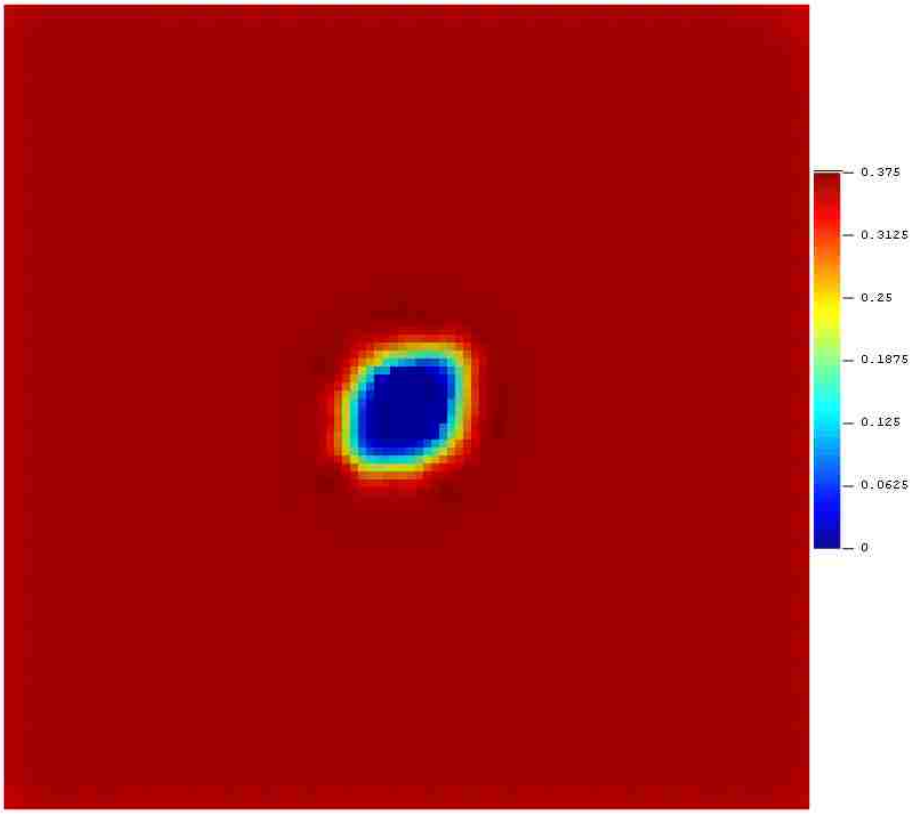

Figure 36 Contour of Thickness Distribution from Surfer for the Second Arrangement

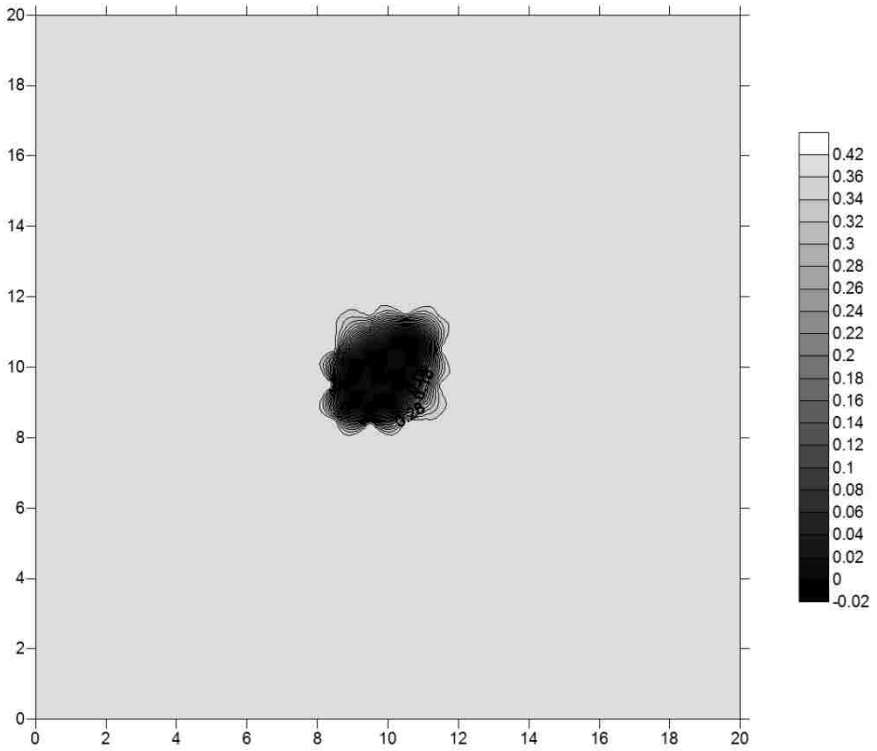

Figure 37 Contour of Thickness Distribution from SGeMS for the Second Arrangement

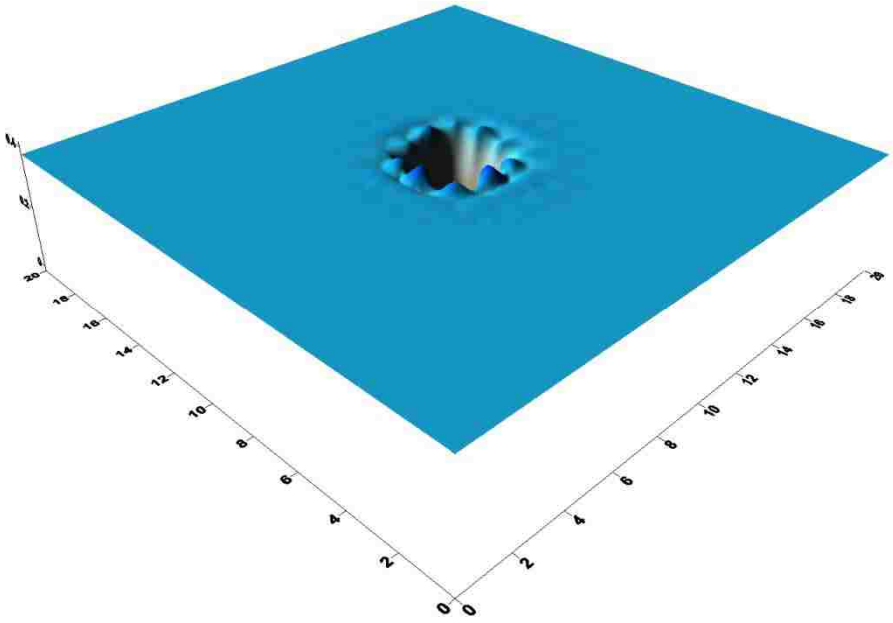

Figure 38 3-D Model of Thickness Distribution from SGeMS for the Second Arrangement

The damage effect ration (φ) was measured from Figures 35, 36 and 37 by Image Pro-Plus, and Table 2 contains the results.

3.4.4 Simulation of the Third Holes Arrangement

3.4.4.1 Setting up Parameters

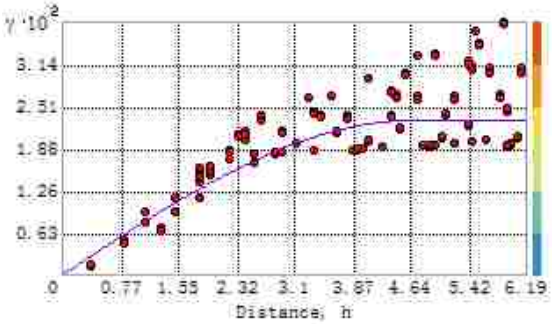

Figure 39 Curve of Variogram Function for the Third Arrangement

Based on this curve, the spherical effect model was selected. The other parameters of the spherical model are as following:

Mean Value: 0.32213 Major range: 4.68911

3.4.4.2 Displaying the Images

Using the above parameters in the three softwares, the estimated thickness distribution was computed. Given on these files, the four figures are developed from the packages. Every software gives a contour map of the distribution and Surfer yields a 3-D distribution map.

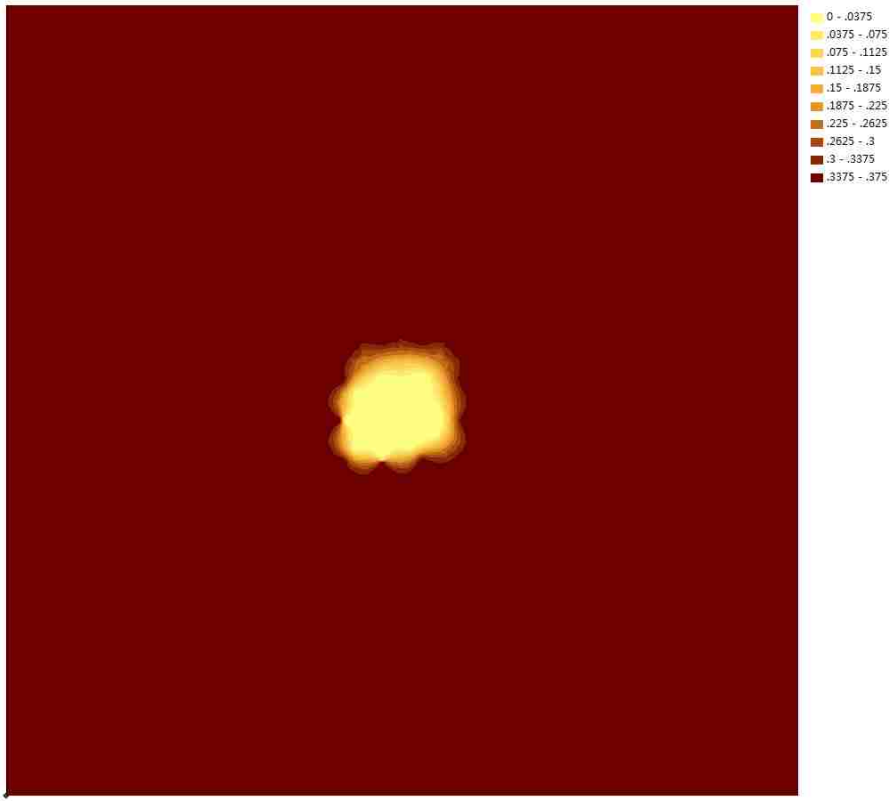

Figure 40 Contour of Thickness Distribution from ArcGIS for the Third Arrangement

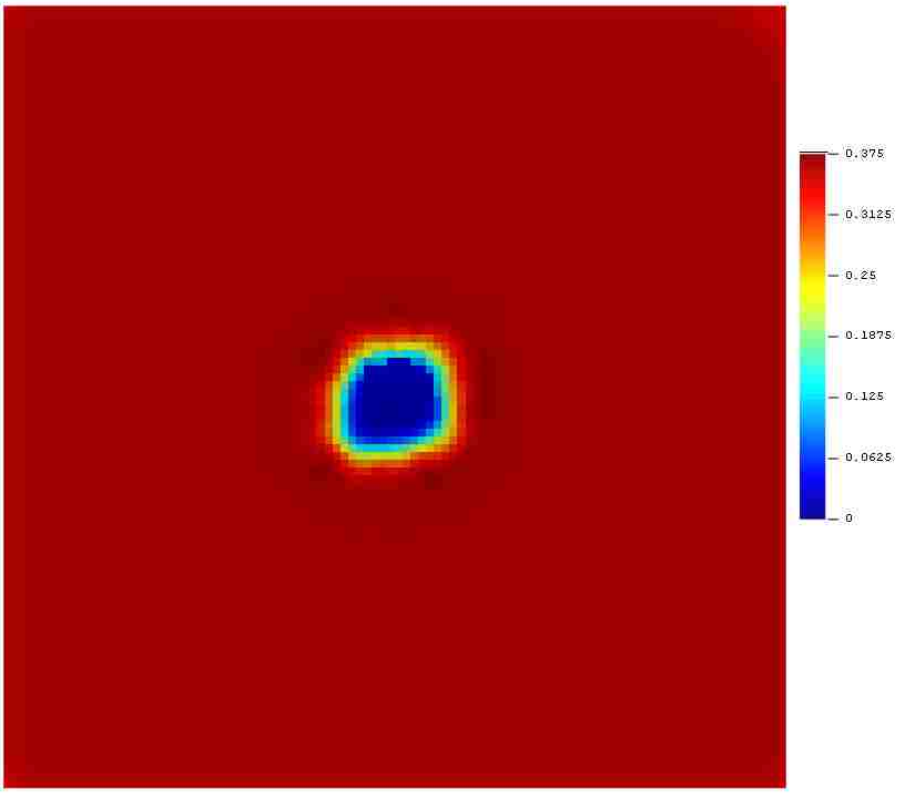

Figure 41 Contour of Thickness Distribution from Surfer for the Third Arrangement

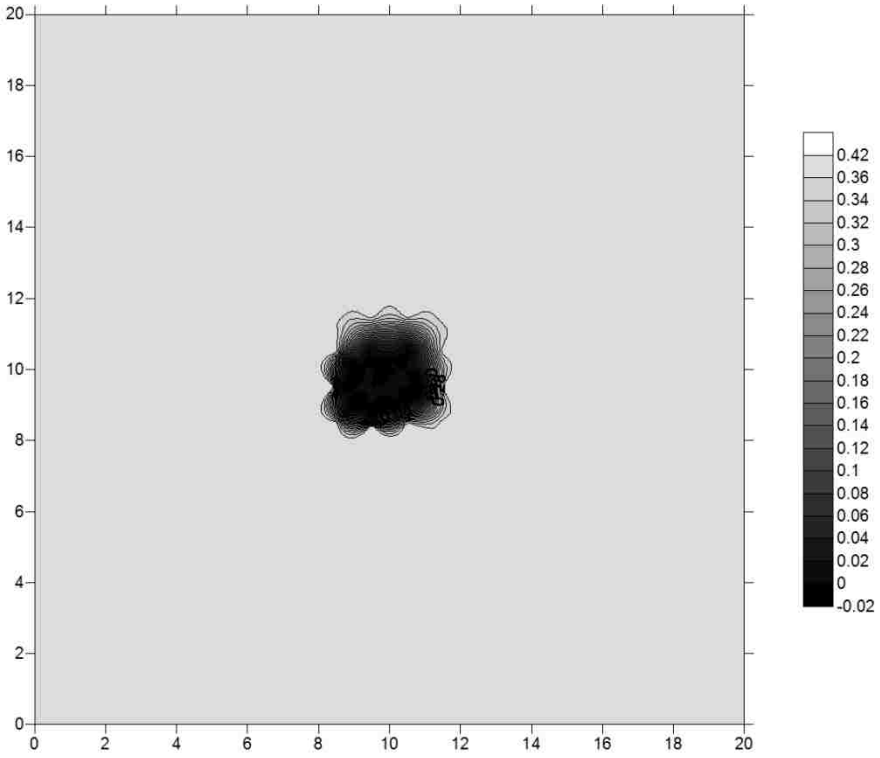

Figure 42 Contour of Thickness Distribution from SGeMS for the Third Arrangement

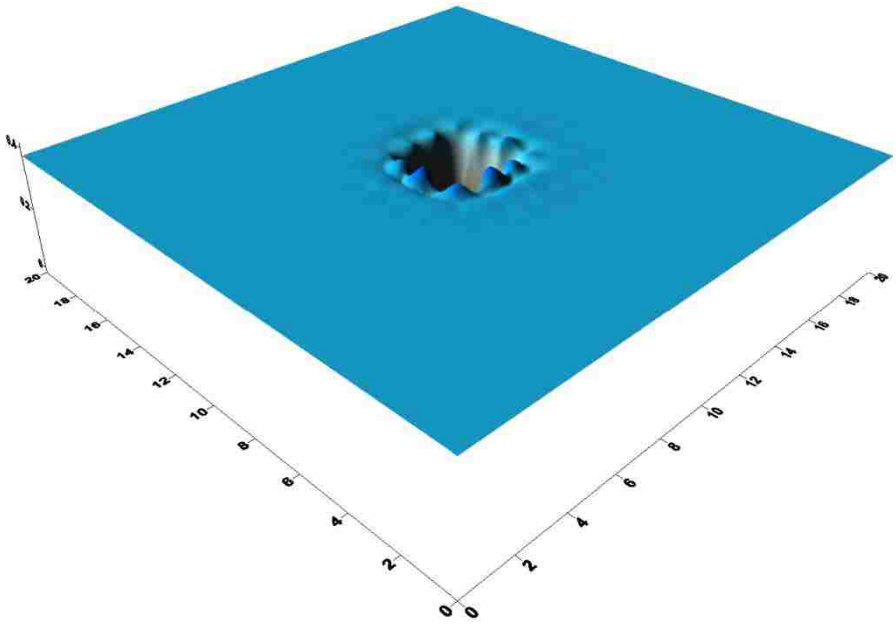

Figure 43 3-D Model of Thickness Distribution from SGeMS for the Third Arrangement

The damage effect ration (φ) was measured from Figures 40, 41 and 42 by Image Pro-Plus, and Table 2 contains the results.

3.4.5 Conclusion of Different Holes Arrangement Effect

By combined the above gained damage effect ratio, **Table 2** is easy to illustrate the damage effect ratio from changing arrangement of holes with different radii.

Different Holes Arrangements (clockwise)	**Damage Effect Ratio (φ): (%)**		
	ArcGIS	**Surfer**	**SGeMS**
1ft → 1/8ft → 1/16ft → 1/2ft	1.53	1.55	1.85
1ft → 1/16ft → 1/2ft → 1/8ft	1.57	1.60	1.94
1ft → 1/16ft → 1/8ft → 1/2ft	1.53	1.56	1.87

Table 2 Damage Effect Ratio with Different Radii Holes Arrangement

Using the Table 2 and the above figures, the conclusions about the radius effect

are stated as following:

(1) The various radius holes arrangements cause more damage than that indicated in Table 1, but the effect is small between the different cases.

(2) The damage effect ratio tends to increase with the increasing distance between the two adjacent holes whose radii are the largest and the next largest. That means the damage effect ratio for the two holes whose radii are the largest and the next largest are adjacent is larger than those are located in the diagonal.

3.5 Effect of Different Distance between Holes

3.5.1 Creating Data Set

The circumstance of this part is that the 20ft × 20ft plate is divided into 400 cells, and 396 are represented by a single point located in the center, and 4 cells near the center of the plate contain damage. The thicknesses of the 396 points are 0.375 in. The other 4 cells have known damage. These simulations will consider the effect of different distances between two adjacent holes varied from 1ft, 3ft and 5ft.

3.5.2 Simulation of Separation is 3 ft

3.5.2.1 Setting up Parameters

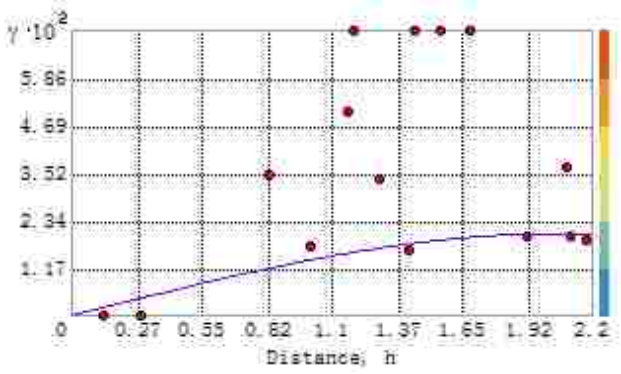

Figure 44 Curve of Variogram Function for Separation is 3ft

Based on this curve, the spherical effect model was selected. The other parameters of the spherical model are as following:

Mean Value: 0.32004

Major range: 2.05927

3.5.2.2 Displaying the Images

Using the above parameters in the three softwares, the estimated thickness distribution was computed. Given on these files, the four figures are developed from the packages. Every software gives a contour map of the distribution and Surfer yields a 3-D distribution map.

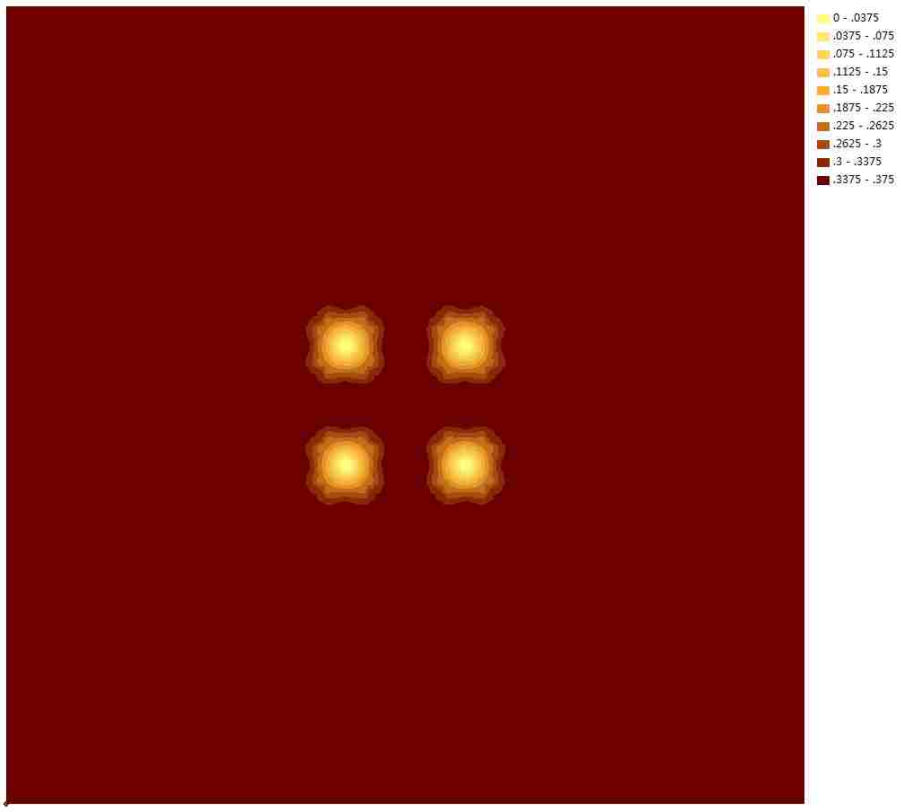

Figure 45 Contour of Thickness Distribution from ArcGIS for Separation is 3ft

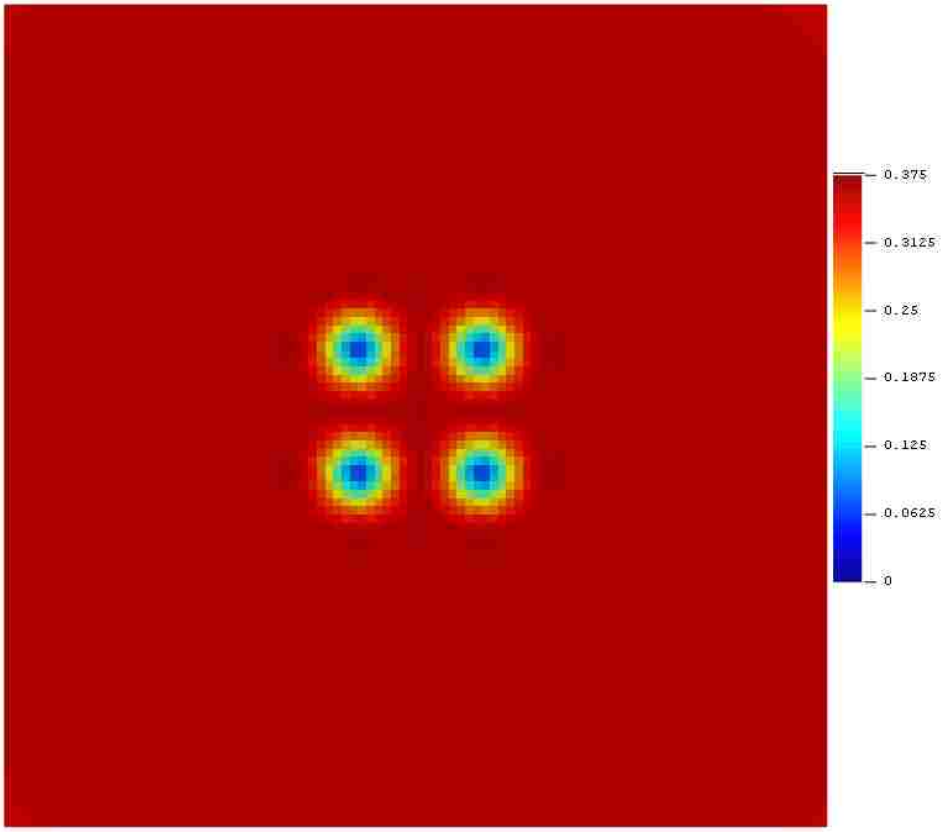

Figure 46 Contour of Thickness Distribution from Surfer for Separation is 3ft

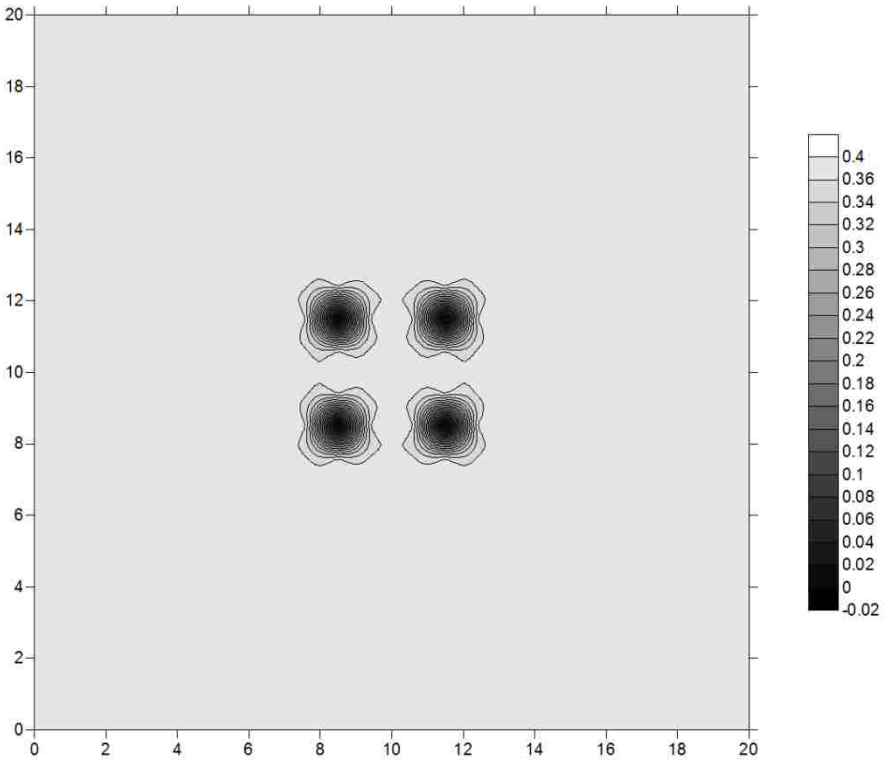

Figure 47 Contour of Thickness Distribution from SGeMS for Separation is 3ft

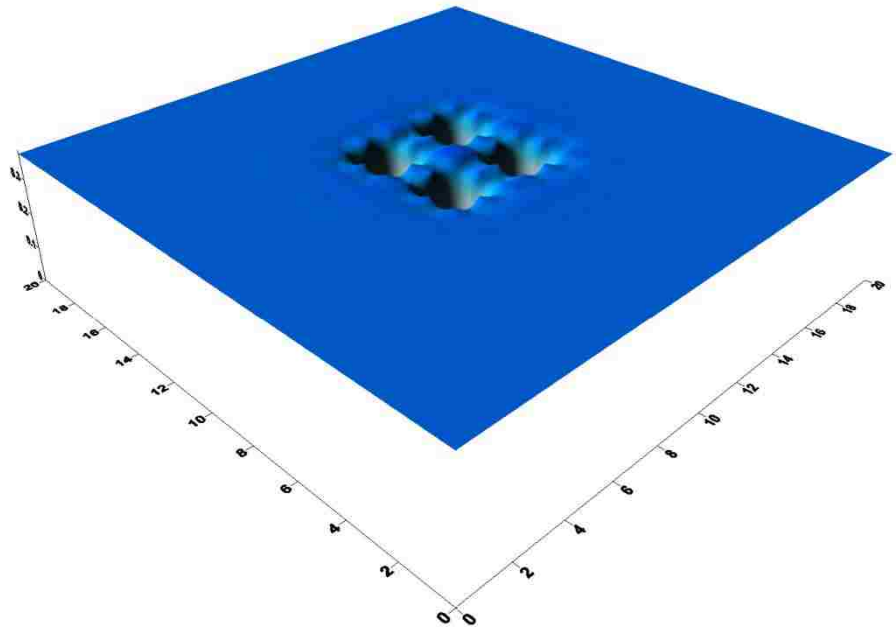

Figure 48 3-D Model of Thickness Distribution from SGeMS for Separation is 3ft

The damage effect ration (φ) was measured from Figures 45, 46 and 47by Image Pro-Plus, and Table 3 contains the results.

3.5.3 Simulation of Separation is 5 ft

3.5.3.1 Setting up Parameters

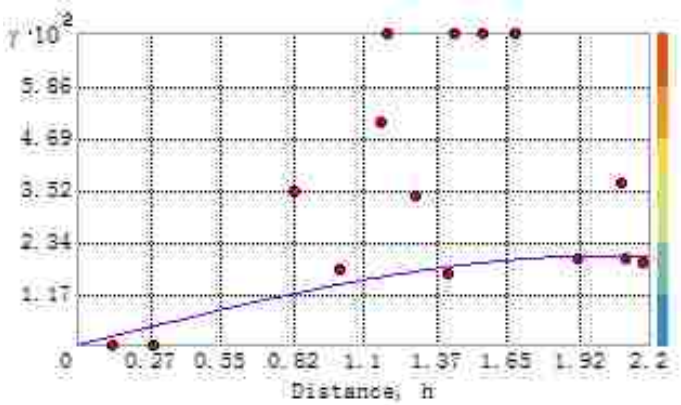

Figure 49 Curve of Variogram Function for Separation is 5ft

Based on this curve, the spherical effect model was selected. The other parameters of the spherical model are as following:

Mean Value: 0.32004

Major range: 2.05927

3.5.3.2 Displaying the Images

Using the above parameters in the three softwares, the estimated thickness distribution was computed. Given on these files, the four figures are developed from the packages. Every software gives a contour map of the distribution and Surfer yields a 3-D distribution map.

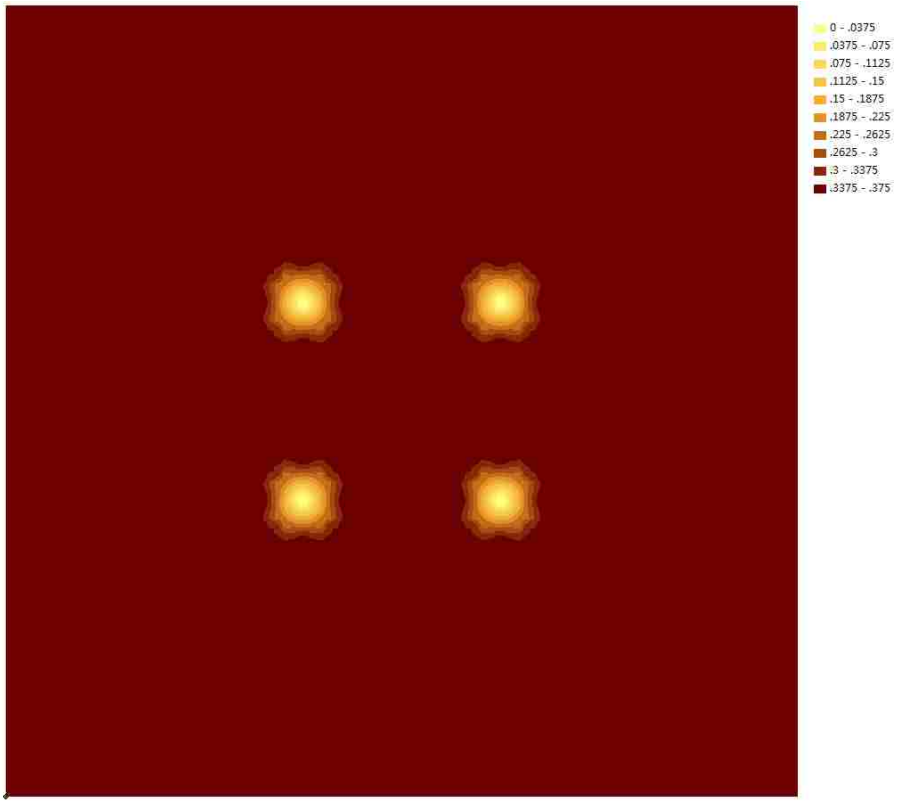

Figure 50 Contour of Thickness Distribution from ArcGIS for Separation is 5ft

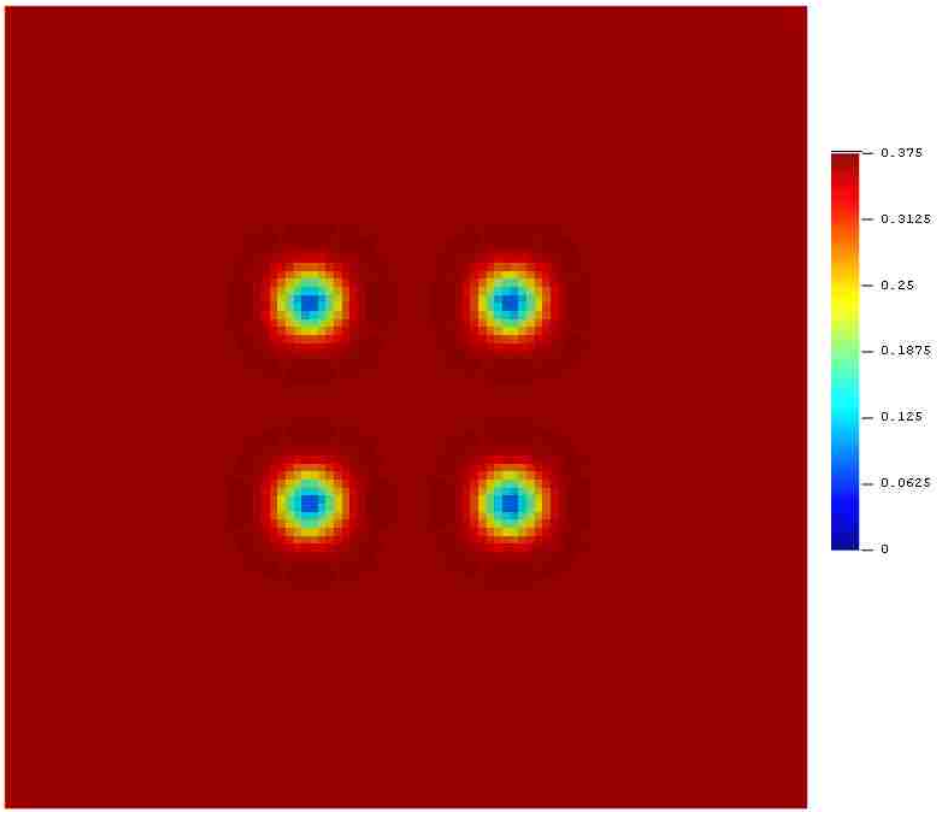

Figure 51 Contour of Thickness Distribution from Surfer for Separation is 5ft

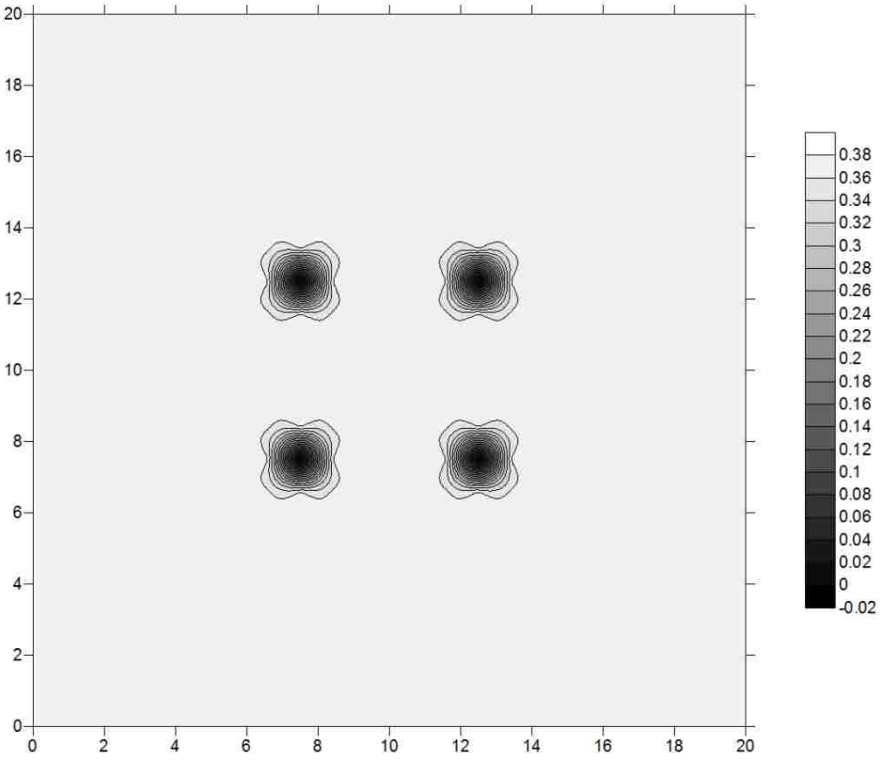

Figure 52 Contour of Thickness Distribution from SGeMS for Separation is 5ft

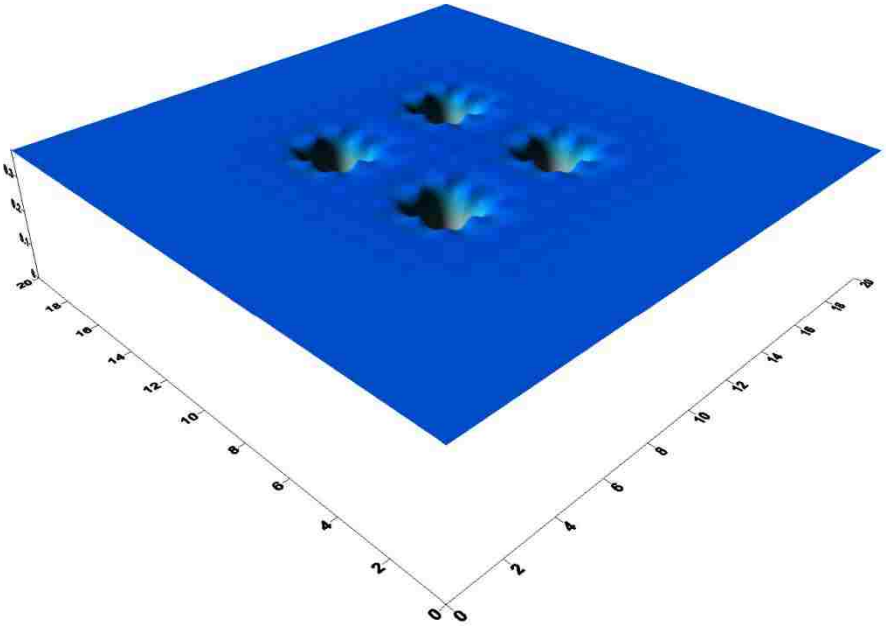

Figure 53 3-D Model of Thickness Distribution from SGeMS for Separation is 5ft

The damage effect ration (φ) was measured from Figures 50, 51 and 52 by Image Pro-Plus, and Table 3 contains the results.

3.5.4 Conclusion of Different Distance between Holes

By combined the above damage effect ratio, **Table 3** is easy to illustrate the damage effect ratio which is caused by changing the distance between the holes.

Different Distances	**Damage Effect Ratio (φ): (%)**		
	ArcGIS	**Surfer**	**SGeMS**
1 ft	0.99	0.97	1.58
3 ft	0.82	0.7	1.78
5ft	0.8	0.71	1.76

Table 3 Damage Effect Ratio with Different Radii Holes Arrangement

Comparing the Table 3 and the above figures, the conclusions are as following:

(1) The damage effect ratio reduces with the increasing separation of the holes. There will be nearly no change when the separation exceeds a certain value, because these holes will not interact with each other after that amount of separation. The relationship between distance and radius will be studied in the following part.

(2) When the distances are 3ft and 5ft, holes will not interact. Thus, every hole only affects its adjacent areas; and the patterns around the holes are similar.

3.6 Effect of Different Patterns of Holes

3.6.1 Creating Data Set

The condition for this section is that the 20ft × 20ft plate is divided into 400 cells

with 396 cells represented by the nominal thickness of 0.375in which are located in the center of these cells. The other 4 cells consisted to a square. There are from 1 to 6 holes which make up patterns are symmetry with the corner of square. The radii of these holes are 1/16ft. These patterns that are considered are shown in Figure 54. Expect that the first 1 point was located in the center of a circle, all the other points were located on a circumference with radius of 1.414ft centered on the center of the pleat. Four hole patterns have been considered in **3.3.2 .**

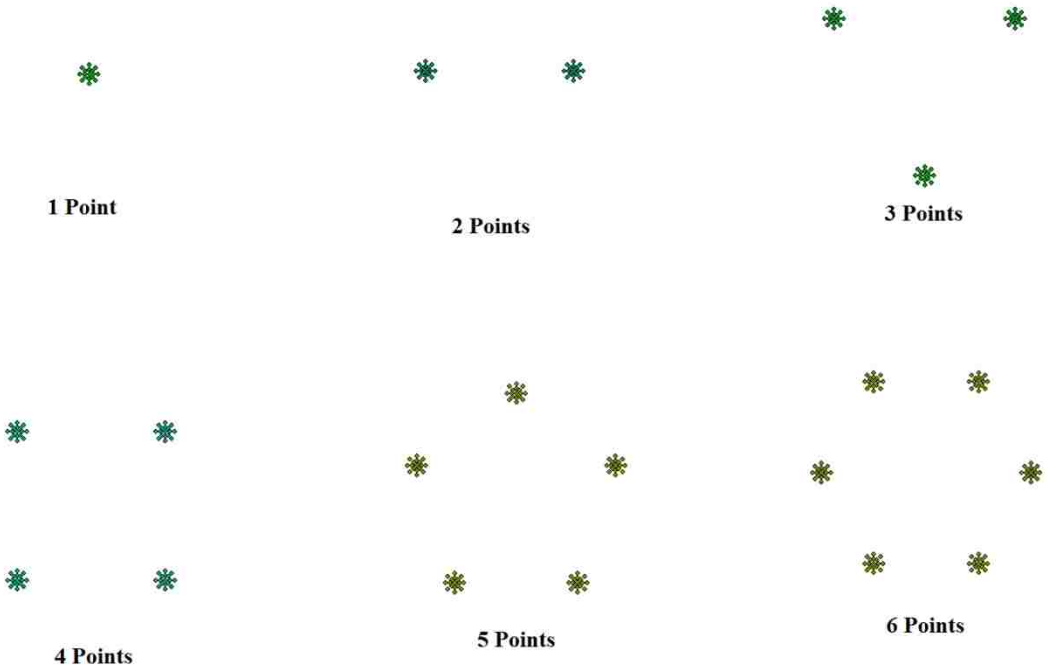

Figure 54 Different Patterns

3.6.2 Simulation of 1 Hole

3.6.2.1 Setting up Parameters

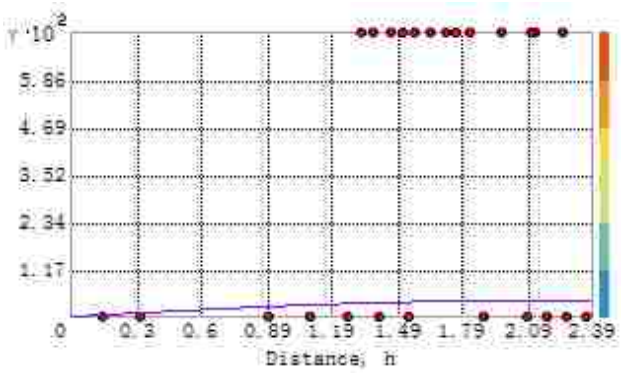

Figure 55 Curve of Variogram Function for 1 Hole

Based on this curve, the spherical effect model was selected. The other parameters of the spherical model are as following:

Mean Value: 0.35956

Major range: 1.97907

3.6.2.2 Displaying the Images

Using the above parameters in the three softwares, the estimated thickness distribution was computed. Given on these files, the four figures are developed from the packages. Every software gives a contour map of the distribution and Surfer yields a 3-D distribution map.

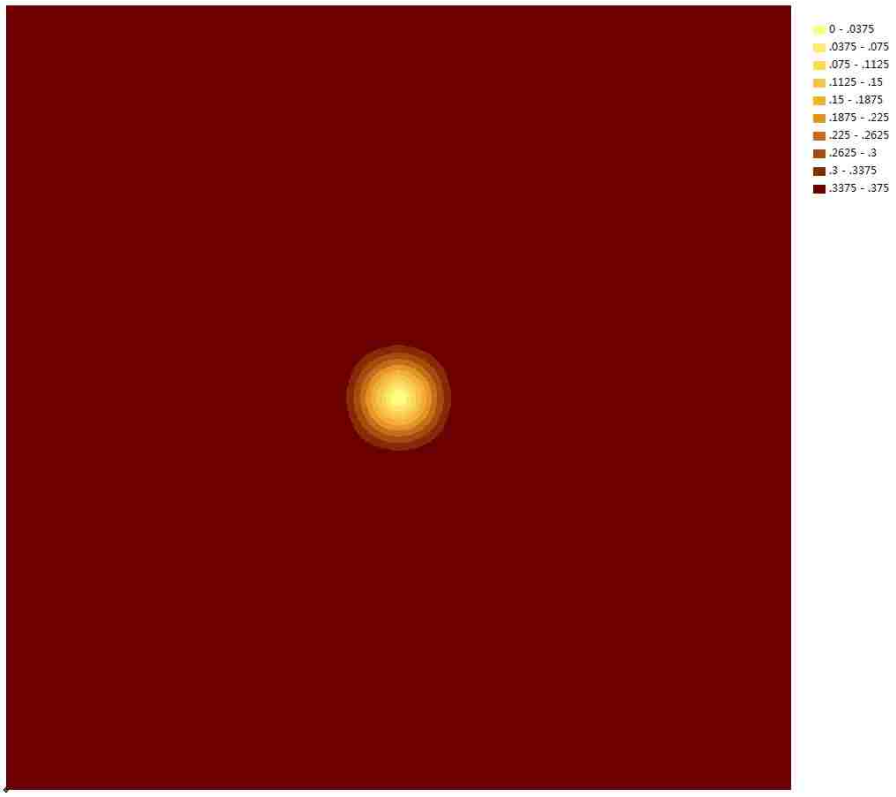

Figure 56 Contour of Thickness Distribution from ArcGIS for 1 Hole

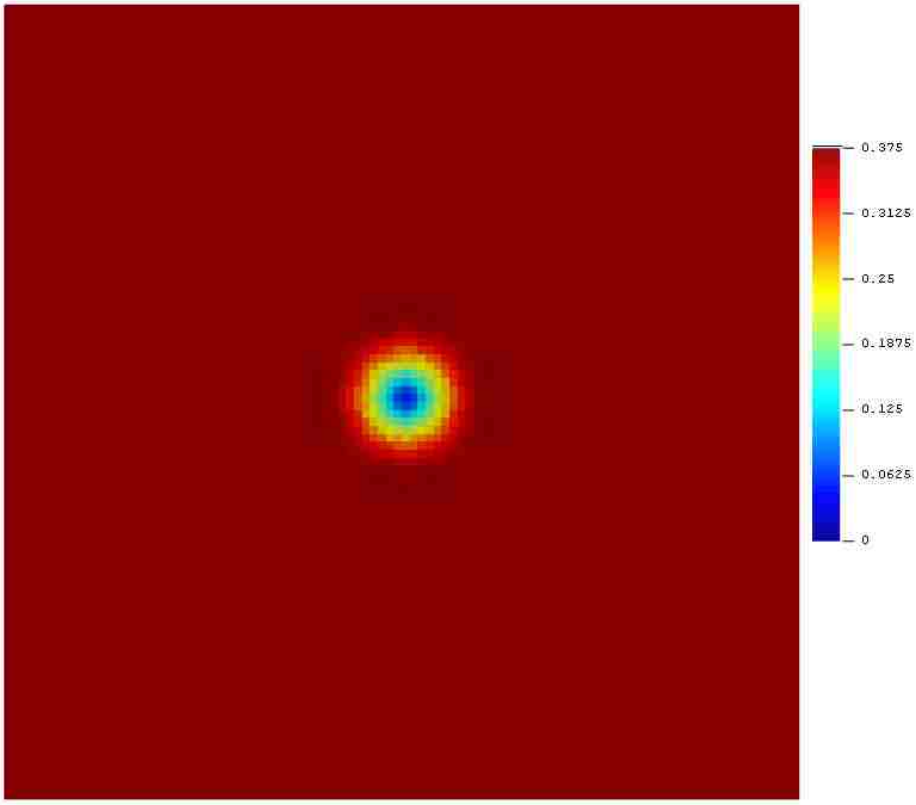

Figure 57 Contour of Thickness Distribution from Surfer for 1 Hole

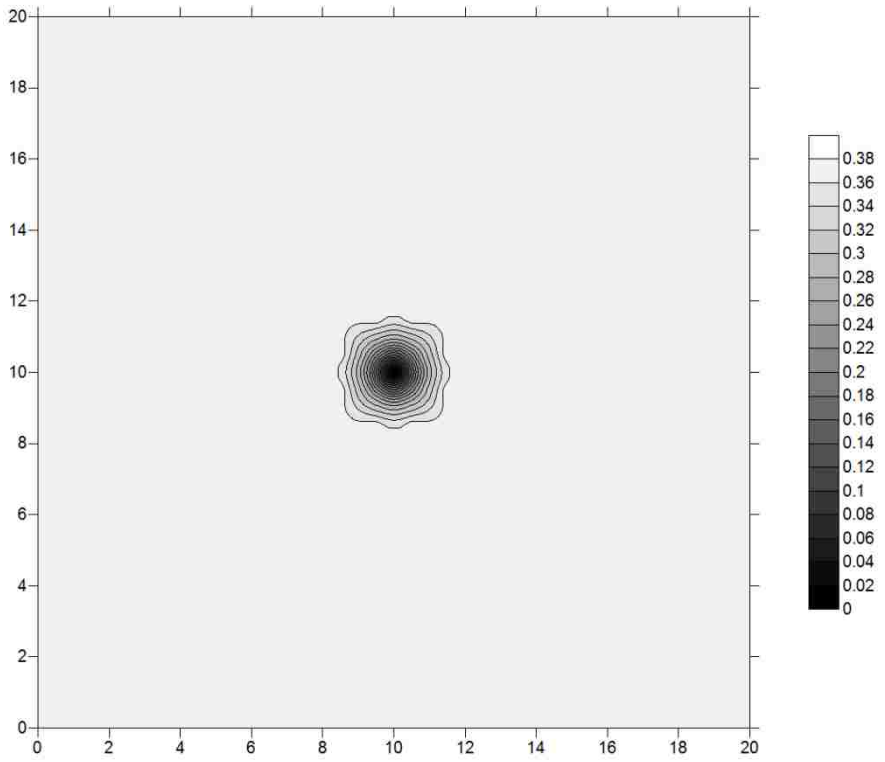

Figure 58 Contour of Thickness Distribution from SGeMS for 1 Hole

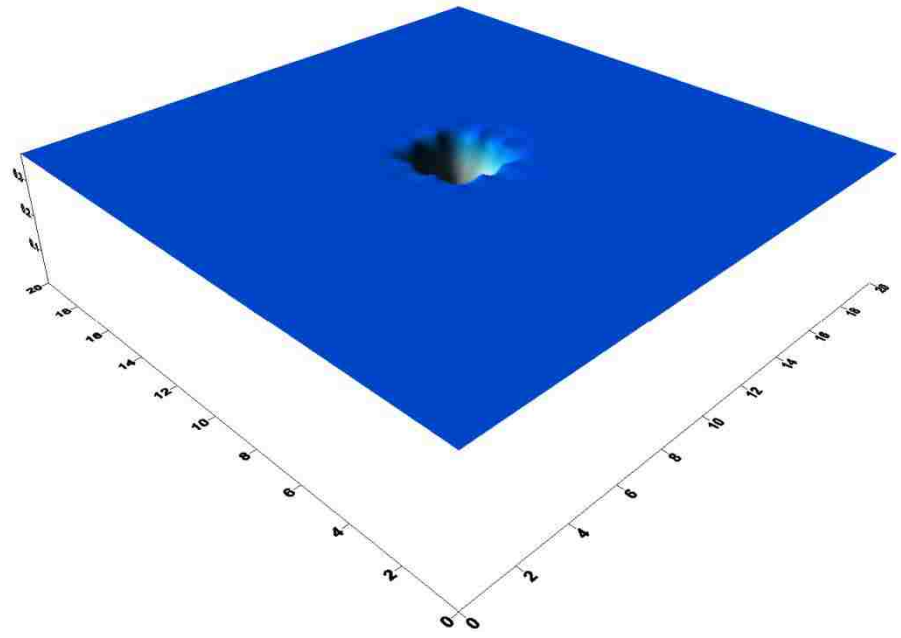

Figure 59 3-D Model of Thickness Distribution from SGeMS for 1 Hole

The damage effect ration (φ) was measured from Figures 56, 57 and 58 by Image Pro-Plus, and Table 4 contains the results.

3.6.3 Simulation of 2 Holes

3.6.3.1 Setting up Parameters

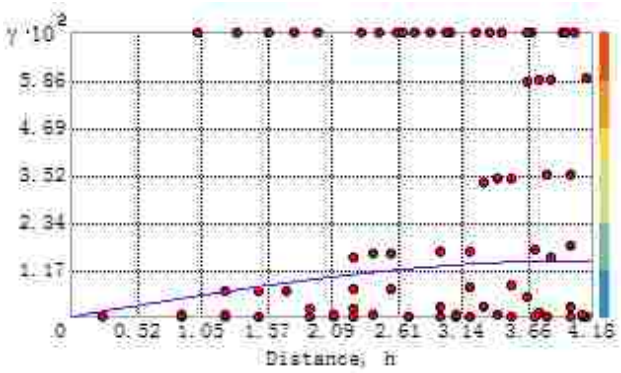

Figure 60 Curve of Variogram Function for 2 Holes

Based on this curve, the spherical effect model was selected. The other parameters of the spherical model are as following:

Mean Value: 0.34535

Major range: 4.00929

3.6.3.2 Displaying the Images

Using the above parameters in the three softwares, the estimated thickness distribution was computed. Given on these files, the four figures are developed from the packages. Every software gives a contour map of the distribution and Surfer yields a 3-D distribution map.

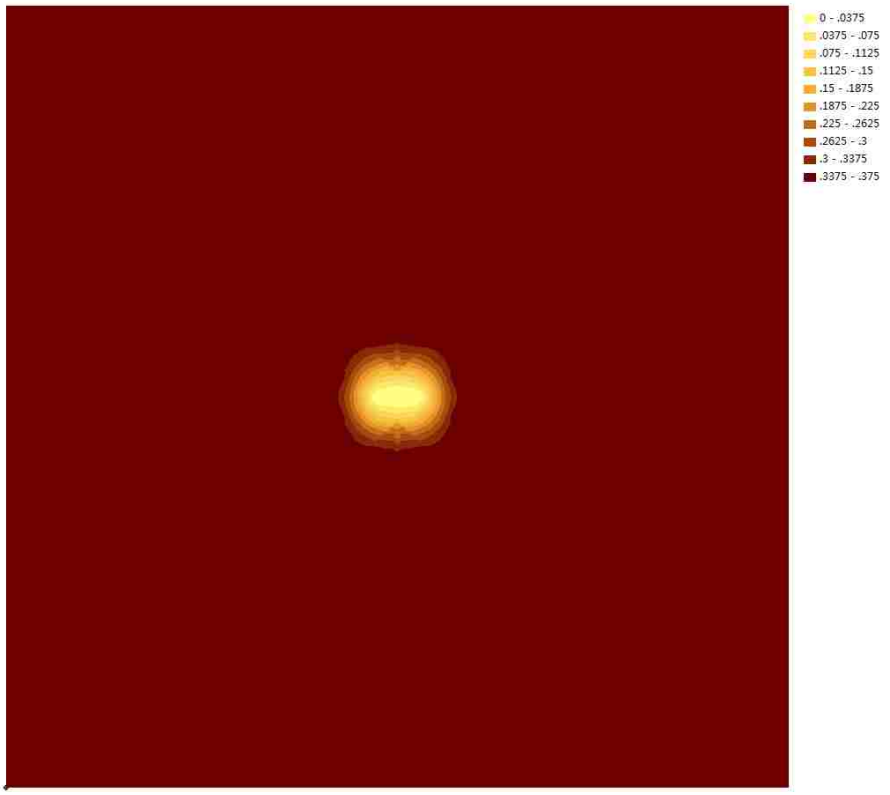

Figure 61 Contour of Thickness Distribution from ArcGIS for 2 Holes

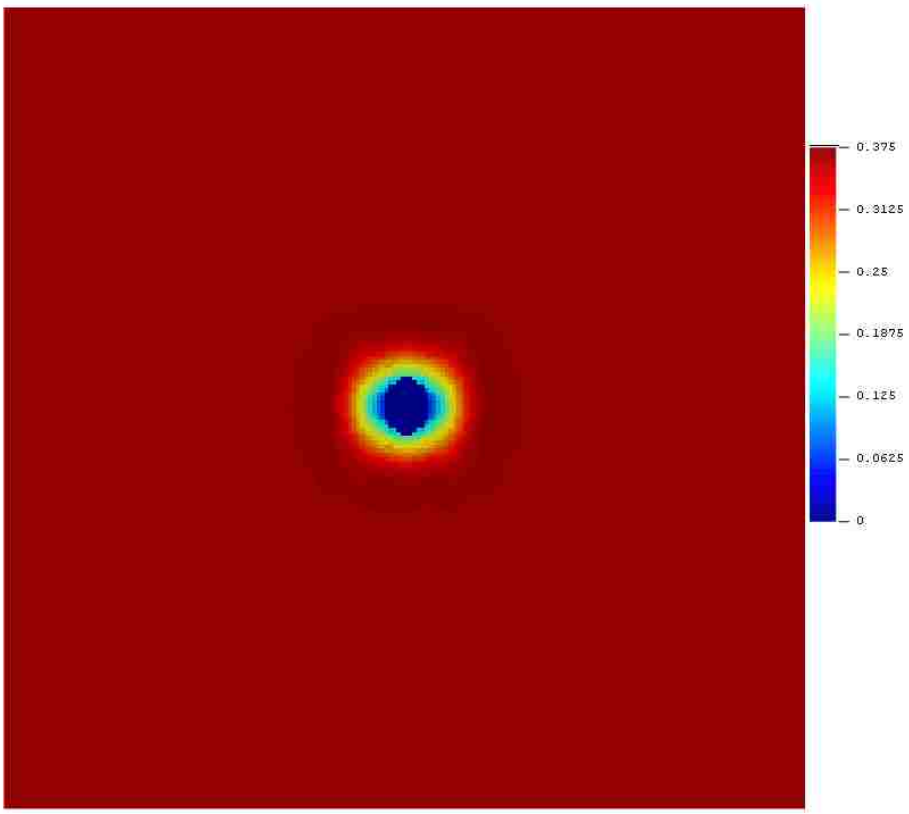

Figure 62 Contour of Thickness Distribution from Surfer for 2 Holes

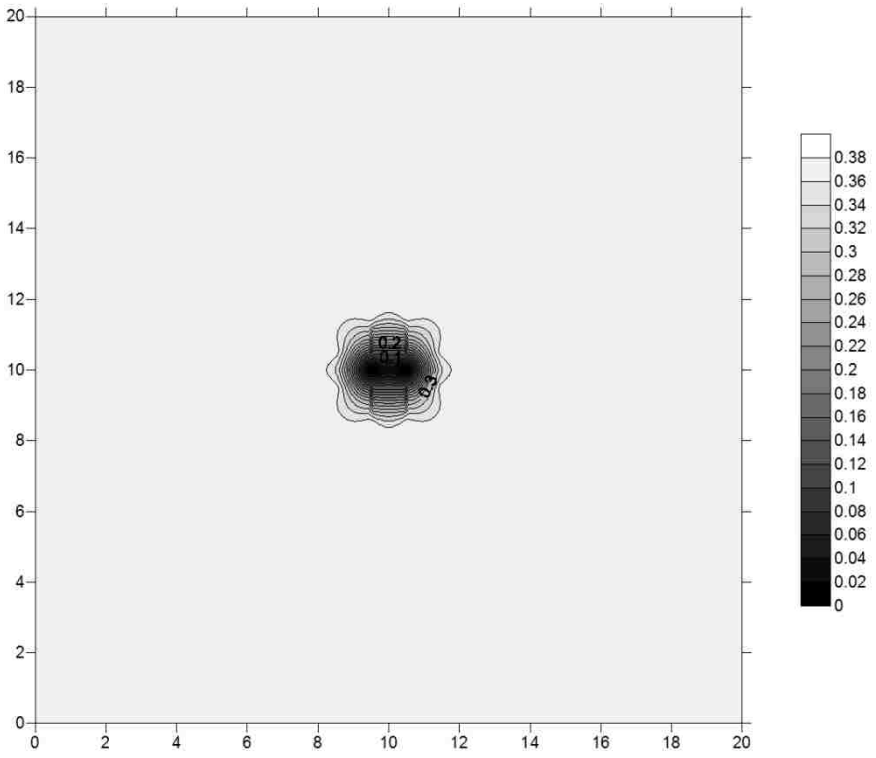

Figure 63 Contour of Thickness Distribution from SGeMS for 2 Holes

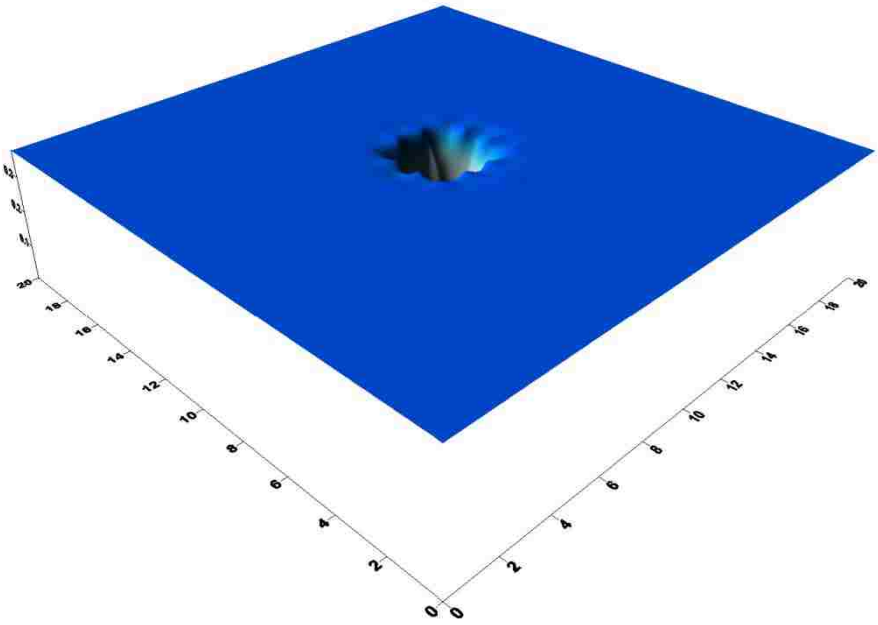

Figure 64 3-D Model of Thickness Distribution from SGeMS for 2 Holes

The damage effect ration (φ) was measured from Figures 61, 62 and 63 by Image Pro-Plus, and Table 4 contains the results.

3.6.4 Simulation of 3 Holes

3.6.4.1 Setting up Parameters

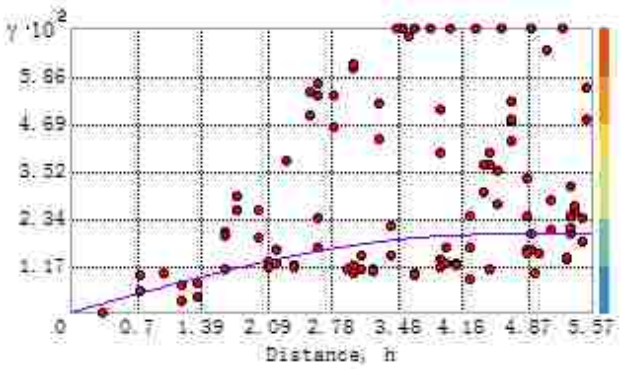

Figure 65 Curve of Variogram Function for 3 Holes

Based on this curve, the spherical effect model was selected. The other parameters of the spherical model are as following:

Mean Value: 0.33221

Major range: 4.44091

3.6.4.2 Displaying the Images

Using the above parameters in the three softwares, the estimated thickness distribution was computed. Given on these files, the four figures are developed from the packages. Every software gives a contour map of the distribution and Surfer yields a 3-D distribution map.

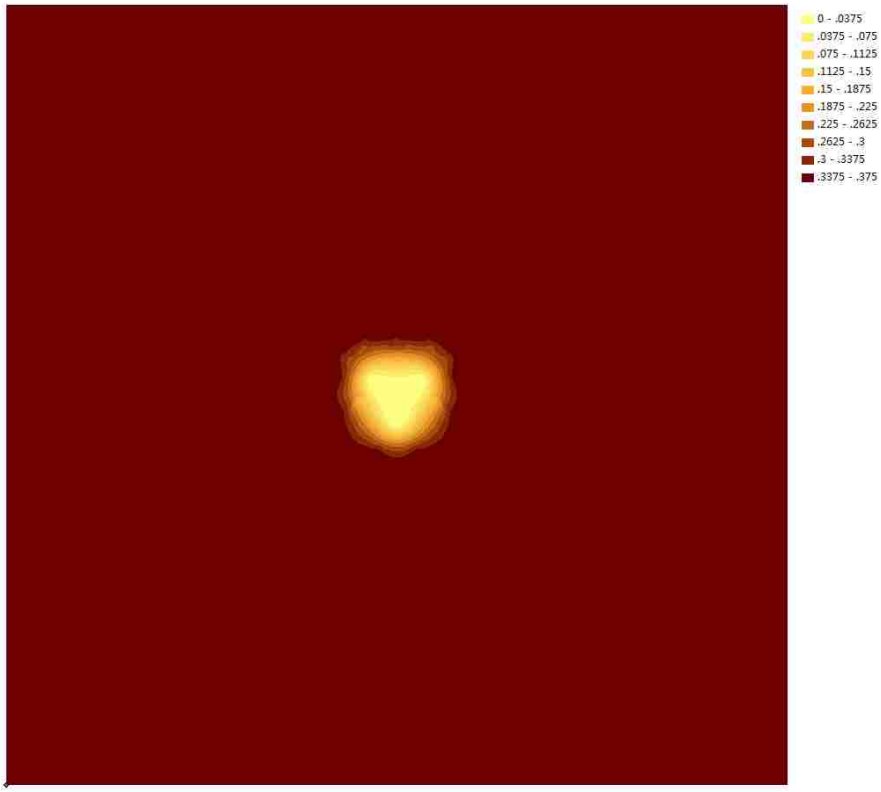

Figure 66 Contour of Thickness Distribution from ArcGIS for 3 Holes

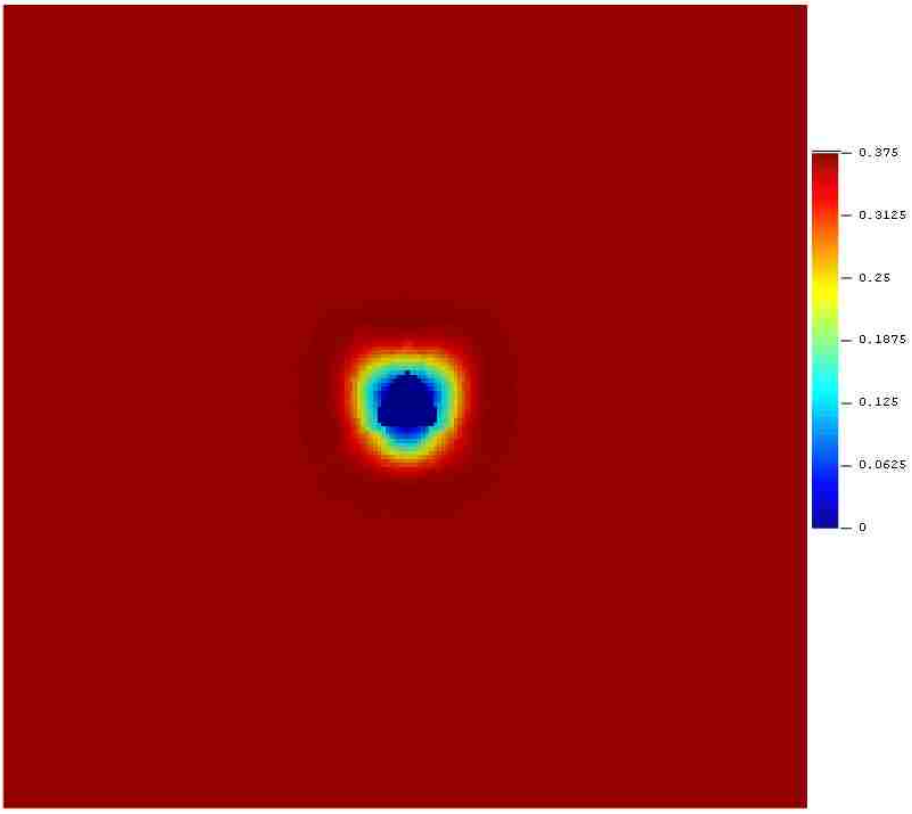

Figure 67 Contour of Thickness Distribution from Surfer for 3 Holes

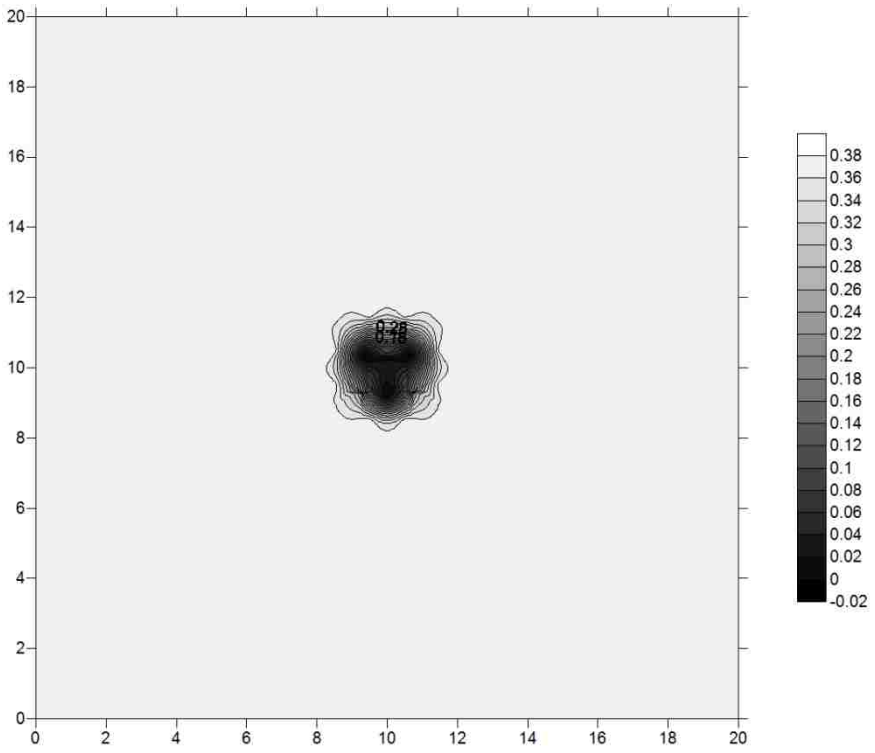

Figure 68 Contour of Thickness Distribution from SGeMS for 3 Holes

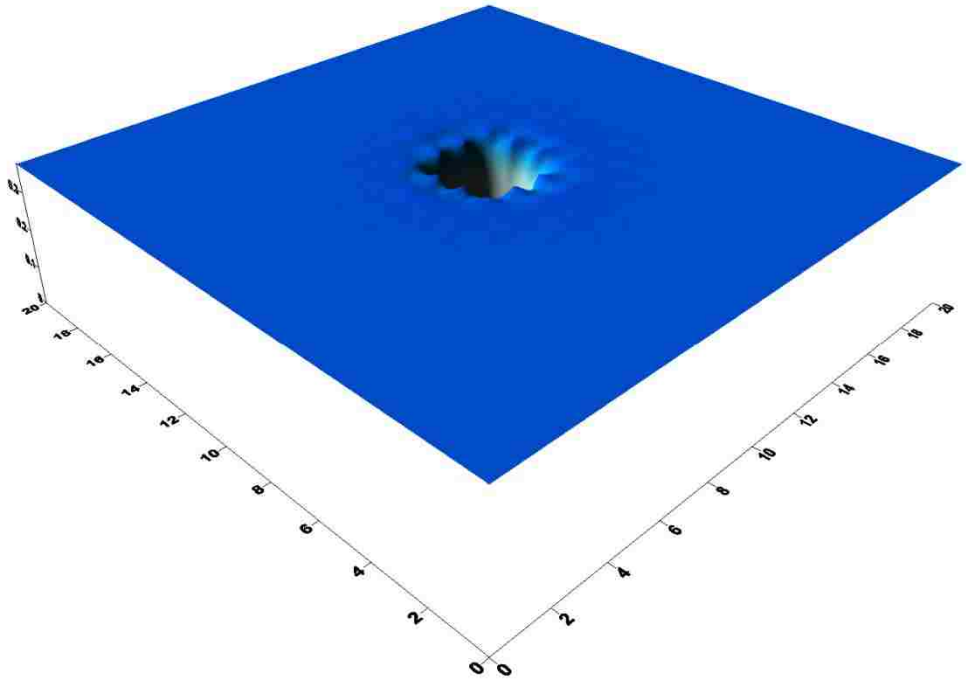

Figure 69 3-D Model of Thickness Distribution from SGeMS for 3 Holes

The damage effect ration (φ) was measured from Figures 66, 67 and 68 by Image Pro-Plus, and Table 4 contains the results.

3.6.5 Simulation of 5 Holes

3.6.5.1 Setting up Parameters

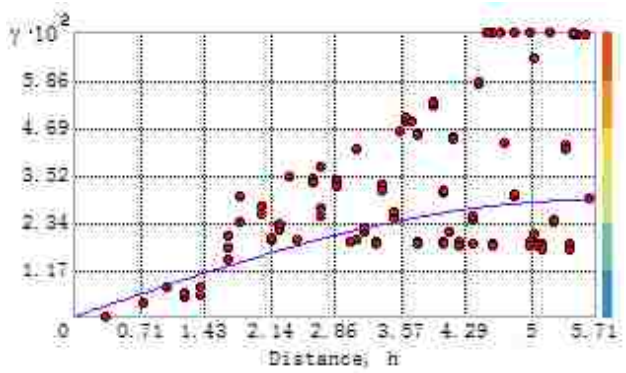

Figure 70 Curve of Variogram Function for 5 Holes

Based on this curve, the spherical effect model was selected. The other parameters of the spherical model are as following:

Mean Value: 0.30873

Major range: 5.64382

3.6.5.2 Displaying the Images

Using the above parameters in the three softwares, the estimated thickness distribution was computed. Given on these files, the four figures are developed from the packages. Every software gives a contour map of the distribution and Surfer yields a 3-D distribution map.

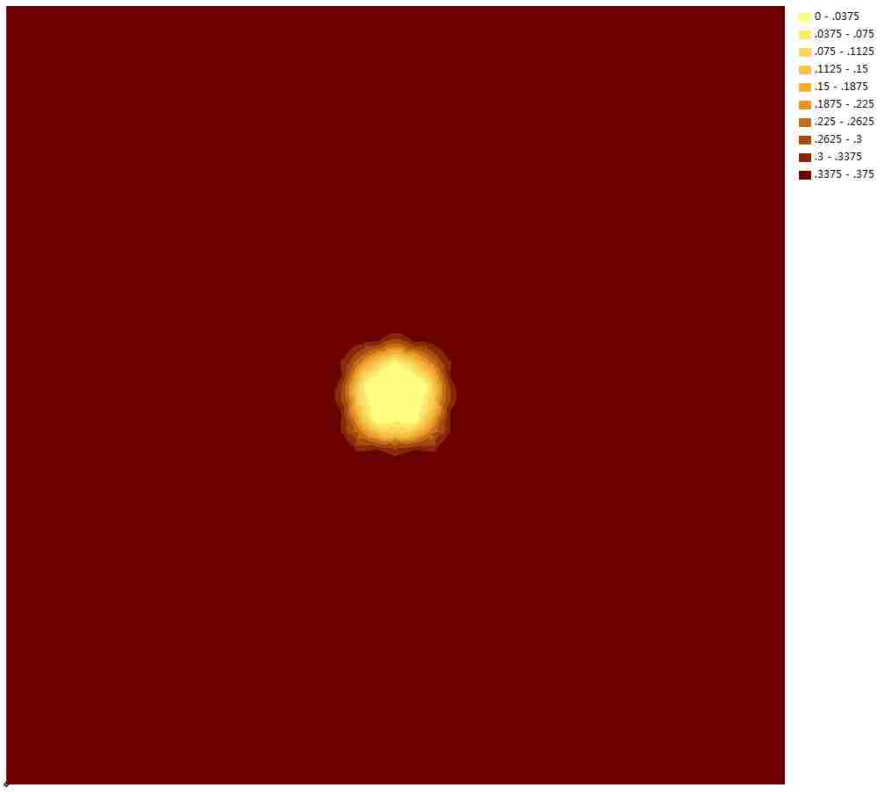

Figure 71 Contour of Thickness Distribution from ArcGIS for 5 Holes

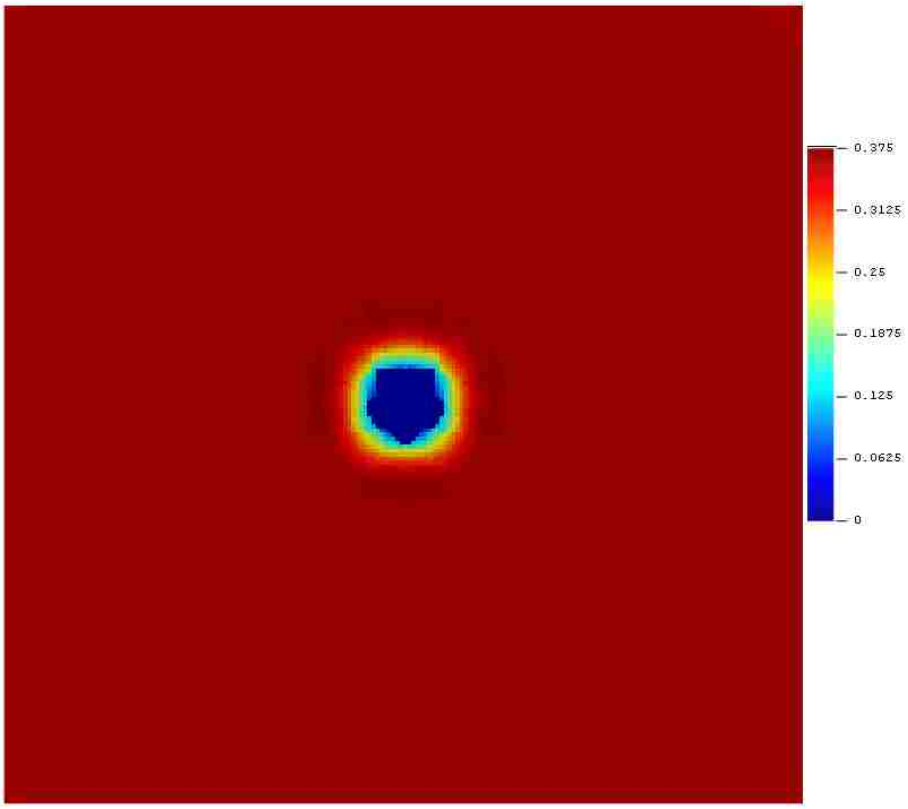

Figure 72 Contour of Thickness Distribution from Surfer for 5 Holes

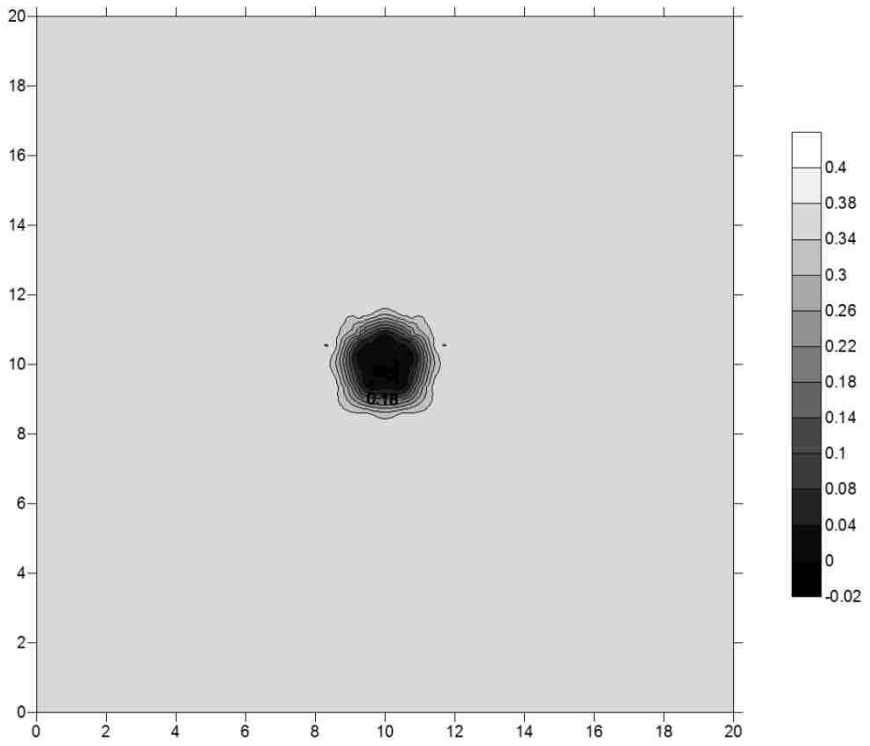

Figure 73 Contour of Thickness Distribution from SGeMS for 5 Holes

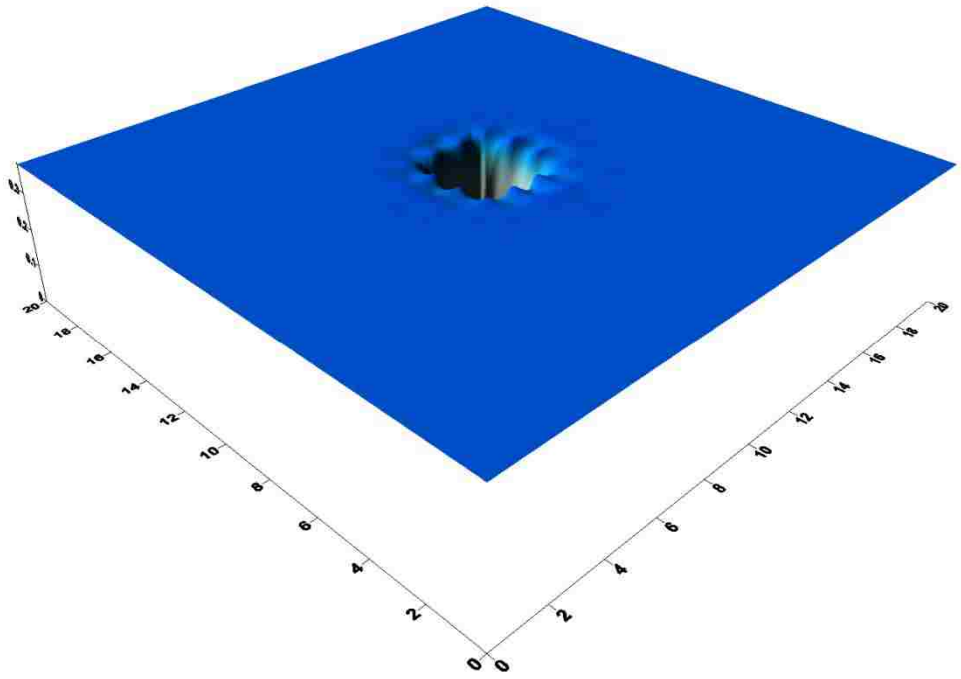

Figure 74 3-D Model of Thickness Distribution from SGeMS for 5 Holes

The damage effect ration (φ) was measured from Figures 71, 72 and 73 by Image Pro-Plus, and Table 4 contains the results.

3.6.6 Simulation of 6 Holes

3.6.6.1 Setting up Parameters

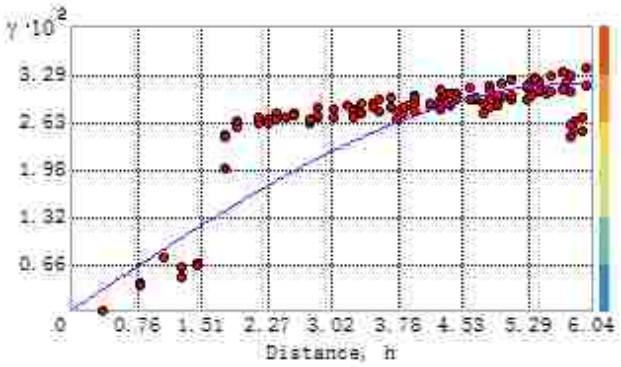

Figure 75 Curve of Variogram Function for 6 Holes

Based on this curve, the spherical effect model was selected. The other parameters of the spherical model are as following:

Mean Value: 0.29819

Major range: 5.92179

3.6.6.2 Displaying the Images

Using the above parameters in the three softwares, the estimated thickness distribution was computed. Given on these files, the four figures are developed from the packages. Every software gives a contour map of the distribution and Surfer yields a 3-D distribution map.

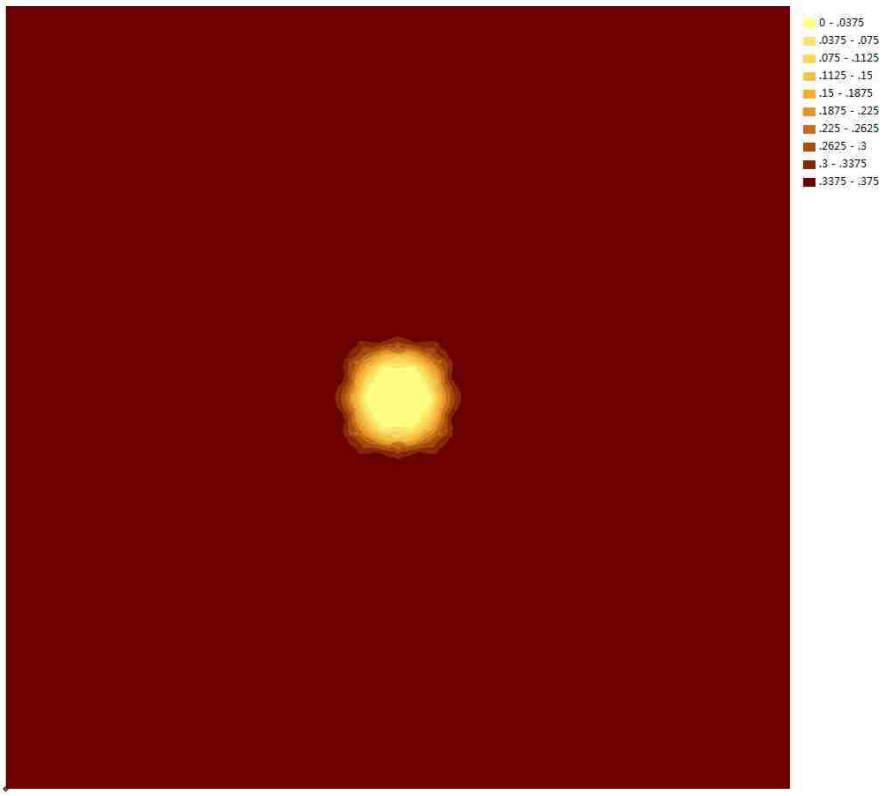

Figure 76 Contour of Thickness Distribution from ArcGIS for 6 Holes

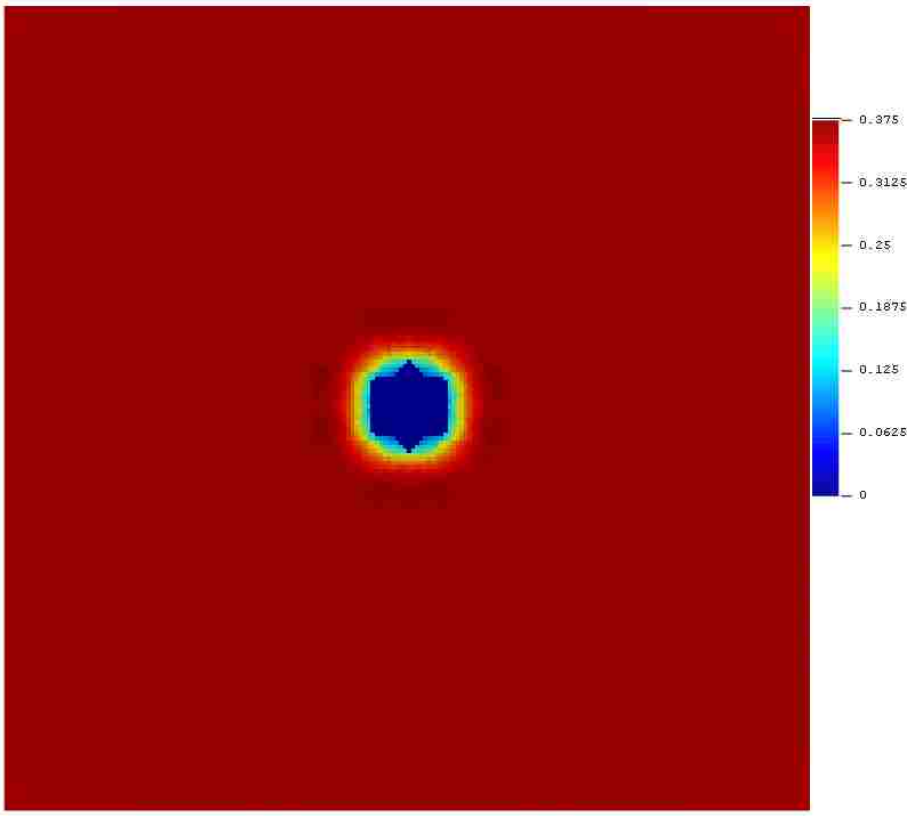

Figure 77 Contour of Thickness Distribution from Surfer for 6 Holes

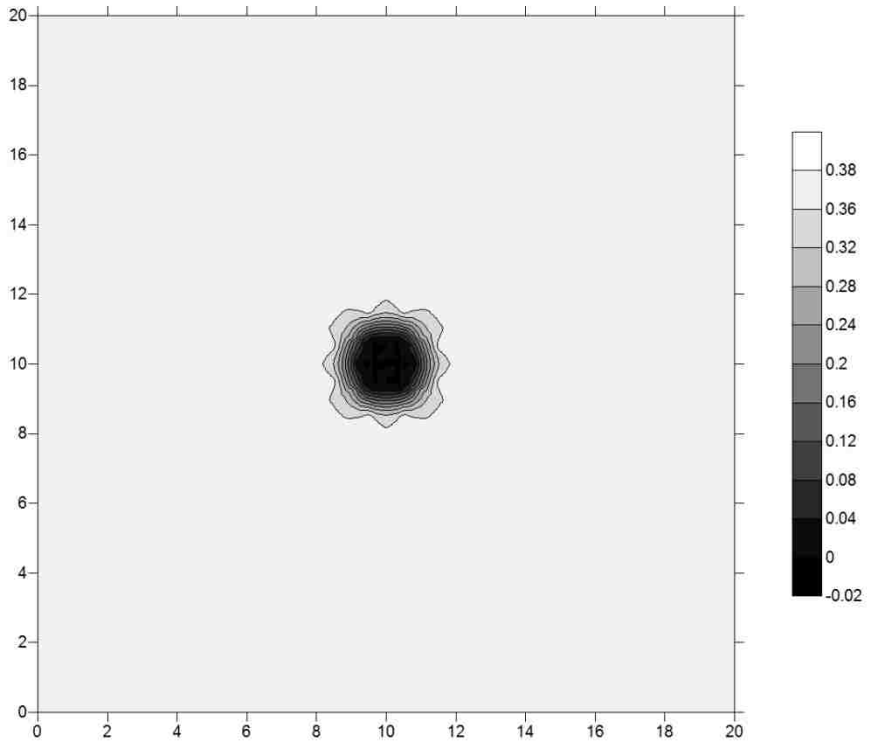

Figure 78 Contour of Thickness Distribution from SGeMS for 6 Holes

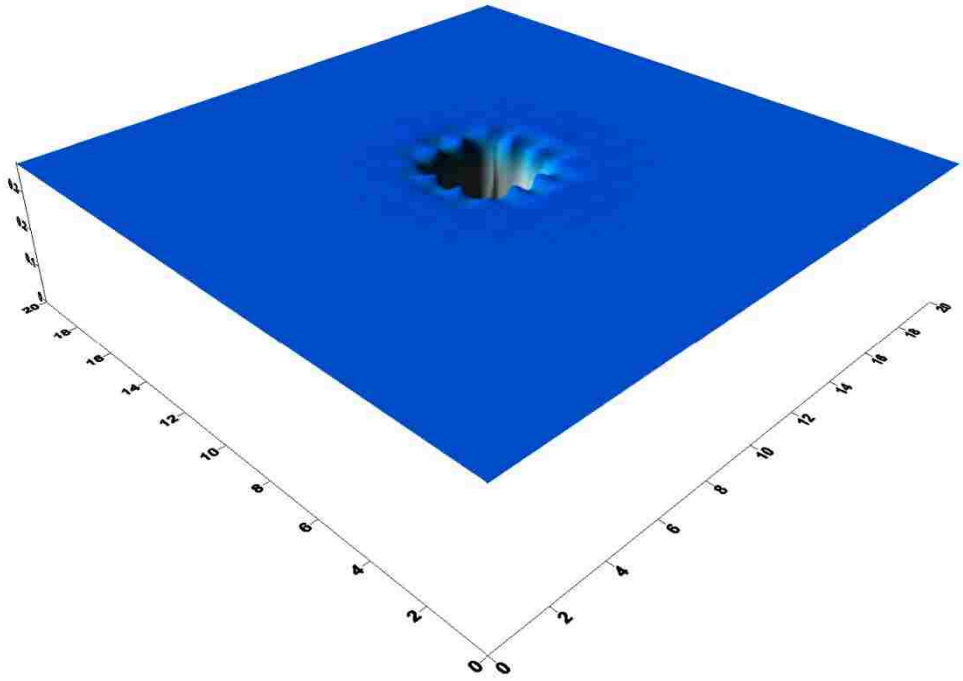

Figure 79 3-D Model of Thickness Distribution from SGeMS for 6 Holes

The damage effect ration (φ) was measured from Figures 76, 77 and 78 by Image Pro-Plus, and Table 4 contains the results.

3.6.4 Conclusion of Different Patterns of Holes

By combined the above damage effect ration, **Table 4** illustrates the damage effect ratio which is altered by different patterns of holes.

Different Patterns	Damage Effect Ratio (φ): (%)		
	ArcGIS	**Surfer**	**SGeMS**
1 hole	0.39	0.26	0.94
Line pattern of 2 holes	0.64	0.59	1.18
Triangular pattern of 3 holes	0.90	0.88	1.33
Square pattern of 4 holes	0.99	0.97	1.41
Pentagon pattern of 5 holes	1.02	1.02	1.48
Hexagon pattern of 6 holes	1.04	1.06	1.54

Table 4 Damage Effect Ratio with Different Patterns of Holes

Comparing the Table 18 and the above figures, the conclusions about the effect of the patterns constituted by different number of holes are as follows:

(1) The damage effect ratio tends to increase as the number of holes in a fix area increases.

(2) The damaged areas caused by the holes have a similar pattern as that of the holes.

3.7 Relationship between Radius and Distance

As shown in **3.3.2** and **3.5**, when the distance between two holes exceeds 3ft or

5ft, there is minimal interaction between them, but when the distance is less than 3ft, their interaction with each other can be substantial. This is an interesting issue. This part of the study will consider this problem to seek a value of distance so that the holes do not interact with each other for different radii, which are 1/16ft, 1/8ft and 1/2ft. From above parts, the value of the distance is located between 1ft and 3 ft for a 1/16ft hole. The solution from ArcGIS and Surfer are similar, so only ArcGIS is used to estimate the thickness distribution.

3.7.1 Creating Data Set

The condition for this section is that the 20ft × 20ft plate is divided into 400 cells with 396 cells represented by the nominal thickness of 0.375in which located in the center of these cells. The other 4 cells contain holes which have known damage. The separation of the other 4 cells corner is from 1ft to 3ft for the 1/16ft radius. The separation for 1/8ft and 1/2 ft is investigated in the following.

3.7.2 Relationship of Radius and Distance for 1/16ft radius

The 1ft distance for 1/16ft has been estimated in **3.3.2**, and 3ft distance for 1/16ft has been estimated in **3.5.2.** The next step is estimating the 2ft distance for 1/16ft radius, which is shown in **Figure 80**.

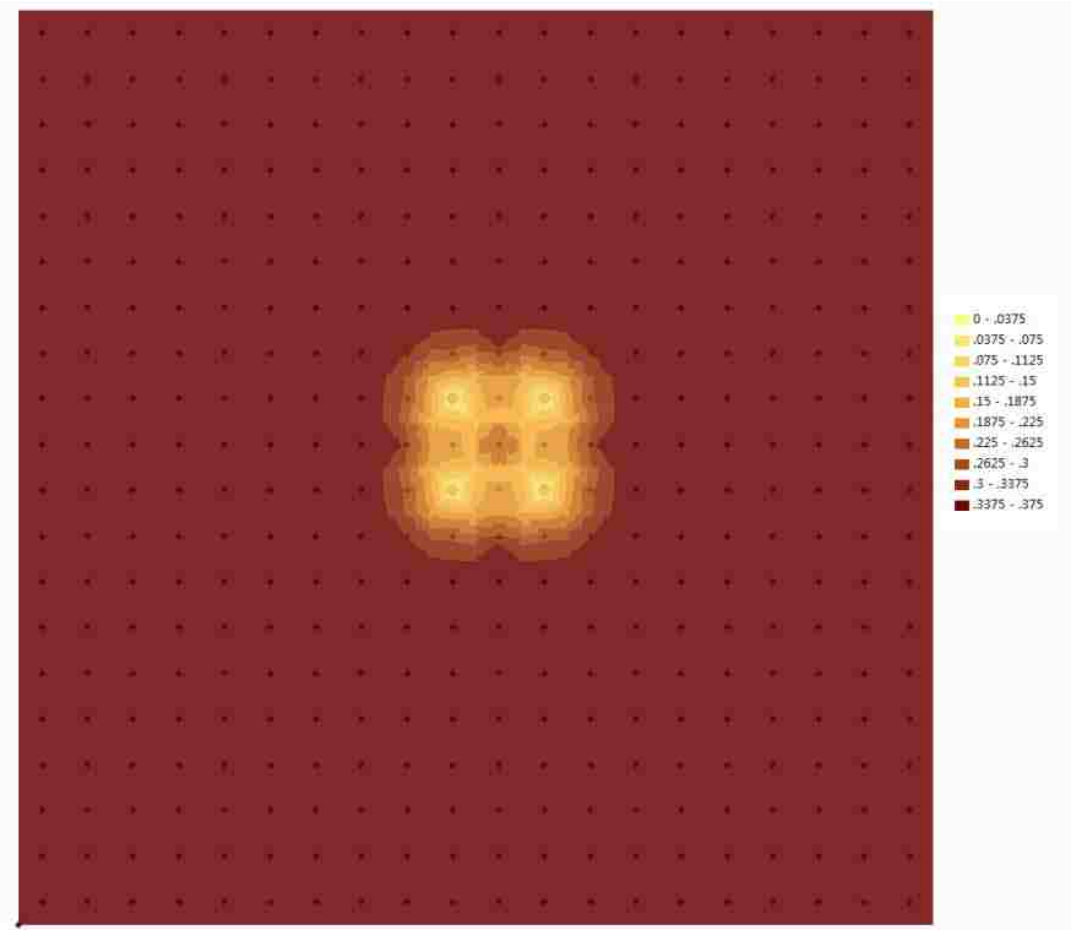

Figure 80 Contour of Thickness Distribution from ArcGIS for 2ft Distance

The above figure illustrates that the holes also interact with each other at 2ft distance, so other distances should be checked. The value of distance should be correct to two decimal values. At the end, the value of distances was found between 2.67ft and 2.68ft, whose distribution shown in figures 81 and 82.

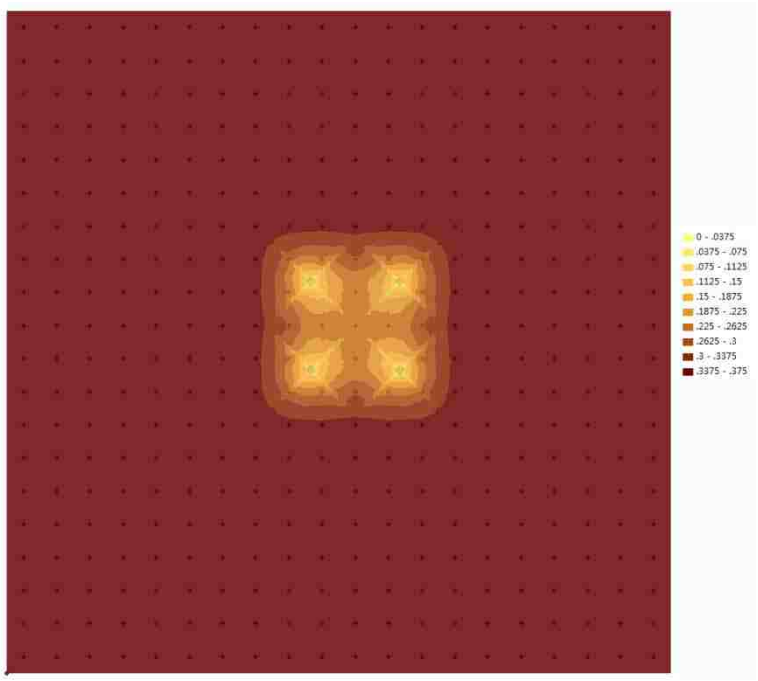

Figure 81 Contour of Thickness Distribution from ArcGIS for 2.67ft Distance

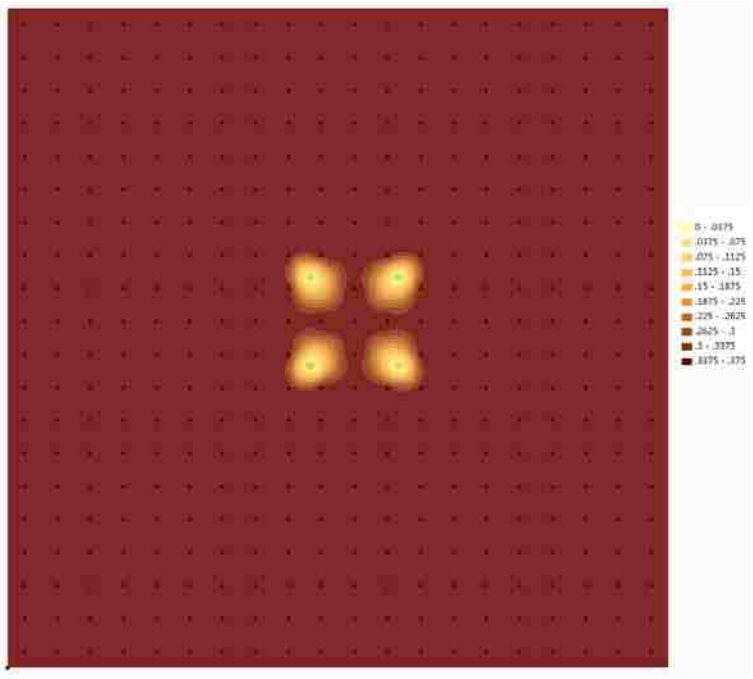

Figure 82 Contour of Thickness Distribution from ArcGIS for 2.68ft Distance

From these figures, it is obvious that there is no interaction when the distance of two radius 1/16ft holes corner is more than 2.68ft. For the distances which are less than 2.67ft, the interaction would exist.

3.7.3 Relationship of Radius and Distance for 1/8ft radius

The 1ft distance for 1/8ft has been estimated in **3.3.3**. Based on the result of 3.7.2, the no interaction distance for 1/8 ft must be around 2.68ft because all the conditions are same except the small separation of radius from 1/16ft to 1/8ft. From **3.5.2**, there is no interaction when distance is 3ft. Firstly, distances of 2.68ft and 3ft would be checked, which are shown in Figure 83 for 3ft and Figure 84 for 2.68ft.

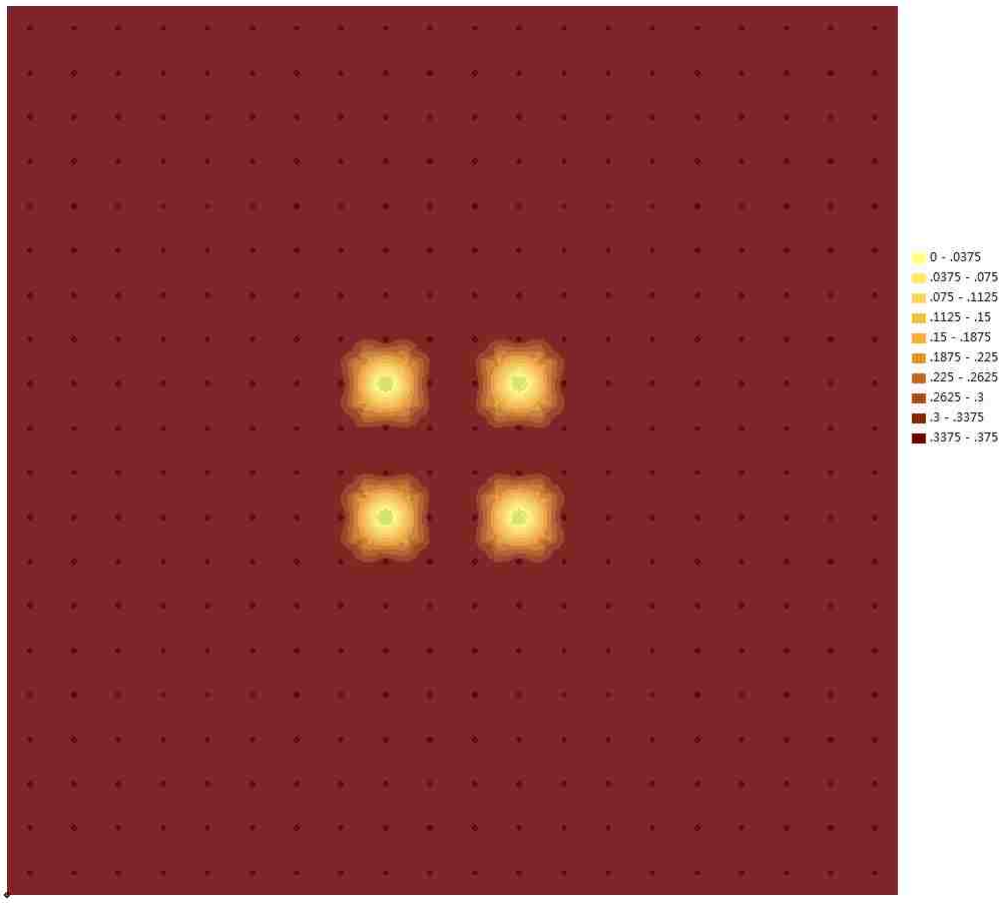

Figure 83 Contour of Thickness Distribution from ArcGIS for 3ft Distance

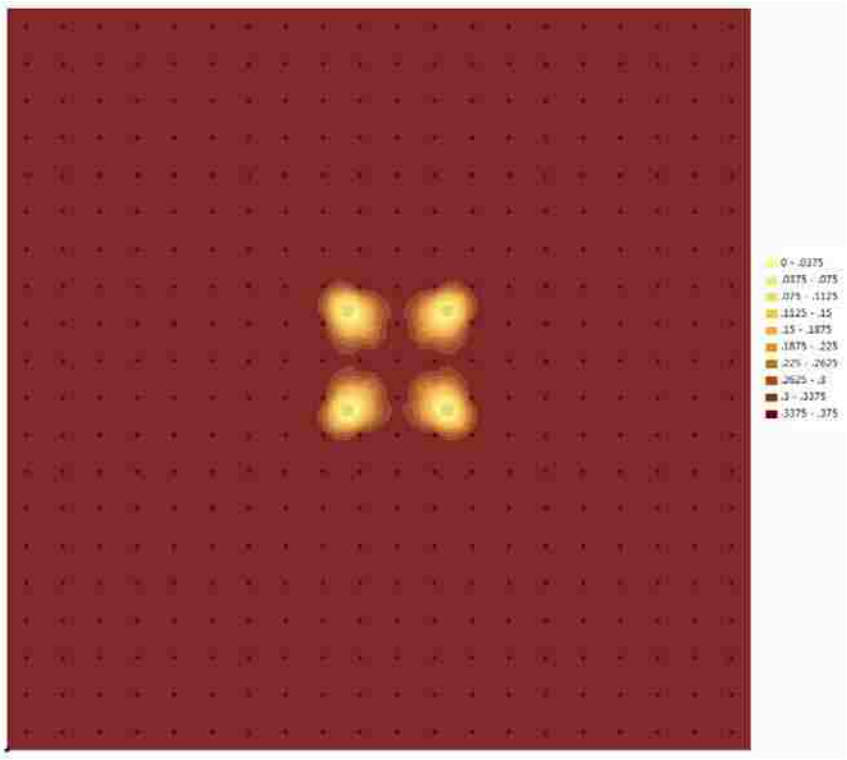

Figure 84 Contour of Thickness Distribution from ArcGIS for 2.68ft Distance

After reducing the distance, 2.67ft distance was found to be a value that the holes were interaction, which is shown in **Figure 85**

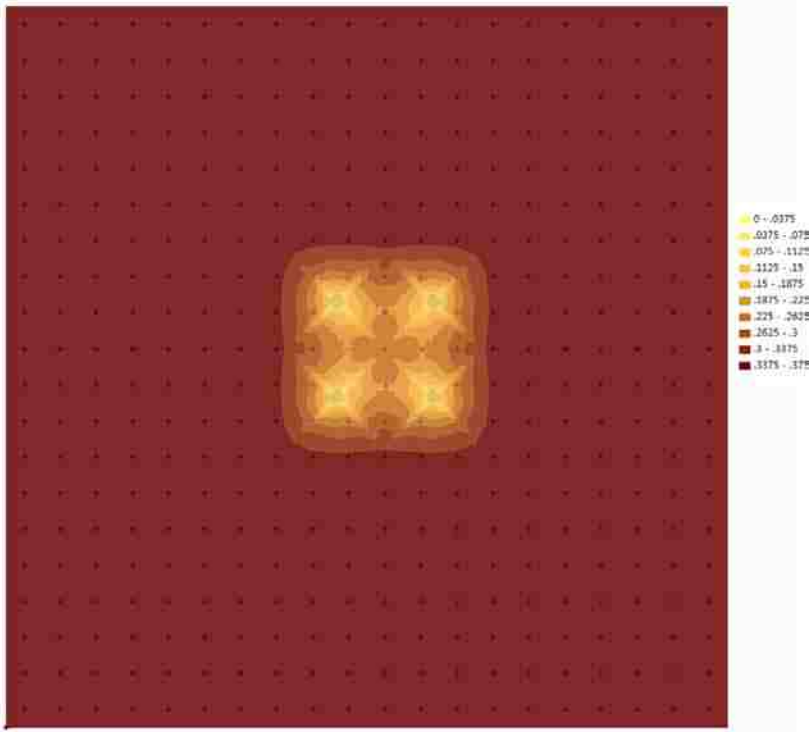

Figure 85 Contour of Thickness Distribution from ArcGIS for 2.67ft Distance

From these figures, it is obvious that there is no interaction when the distance of two radius 1/8ft holes' center is more than 2.68ft. For the distances which are less than 2.67ft, the interaction would exist. The result is same as the result for 1/16ft, but it is obvious that the effect for 1/8ft radius is more than that for 1/16ft radius whose distances are both 2.67ft and 2.68ft.

3.7.4 Relationship of Radius and Distance for 1/2ft radius

The 1ft distance for 1/2ft radiushas been estimated in **3.3.4**. The radius increases from 1/8ft to 1/2ft. The changing is very large, so the result from above parts could not be used. As the first step, 3ft distance should be checked, which is illustrated in Figure 86.

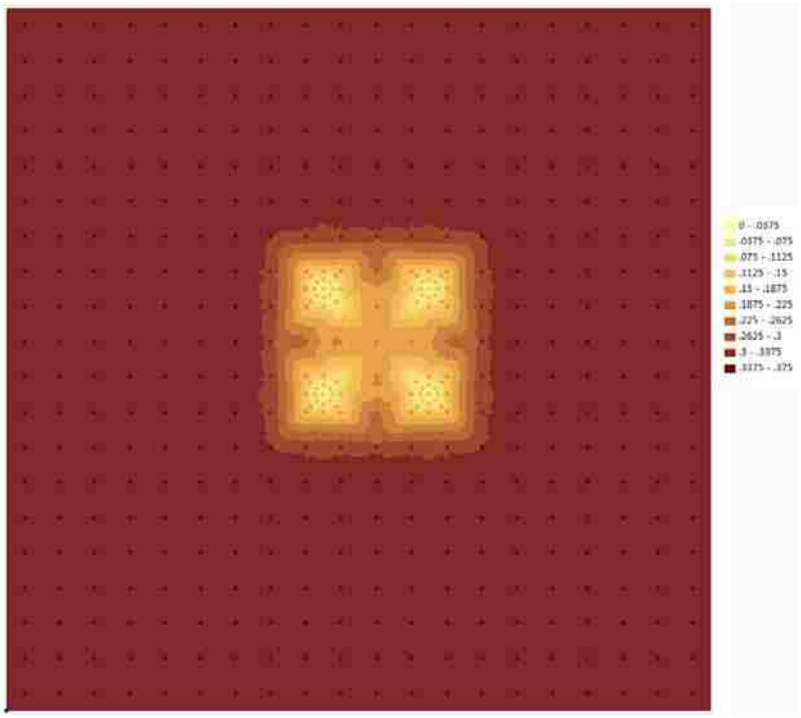

Figure 86 Contour of Thickness Distribution from ArcGIS for 2.67ft Distance with No Additional Points.

When the distance is 3ft, the centers of holes are located the sides of the 4 damage cells and there are no points on the corner of these cells. After checking no additional points in Figure 86, some points were added in this location and checked to show in Figure 87.

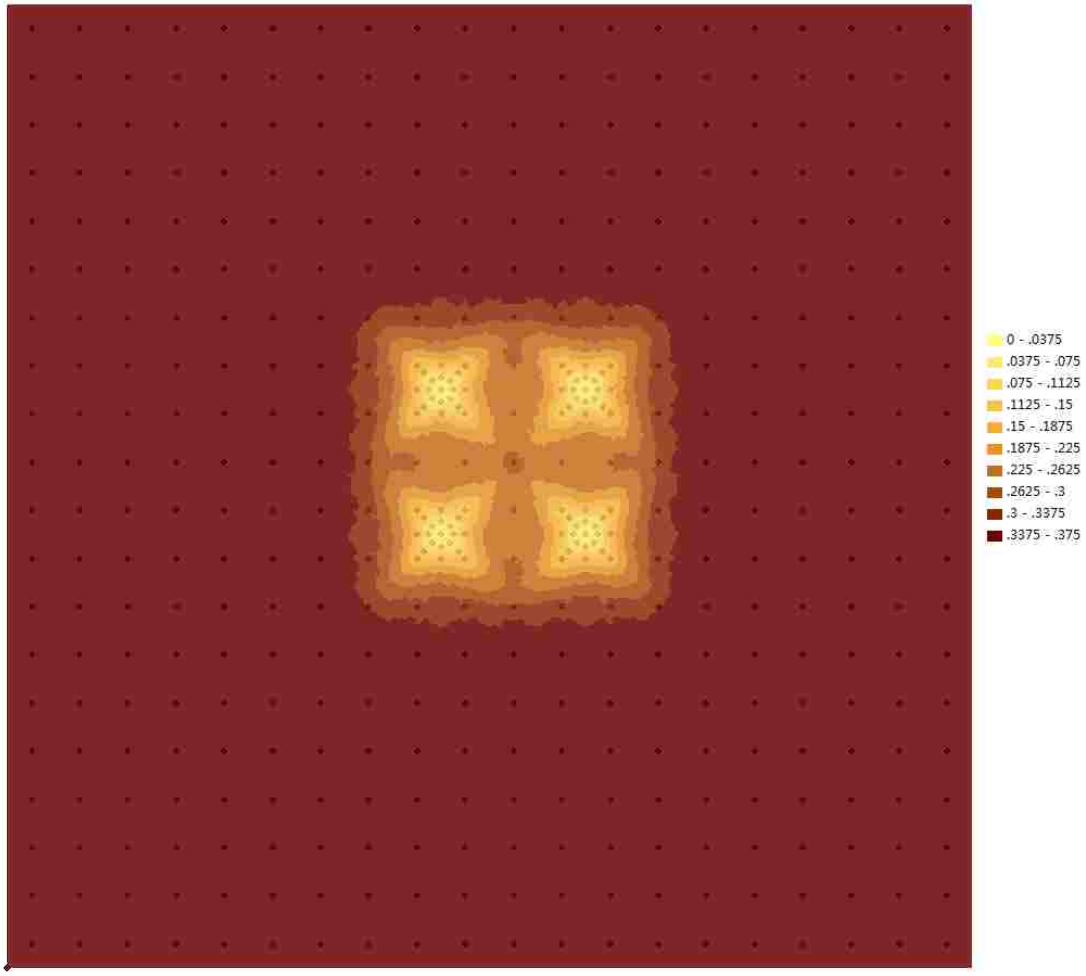

Figure 87 Contour of Thickness Distribution from ArcGIS for 2.67ft Distance with Additional Points.

From figure 86 and 87, the difference between them is not large, so these points will be added in the following estimation to make them reasonable. In order to seek the value so that there is no interaction, the separation of the next steps is 0.2ft, and other separations would be adjusted according to the testes. Along with the increasing

of distance, some points in above assumption would locate in the holes. These points will be removed. The following figures will show the thickness distribution.

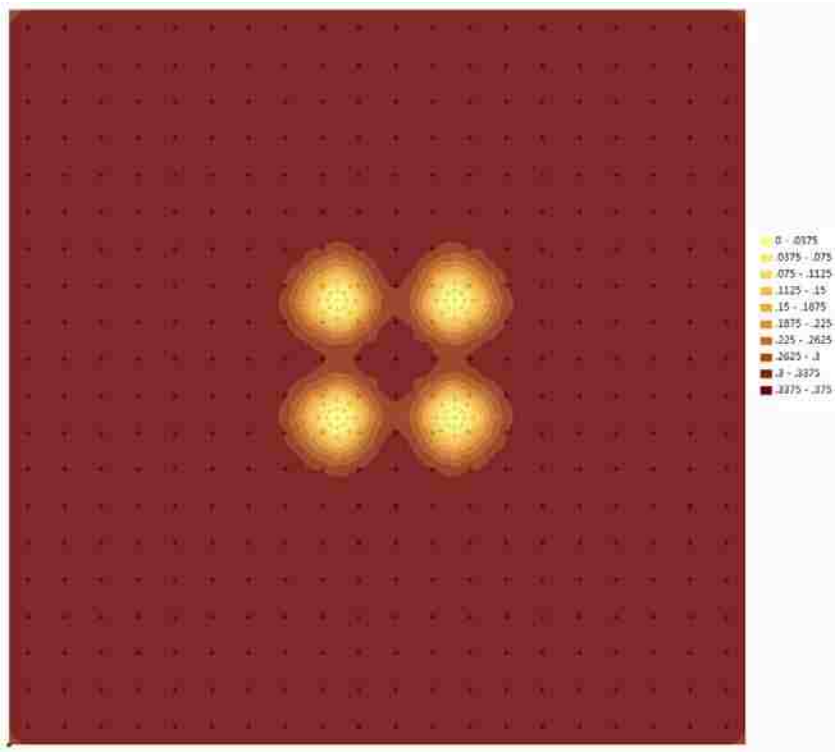

Figure 88 Contour of Thickness Distribution from ArcGIS for 3.2ft Distance

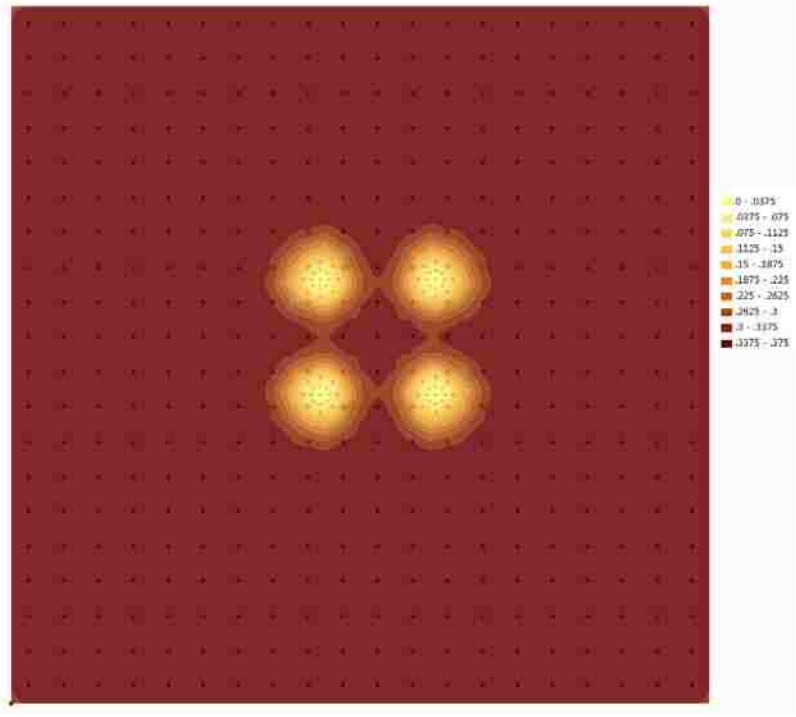

Figure 89 Contour of Thickness Distribution from ArcGIS for 3.3ft Distance

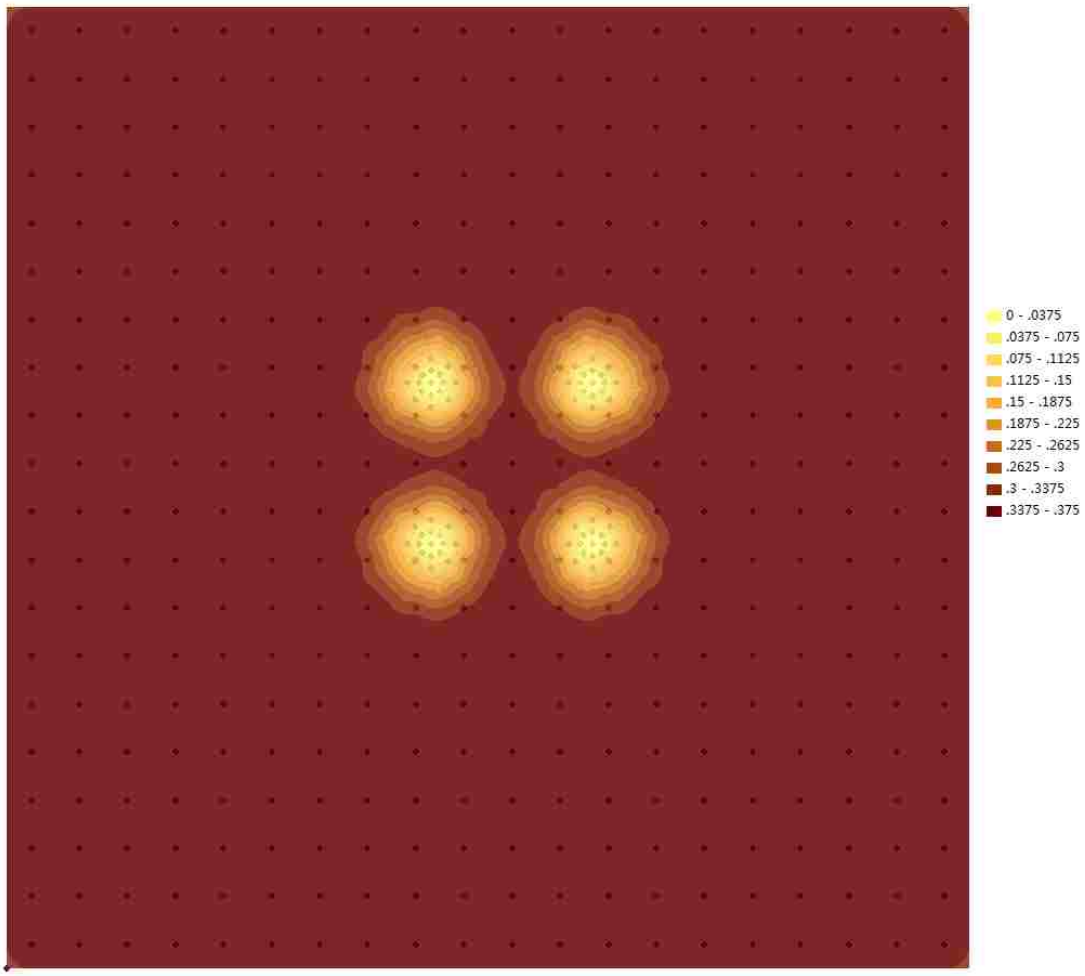

Figure 90 Contour of Thickness Distribution from ArcGIS for 3.35ft Distance

The value of distance with no interaction finally located between 3.3ft and 3.35ft which are shown in figure 89 and 90.

3.7.5 Conclusion of Relationship between Radius and Distance

(1) Along with increasing the distance, the interaction between holes tends to reduce, and at an appropriate value of distance, the interaction will disappear.

(2) The value of the distance with no interaction tends to increase with increasing radius, but the separations of two closest points of two neighboring holes are not much different for different radii.

Chapter 4

Conclusion and Future Work

In this chapter, some conclusions based on the results illustrated in the previous chapters are presented. Some extended work for future applications are also recommended.

4.1 Conclusion

The aim of this thesis is to apply kriging methods to investigate the effect of damage areas in a large plate by estimating the thickness distribution. All simulations were computed for a 20ft × 20ft plate The major conclusions obtained in this research are the following:

(1) Kriging can be used to estimate thickness distributions quickly and easily by using proven software packages, given the observed data.

(2) The applied software, ArcGIS, Surfer and SGeMS, predict similar thickness distributions. ArcGIS and Surfer yield similar predictions of the damage effect ratio, and SGeMS gives slightly bigger results. The reason for this is that the accuracy of SGeMS is lower than the other two softwares.

(3) The damage holes only affect their adjacent areas, with nearly no affect on farther areas.

(4) The damage effect ration tends to rise with increasing hole radius, and the

relationship between them is non-linear.

(5) The various holes radii arrangements influence the damage effect ratio and the pattern is different, but the difference of in the pattern is small.

(6) For arrangement of several holes whose radii are different, the damage effect ratio for the two holes whose radii are the largest and the next largest are adjacent is larger than those are located in the diagonal.

(7) The damage effect ratio tends to decrease with the increasing separation of two holes and that will nearly change when the separations close to a value. Because these holes will not interact with each other after the separation closes to the value.

(8) The damage effect ratio tends to increase with an increasing number of holes in a fix area, but the difference of ratios will be smaller with the increasing. The damaged areas influenced by damage holes have the similar pattern as the patterns of damage holes.

(9) Along with increasing the distance, the interaction between holes tends to reduce, and at an appropriate value of distance, the interaction will disappear.

(10) The value of the distance with no interaction tends to increase with increasing radius, but the separations of two closest points of two neighboring holes are not much different for different radii.

4.2 Suggestions for Future Work

Although kriging methods has been applied in geology and mining for more than

50 years and plenty of commercial and non-commercial softwares that were programmed by this algorithm have been proven to work well, it has not been applied in Mechanical Engineering very much. Considering the differences among Mechanics, Geology and Mining, there is still room to update and examine kriging methods for Mechanics. Some works are given below.

(1) The data sets used in this thesis are assumed, but the practical data sets are very different. Kriging methods maybe better than other algorithms, but they are also linear least squares estimation algorithms, which predict the distribution. Some experiments should be done to test the accuracy of kriging methods.

(2) Based on the above results, the minimum thickness in some figures is less than 0, which is not reality. Some work should be done to eliminate this situation to make the results reality.

(3) Besides simple kriging, there are also other kriging methods like ordinary kriging, universal kriging. These methods could also be used to estimate the thickness distribution to compare the results with real situation so that the best kriging methods could be implemented in this problem.

REFERENCE

[1] Krige, D. G (1951), A statistical approach to some mine valuations and allied problems at the Witwatersrand, Witwatersrand, University of Witwatersrand.

[2] Pierre Goovaerts (1997), Geostatistics for Natural Resources Evaluation, New York, Oxford University Press

[3] Geoff Bohling (2005), Kriging, Kansas Geological Survey, http://people.ku.edu/~gbohling/cpe940

[4] Chilès, J. and Delfiner,P. (1999), Geostatistics: Modeling spatial unvertainty, New York, John Wiley & Sons.

[5] Tran, T. (1994), Improving variogram reproduction on dense simulation grids, Computer & Geosciences 20(7), 1161-1168

[15] Nicolas Remy, Alexandre Boucher and Jianbing Wu (2009), Applied Geostatistics With SGeMS: A User's Guide, (1 Har/Cdr editon), Stanford, Cambridge University Press

[6] Armstrong M (1998), Basic linear geostatistics, Berlin, Springer Verlag

[7] Isaaks, E. and Srivastava, R. (1989), An Introduction to Applied Geostatistics, New York, Oxford University Press.

[8] Rincock, Allen and Holt (2008), Consultants for Mining and Financial Solutions: About Kriging, ISSUE NO.88, Toronto, A Division of Runge Inc.

[16] Barris, J. (2008), An expert system for appraisal by the method of comparison, Barcelona, UPC.

[9] Cressie, N, (1993), Statistics for spatial data, New York, Wiley.

[10] Journel, A. G. (1989), Fundamentals of Geostatistics in Five Lessons, Washington D.C. American Geophysical Union.

[11] Stein, M. L. (1999), Statistical Interpolation of Spatial Data: Some Theory for Kriging, New York, Springer.

[12] Merriam, D F (1970), Geostatistics, a colloquium, New York, Plenum Press.

[13] Sakata S, Ashida F, Zako M (2003), Structural optimization using kriging approximation, Computer Methods in Applied Mechanics and Engineering 192:923

[14] Golden Software, Inc. (2010), Surfer Quick Start Guide, Golden, Golden Software, Inc. www.GoldenSoftware.com

[15] Nicolas Remy, Alexandre Boucher and Jianbing Wu (2009), Applied Geostatistics With SGeMS: A User's Guide, (1 Har/Cdr editon), Stanford, Cambridge University Press

[16] Barris, J. (2008), An expert system for appraisal by the method of comparison, Barcelona, UPC.

[17] Zekai Sen, Spatial modeling principles in earth sciences, New York, Springer.

[18] Fatima – Zohra Benmostefa Largueche, Estimating soil contamination with kriging interpolation method, American Journal of Applied Sciences.

[19] Ricardo A. Olea (1999), Geostatistics for Engineers and Earth Scientists, New York, Springer.

[20] Vera Pawlowsky-Glahn and Ricardo A. Olea (2004), Geostatistical analysis of compositional data, New York, Oxford University Press.

[21] Clayton V. Deutsch (2002), Geostatistical Reservoir Modeling, New York, Oxford University Press.

APPENDIX

This program is used to calculate the locations of 17 points which represent circular damage.

```
% This program is to calculate the location of 17 points which express
a
% circle and transfer them into .xls file

clear all;
clc;
r=input('Radius = '); % Input the radius of the hole

% Determine the distance between each 16 points and circle center
L_far=[-r,0];
L_close=[-r/2,0];
LU_far = [-2^0.5/2*r,2^0.5/2*r];
LU_close = [-2^0.5/4*r,2^0.5/4*r];
U_far = [0,r];
U_close = [0,r/2];
RU_far = [2^0.5/2*r,2^0.5/2*r];
RU_close = [2^0.5/4*r,2^0.5/4*r];
R_far = [r,0];
R_close = [r/2,0];
RD_far = [2^0.5/2*r,-2^0.5/2*r];
RD_close = [2^0.5/4*r,-2^0.5/4*r];
D_far = [0,-r];
D_close = [0,-r/2];
LD_far = [-2^0.5/2*r,-2^0.5/2*r];
LD_close = [-2^0.5/4*r,-2^0.5/4*r];

p=input('Point location = '); % Input the location of circle center

% Gaining the location of other 16 points
p_L_far= p - L_far;
p_L_close= p - L_close;
p_LU_far = p - LU_far;
p_LU_close = p - LU_close;
p_U_far = p - U_far;
p_U_close = p - U_close;
```

```
p_RU_far = p - RU_far;
p_RU_close = p - RU_close;
p_R_far = p - R_far;
p_R_close = p - R_close;
p_RD_far = p - RD_far;
p_RD_close = p - RD_close;
p_D_far = p - D_far;
p_D_close = p - D_close;
p_LD_far = p - LD_far;
p_LD_close = p - LD_close;

% Output the location of 17 points as a matrix
P(1,:)=p_LD_close;
P(2,:)=p_LD_far;
P(3,:)=p_D_close;
P(4,:)=p_D_far;
P(5,:)=p_RD_close;
P(6,:)=p_RD_far;
P(7,:)=p_R_close;
P(8,:)=p_R_far;
P(9,:)=p_RU_close;
P(10,:)=p;
P(11,:)=p_RU_far;
P(12,:)=p_U_close;
P(13,:)=p_U_far;
P(14,:)=p_LU_close;
P(15,:)=p_LU_far;
P(16,:)=p_L_close;
P(17,:)=p_L_far;
P
```